# Applications Potential of

# RADARSAT-2

## A Preview

Edited by:

J.J. van der Sanden

S.G. Ross

April 2001

Natural Resources Canada | Ressources naturelles Canada

Canada

BLANK PAGE

# Applications Potential of RADARSAT-2 A Preview

Prepared by:
Canada Centre for Remote Sensing
in collaboration with
Canadian Ice Service
For
Canadian Space Agency

Edited by:
J.J. van der Sanden
S.G. Ross

Contributors:
P. Budkewitsch
D.G. Flett
A.L. Gray
R.K. Hawkins
R. Landry
T.I. Lukowski
H. McNairn
T.J. Pultz
V. Singhroy
J. Sokol
Th. Toutin
R. Touzi
P.W. Vachon
J.J. van der Sanden

April 2001

BLANK PAGE

# Abstract

van der Sanden, J.J. and S.G. Ross (eds). (2001). *Applications Potential of RADARSAT-2 – A Preview*. Ottawa (Natural Resources Canada, Canada Centre for Remote Sensing), report compiled for and with funding from the Candian Space Agency, 117 p.

This report describes the state-of–the-art with respect to the extraction of information from RADARSAT-2 type Synthetic Aperture Radar data for 32 applications in fields of agriculture, cartography, disaster management, forestry, geology, hydrology, oceans, and sea and land ice. As such, the report offers a preview of the application potential associated with the data products from the future RADARSAT-2 satellite. In addition, it facilitates the identification of application fields and information extraction techniques that require further research and development. In terms of application potential, the report focuses on an assessment of the data information content. Comparison of the ratings for the overall application potential of RADARSAT-1 and –2 shows that the biggest improvement is projected to be associated with the crop type, crop condition and sea ice topography / structure fields. This is primarily the result of the enhancement of RADARSAT-2 in terms of polarization. For 18 out of the 32 application fields considered the introduction of RADARSAT-2 is expected to result in a modest increase in application potential. The application potential for 10 fields is projected to remain unchanged. The recommendations for applications research and development focus on the new RADARSAT-2 data products. A widespread lack of understanding with regard to the relationship between the image information content and the polarization of the radar signal is identified. The report is based on first-hand experience of applications specialists at the Canada Centre for Remote Sensing and the Canadian Ice Service as well as on findings that other researchers have published in the literature. It constitutes one of the first results of the RADARSAT-2 Applications Development Programme. This programme is led by the Canada Centre for Remote Sensing and financed by the Canadian Space Agency with Canadian Space Plan funds.

Keywords: RADARSAT, application, Canada, remote sensing, satellite, radar, polarimetry

BLANK PAGE

# Executive Summary

Canada's second Earth observation satellite, that is, RADARSAT-2 is scheduled for launch in 2003. Like its predecessor, RADARSAT-2 will image by means of a Synthetic Aperture Radar (SAR) system. RADARSAT-2 will provide all imaging modes of the current RADARSAT-1 satellite, as well as some new modes that incorporate significant technical innovations and improvements. Hence, the satellite will offer data continuity to RADARSAT-1 users and new data that will support development of new applications and refinement of existing ones. The most important technical enhancements embodied by RADARSAT-2 are reflected in its specifications in terms of look direction, spatial resolution, polarization, and orbit control.

Given the investment, it is important to all parties involved that the future RADARSAT-2 data can be applied to its full extent to meet information needs from users both within Canada and abroad. Preparation for RADARSAT-2 through applications research and development is therefore crucial to the overall success of the mission. Here, the Canadian government must take a leadership role since industry and academia generally lack the required continuity in terms of financial and human resources. The Canadian Space Agency (CSA) is well aware of this and has therefore decided to allocate Canadian Space Plan (CSP) funds to the RADARSAT-2 Applications Development Programme as proposed by the Canada Centre for Remote Sensing (CCRS).

This report constitutes one of the first results of the RADARSAT-2 Applications Development Programme. It describes the state-of–the-art with respect to the extraction of information from RADARSAT-2 type data for 32 applications in fields of agriculture, cartography, disaster management, forestry, geology, hydrology, oceans, and sea and land ice. In doing so, it allows us to preview the application potential of RADARSAT-2 and to identify application fields and information extraction techniques that require further research and development. The applicability of the current RADARSAT-1 data products is often taken as a starting-point for discussions concerning the application potential of the future RADARSAT-2 data products. In terms of application potential, the report focuses on an assessment of the data information content and thus pays little attention to other issues that may affect the promise of an application, e.g. economic or legal preconditions. After all, these preconditions may vary widely from one geographical area to another. The report is based on first-hand experience of applications specialists at CCRS and the Canadian Ice Service (CIS) as well as on findings that other researchers have published in the literature.

To summarise our assessments, we have rated the anticipated effects of RADARSAT-2's most important technical enhancements on its potential for application to each of the fields studied as 'minor', 'moderate', or 'major'. Similarly, we have ranked the overall potential of both RADARSAT-1 and RADARSAT-2 for each of the applications as 'minimal', 'limited', 'moderate', or 'strong'. Comparison of the ratings for the overall application potential of RADARSAT-1 and –2 shows that the biggest improvement is projected to be associated with the crop type, crop condition and sea ice topography / structure fields (change in ratings from 'limited' to 'strong'). This is primarily the result of the enhancement of RADARSAT-2 in terms of polarization. Of the 29 remaining applications fields, the DEM polarimetry field is one that cannot currently be attended to with data from RADARSAT-1. The potential of RADARSAT-2 for this particular application is rated as 'limited' because of the minimal flexibility in terms of viewing geometry and the fact that the elevation information is limited to

the azimuth direction. For 18 out of the 32 fields considered we predict that the introduction of RADARSAT-2 will result in a modest increase in application potential. Going from RADARSAT-1 to RADARSAT-2 the potentials associated with these applications are ranked one category higher. The RADARSAT-2 features that instigate these changes in application potential may differ from one application to another. For 10 fields we foresee no increase in application potential. Among these are the applications concerned with DEM stereoscopy and floods, that is, applications for which the potential of RADARSAT-1 data products is already ranked as 'strong'. For the DEM interferometry and hurricanes fields the application potential stalls at the 'moderate' rating because of restraints imposed by atmospheric conditions and swath width, respectively. The orbital characteristics of RADARSAT-1 and RADARSAT-2 make that the application potential for the waves field halts at the 'limited' rating. Generally speaking, the information requirements of the five remaining applications can only be better satisfied by low- or multi-frequency SAR systems (e.g. forest type, forest biomass, sea ice type) or by optical remote sensing systems (e.g. oil spills, lithology).

Consistent with the objectives, the recommendations for applications research and development (R&D) focus on the new RADARSAT-2 data products. Outstanding R&D issues that relate to the application of current SAR satellite data can be expected to carry forward into the RADARSAT-2 era. The most important recommendations arising from the study read as follows:

- R&D in the context of RADARSAT-2 should focus on alleviating the lack of understanding with regard to the relationship between the image information content and the polarization of the radar signal.
- The primary R&D challenge lies in the extraction and application of the information as contained in the data acquired in the Quad Polarization image mode.
- R&D to prepare for the exploitation of RADARSAT-2's extended polarization capabilities should focus on application fields that hold the most promise for operational use of the relevant products.
- Successful application of the new high-resolution RADARSAT-2 image products does not require major research efforts at this time. Existing techniques for information extraction are expected to be applicable to these data products without further ado.
- The airborne Convair-580 SAR system is the sensor of choice for the acquisition of RADARSAT-2 type radar data in Canada.
- Data from the Envisat-1 ASAR system (launch October 2001) will make a valuable basis for applications R&D in preparation for RADARSAT-2.
- Progress in R&D is likely to advance our knowledge and may therefore call for the adjustment of the presented preliminary assessment regarding the application potential of RADARSAT-2.
- The application potential of products in which RADARSAT-2 data are fused with other data sources, both in-situ and remote, should be considered in subsequent assessments.

# Preface

The Canada Centre for Remote Sensing (CCRS) in partnership with the Canadian Ice Service (CIS) compiled this report in the framework of the RADARSAT-2 Applications Development Programme. This programme aims to prepare the remote sensing community for the application of data products from Canada's second radar satellite which is scheduled for launch in 2003. While led by the Canada Centre for Remote Sensing, the programme is financed by the Canadian Space Agency with Canadian Space Plan funds.

The report is based on first-hand experience of CCRS and CIS applications specialists as well as on findings that other researchers have published in the literature. The editors wish to acknowledge the technical contributions of the following colleagues:

| | |
|---|---|
| Paul Budkewitsch | Sections 3.5.2, 3.5.3 |
| Dean Flett | Sections 3.8.1, 3.8.2, 3.8.3, 3.8.4 |
| Laurence Gray | Sections 3.2.1, 3.8.5 |
| Robert Hawkins | Appendix I |
| Robert Landry | Sections 3.4.1, 3.4.2, 3.4.3, 3.4.4 |
| Tom Lukowski | Sections 3.3.5 |
| Heather McNairn | Sections 3.1.1, 3.1.2, 3.1.3 |
| Terry Pultz | Sections 3.3.1, 3.6.1, 3.6.2, 3.6.3 |
| Vern Singhroy | Sections 3.3.2, 3.5.1 |
| Jennifer Sokol | Sections 3.3.1, 3.6.1, 3.6.2, 3.6.3 |
| Thierry Toutin | Sections 3.2.2, 3.2.3, 3.2.4 |
| Ridha Touzi | Sections 3.4.1, 3.7.2 |
| Paris Vachon | Sections 3.3.3, 3.7.1, 3.7.2, 3.7.3, 3.7.4 |
| Joost van der Sanden | Sections 3.3.4, 3.7.5 |

Tom Lukowski's critical review of Chapter 2 and Paris Vachon's suggestions regarding the keys for the summarising tables in Section 3.9 were also much appreciated. Julie Allard of the CCRS Training and Technology Transfer Section is acknowledged for the design of the front cover.

Lastly, the editors would like to encourage the readers of this report to inform them of their questions and comments by sending an email to one of the following two addresses: Joost.van_der_Sanden@ccrs.nrcan.gc.ca or Shannon.Ross@ccrs.nrcan.gc.ca.

BLANK PAGE

# Contents

# List of Tables

BLANK PAGE

# List of Figures

# List of Abbreviations

| Abbreviation | Description |
|---|---|
| ADRO | Applications Development and Research Opportunity |
| ASAR | Advanced Synthetic Aperture Radar |
| AVHRR | Advanced Very-High-Resolution Radiometer |
| CCRS | Canada Centre for Remote Sensing |
| CSA | Canadian Space Agency |
| DEM | Digital Elevation Model |
| EEZ | Exclusive Economic Zone |
| ELT | Emergency Locator Transmitter |
| ENVISAT-1 | First Environmental Satellite |
| ERS | European Remote Sensing Satellite |
| GOES | Geostationary Operational Environment Satellites |
| GPS | Global Positioning System |
| HH | Horizontal transmit – Horizontal receive polarization |
| HV | Horizontal transmit – Vertical receive polarization |
| InSAR | Interferometric SAR |
| JERS-1 | Japanese Earth Resources Satellite |
| JPL | Jet Propulsion Laboratoty |
| SAR | Synthetic Aperture Radar |
| SWE | Snow Water Equivalent |
| LL | Left-hand circular transmit – Left-hand circular receive polarization |
| LR | Left-hand circular transmit – Right-hand circular receive polarization |
| MABL | Marine Atmospheric Boundary Layer |
| MDA | MacDonald, Dettwiler, and Associates |
| MODEX | Moving Object Detection Experiment |
| MTI | Moving Target Indication |
| NASA | National Aeronautics and Space Administration |
| NOAA | National Oceanic and Atmospheric Administration |
| QP | Quad Polarization (full polarimetric) |
| RAR MTF | Real Aperture Radar Modulation Transfer Function |
| RL | Right-hand circular transmit – Left-hand circular receive polarization |
| RR | Right-hand circular transmit – Right-hand circular receive polarization |
| SIR-C | Shuttle Imaging Radar C |
| SDP | Selective Dual Polarization |
| SSP | Selective Single Polarization |
| VH | Vertical transmit – Horizontal receive polarization |
| VV | Vertical transmit – Vertical receive polarization |

BLANK PAGE

# 1 Introduction

RADARSAT-2, Canada's second Earth observation satellite is being implemented through a unique co-operation between the Canadian Space Agency (CSA) and MacDonald Dettwiler Associates Ltd (MDA) of Richmond, BC. While providing data continuity to RADARSAT-1 users, RADARSAT-2 will contain a series of technical enhancements that augment its imaging capabilities. The Government of Canada and MDA will invest $400 million and $90 million respectively for the development of the satellite. Following the launch in 2003, RADARSAT-2 will be owned, operated and commercialised by MDA. Canada's investment will be recovered through the supply of data to government agencies during the mission lifetime. Canadian businesses other than MDA will benefit from the project through the awarding of subcontracts for the satellite's development and through the sales of RADARSAT-2 derived information products once the satellite becomes operational. The arrangement between CSA and MDA is seen as the first step in the transition of space-borne Earth observation from government to private sector.

Given the investment, it is important to all parties involved that the future RADARSAT-2 data can be applied to its full extent to meet information needs from users both within Canada and abroad. Preparation for RADARSAT-2 through applications research and development is therefore crucial to the overall success of the mission[1]. Here, the Canadian government must take a leadership role since industry and academia generally lack the required continuity in terms of financial and human resources. The CSA is well aware of this and has therefore decided to allocate Canadian Space Plan (CSP) funds to the RADARSAT-2 Applications Development Programme as proposed by the Canada Centre for Remote Sensing (CCRS).

Being led by CCRS and implemented in partnership with other federal agencies the RADARSAT-2 Applications Development Programme aims to:

- carry out research and development needed to devise algorithms and methods to extract information from RADARSAT-2 data in key applications areas
- support government utilization of RADARSAT-2 data by working with user agencies in the development and demonstration of new applications
- link to and support the Earth Observation Applications Development Program (EOADP), whose primary goal is the commercialization of remote sensing data, including those of RADARSAT-2.

The programme was started in 2000 and is expected to continue until the launch of RADARSAT-2. It will enable the Canadian government and, through her, the Canadian industry to build on the successes achieved with RADARSAT-1 and to expand Canada's leading role in the development of SAR-derived information products.

The present report constitutes one of the first results of the RADARSAT-2 Applications Development Programme. It describes the state-of–the-art with respect to the extraction of information from RADARSAT-2 type data in a large number of application fields. In doing so, it allows us to preview the application potential of RADARSAT-2 and to identify application fields and information extraction techniques that require further research and development. Logically, our emphasis will be on those data products that are not currently available from RADARSAT-1. Nevertheless, we will often take the application potential of RADARSAT-1 data products as a starting-point for our discussions. In terms of application potential, we will

[1] The most important text segments in this report have been highlighted for the benefit of the reader.

focus on an assessment of the data information content and thus pay little attention to other issues that may affect the promise of an application, e.g. economic or legal preconditions. After all, these preconditions may vary widely from one geographical area to another. The report is based on first-hand experience of applications specialists at CCRS and the Canadian Ice Service (CIS) as well as on findings that other researchers have published in the literature.

Following this introduction, Chapter 2 will provide some general information with respect to the RADARSAT-2 satellite and highlight certain technical enhancements that are likely to have an important effect on the applicability of its data. Next, in Chapter 3, we review the results of relevant application studies and draw on these to assess the applications potential of RADARSAT-2 data in the fields of agriculture, cartography, disaster management, forestry, geology, hydrology, oceans, and sea and land ice. The report concludes with recommendations for further applications research and development in Chapter 4.

# 2 New Capabilities of RADARSAT-2

RADARSAT-2 will provide all imaging modes of the current RADARSAT-1 satellite, as well as some new modes that incorporate significant innovations and improvements. Hence, the satellite will offer data continuity to RADARSAT-1 users and new data that will support development of new applications and refinement of existing ones. Scheduled for launch in 2003, the satellite is specified to be active for a minimum of 7 years following commissioning. Similar to the Synthetic Aperture Radar (SAR) system onboard RADARSAT-1, the RADARSAT-2 SAR sensor will image in C-band. However, the operating frequencies for RADARSAT-1 and RADARSAT-2 are slightly different, i.e. 5.3 GHz and 5.405 GHz respectively. This change in operating frequency was dictated by a recent decision by the Radio Regulations Board of the International Telecommunication Union to designate the 5.3 GHz channel for use in telecommunications. Unfortunately, it will prohibit the use of RADARSAT-1 and RADARSAT-2 in tandem mode for the purpose of repeat pass interferometry. However, there are plans to launch a third satellite, i.e. RADARSAT-3, about two years after the launch of RADARSAT-2 and operate the two satellites in tandem for topographic mapping in a so-called 'bistatic' interferometry mode. More details on this exciting plan can be found in Section 3.2.1 of this text.

RADARSAT-2 will be the most advanced civilian SAR satellite ever launched. Table 2-1 lists some of its general specifications and selected characteristics of both the SAR sensor and the orbit. A graphical representation of the RADARSAT-2 imaging modes is given in Figure 2-1. RADARSAT-2 and RADARSAT-1 will be offset in time, but otherwise maintain the same orbit characteristics. Operating in a sun-synchronous orbit, the satellite will pass over the same point on the earth at the same local sun time and at fixed intervals (24 days).

**Table 2-1** Selected specifications of RADARSAT-2 (CSA, 2001; MDA, 2001).

| | |
|---|---|
| **General specifications** | |
| Expected launch date | April 2003 |
| Mission life | 7 years after commissioning |
| **SAR characteristics** | |
| Centre frequency | 5.405 GHz (C-band) |
| Bandwidth | 100 MHz |
| Polarization | HH, HV, VH, VV |
| Cross polarization isolation | < -20 dB |
| Aperture length | 15 m |
| Aperture width | 1.37 m |
| Nominal spatial resolution | 3 - 100 m |
| Nominal swath width | 20 – 500 km |
| Nominal incidence angle | 10° - 60° |
| Look direction | right or left |
| Imaging modes | 11 |
| **Orbit characteristics** | |
| Altitude (average) | 798 km |
| Inclination | 98.6° |
| Sun-synchronous | 14 orbits per day |
| Repeat cycle | 24 days |

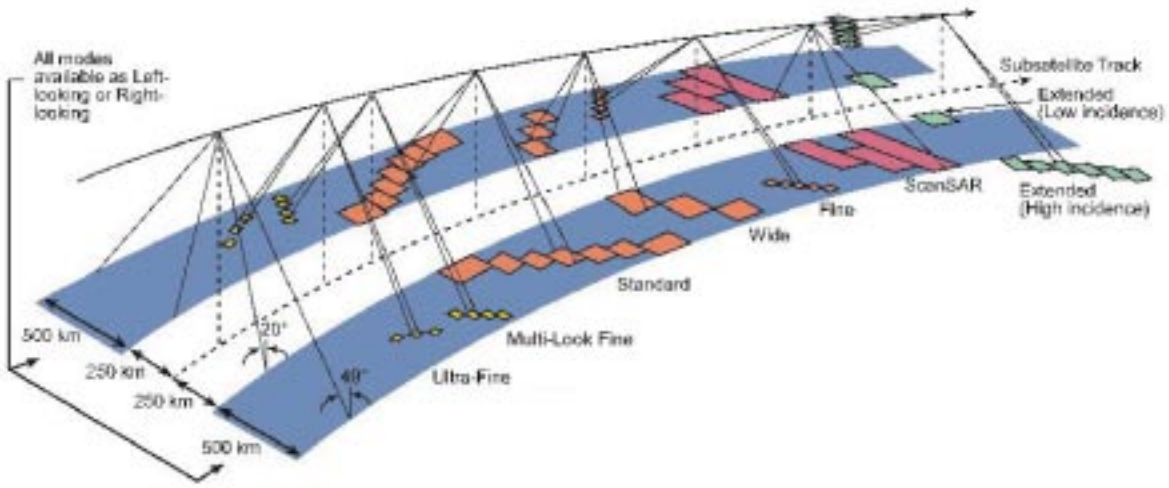


**Figure 2-1** RADARSAT-2 imaging modes (After CSA, 2001).

The 98.6º inclination angle will enable the satellite to provide frequent coverage of polar regions. Thanks to a series of technical enhancements RADARSAT-2 will embody an expansion to the imaging capabilities of RADARSAT-1. Technical improvements that relate to look direction, spatial resolution, polarization, orbit control and moving target indication will be discussed in sections 2.1 through 2.6. Examples of other innovative features are: faster beam mode switching, yaw steering to maintain the antenna beam axis close to the zero Doppler line, higher downlink power density, and onboard solid-state recorders. These features will improve the availability, quality, and retrieval of the image data. Additional information regarding the specifications of RADARSAT-2 may be found at the websites of MacDonald, Dettwiler, and Associates (MDA) (http://radarsat.mda.ca/) and the Canadian Space Agency (CSA) (http://space.gc.ca/csa_sectors/earth_environment/radarsat2/rad_inf/default.asp).

## 2.1 Selective Look Direction

Whereas RADARSAT-1 is a solely right-looking system, RADARSAT-2 will be outfitted with an antenna that can be steered electronically to acquire images to either the right or the left of the sub-satellite track (see Figure 2-1). The switch from one look direction to the other is specified to take less than 10 minutes, that is, about one tenth of the time required to complete one full orbit. Although the look direction switching is an operational feature, the right-looking configuration is regarded as the default mode of operation. Hence, it is expected that about 75% of the imaging will be performed in this particular mode. The left-looking mode will be deployed on occasion; primarily to meet data requirements associated with Antarctic mapping and emergency situations (CSA, 2001).

The capability to image on either side of the sub-satellite track will shorten the response time (on average) and increase the revisit frequency in all but the most northerly regions on earth. Regions located above ca. 79º North will not benefit from the selective look direction capability because they will go unobserved in the left-looking configuration. On the other hand, the left-looking configuration will enable regular imaging of southerly regions that are not routinely covered by RADARSAT-1, e.g. Antarctica. Enhancements in terms of response

**Table 2.2-1** RADARSAT-2 imaging mode specifications; imaging modes not available on RADARSAT-1 are shown in a bold typeface (MDA, 2001).

| Imaging mode | Nominal incidence angle (degrees) | Nominal swath width (km) | Nominal resolution (Gr Rg x Az) (m) | Nominal number of looks (Rg x Az) | Polarization mode [1)] |
|---|---|---|---|---|---|
| Standard | 20 - 49 | 100 | 25 x 28 | 1 x 4 | SSP or SDP |
| Wide | 20 - 45 | 150 | 25 x 28 | 1 x 4 | SSP or SDP |
| Low Incidence | 10 - 23 | 170 | 40 x 28 | 1 x 4 | SSP or SDP |
| High Incidence | 50 - 60 | 70 | 20 x 28 | 1 x 4 | SSP or SDP |
| Fine | 37 - 49 | 50 | 10 x 9 | 1 x 1 | SSP or SDP |
| ScanSAR Wide | 20 - 49 | 500 | 100 x 100 | 4 x 2 | SSP or SDP |
| ScanSAR Narrow | 20 - 46 | 300 | 50 x 50 | 2 x 2 | SSP or SDP |
| **Multi-Look Fine** | 30 - 50 | 50 | 11 x 9 | 2 x 2 | SSP |
| **Ultra-Fine** | 30 - 40 | 20 | 3 x 3 | 1 x 1 | SSP |
| **Standard Quad Polarization** | 20 - 41 | 25 | 25 x 28 | 1 x 4 | QP |
| **Fine Quad Polarization** | 30 - 41 | 25 | 11 x 9 | 1 x 1 | QP |

1) SSP: Selective Single Polarization; HH or HV or VV or VH acquired
SDP: Selective Dual Polarization; HH + HV or VV + VH acquired
QP: Quad Polarization; HH + HV + VV + VH acquired (full polarimetric)

and revisit times will be particularly valuable to time-dependent disaster management applications.

## 2.2 Spatial Resolution

Table 2.2-1 lists the imaging modes that will be available on RADARSAT-2 together with their specifications in terms of nominal incidence angles, swath widths, spatial resolutions, numbers of looks for detected products, and polarizations. Imaging modes that are not currently available on RADARSAT-1 are shown in a bold typeface. In this section we will focus on the spatial resolutions offered, while in section 2.3 we will discuss the available polarizations.

While the highest spatial (ground) resolution offered by RADARSAT-1 is nominally 10 m by 9 m (Fine beam mode), RADARSAT-2 will be capable of acquiring images with spatial (ground) resolutions as high as 3 m by 3 m (Ultra-Fine beam modes). As such, RADARSAT-2 will provide the highest spatial resolution commercially available in spaceborne SAR data. Figure 2.2-1 shows a simulated Ultra-Fine mode image and a RADARSAT-1 Fine mode image of Ottawa, Canada. The data used to generate the simulation were acquired by the airborne Convair-580 SAR system (Please refer to CCRS (2001) for details). The difference in the spatial information content of the two images is evident. Due to technical limitations, very high spatial resolutions can only be offered at the expense of swath width, number of looks and/or polarization. Hence, the images acquired in the Ultra-Fine beam modes will cover a nominal swath no more than 20 km wide and be single look as well as single polarization.

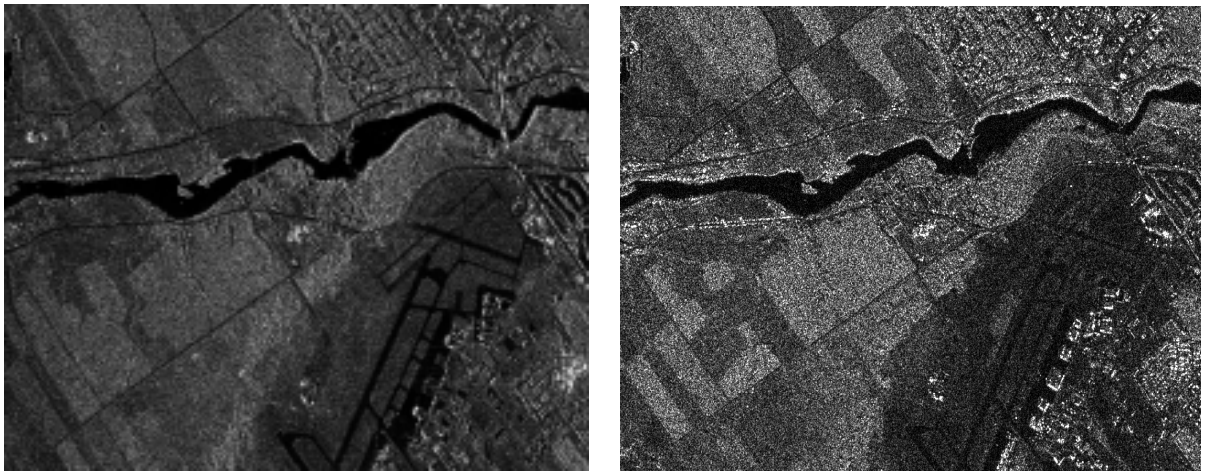

(a) (b)

**Figure 2.2-1 (a-b)** High resolution C-band HH radar images of Ottawa, Ontario (**a**) RADARSAT-2 Ultra-Fine mode simulation (**b**) RADARSAT-1 Fine mode image.

The new Ulltra-Fine beam modes of RADARSAT-2 can be expected to be particularly useful for applications such as vessel tracking / identification, iceberg tracking, digital elevation model (DEM) generation, and cartographic feature extraction.

## 2.3 Polarization

As shown in Table 2.2-1 RADARSAT-2 will have the capability to operate in three different polarization modes. Depending on the beam, images are acquired in the Selective Single Polarization (SSP), the Selective Dual Polarization (SDP) or the Quad Polarization (QP) mode.

Data acquisition in the SSP mode provides radar images that comprise a single channel the polarization of which is HH (Horizontal transmit – Horizontal receive) or HV (Horizontal transmit – Vertical receive) or VV (Vertical transmit – Vertical receive) or VH (Vertical transmit – Horizontal receive). In the SDP mode RADARSAT-2 will acquire images that comprise both a like- and cross-polarized radar channel, i.e. either an HH and HV channel or a VV and VH channel. Finally, in the QP (fully polarimetric) mode, the RADARSAT-2 SAR will operate as a polarimeter and measure the amplitude and phase of the backscattered wave for the four available transmit and receive linear antenna polarization combinations (HH, HV, VV, VH). In combination these measurements make it possible to determine the backscatter for any possible transmit and receive polarization combination.

The polarization capabilities of RADARSAT-2 are much superior to those of RADARSAT-1 since the latter only images in one specific polarization, i.e. HH. Although the Envisat-1 satellite is foreseen to image in SSP and SDP like modes as of late 2001, RADARSAT-2 will be the first civilian satellite to acquire fully polarimetric radar data.

It is well known that the polarization of the incident radar waves and the structural characteristics of features illuminated govern the polarization of the backscattered radar waves. Consequently, the advanced polarization capabilities of RADARSAT-2 can be

expected to facilitate the discrimination of features observed. This, in turn, will enhance the overall application potential of RADARSAT-2 data considerably.

## 2.4 Orbit Control

Unlike RADARSAT-1, RADARSAT-2 will be equipped with onboard GPS receivers and star-trackers. These devices will augment the knowledge about and hence facilitate the control of the satellite's orbit and attitude. Applications will benefit from these enhancements because they ensure a consistently high geometric and radiometric image quality.

The spacecraft orbit control system is specified to maintain ground track repeatability to within at least ± 5 km at any point in the orbit with a goal of ± 1km at any point in the orbit. The orbital position of the spacecraft is specified to be known within 20 m (1 sigma on each axis) in real-time and within 15 m (3 sigma on each axis) after processing of the available satellite position data. This will translate in an image product absolute scene location without ground control points of < 300 m (3 sigma) at down-link time and < 100 m (3 sigma) without ground control points after processing (MDA, 2001). Improved repeat coverage and georeferencing of data will be of benefit to applications that involve long-term monitoring, in particular. Applications that are based on repeat-pass SAR interferometry will gain from more reliable knowledge about the satellite's orbital position since this improves the accuracy with which baselines can be computed.

## 2.5 Moving Target Indication

RADARSAT-2 will contain an experimental moving target indication (MTI) capability known as the Moving Object Detection Experiment (MODEX). MODEX makes use of the fact that the RADARSAT-2 design allows two wings of the SAR antenna to be used independently with two separate receivers. By appropriate processing of the echo data received in this dual-receive mode of operation, objects with non-zero radial velocities can be detected and their radial velocities can be estimated.

Thompson and Livingstone (2000) assess the MTI performance of RADARSAT-2 by using the along-track interferometry processing technique. Their results indicate that reliable detection and estimation of velocities of approach / recession on the order of 6 m $s^{-1}$ should be possible for targets with a radar cross-section of 12 $m^2$ in a clutter background of –13 dB Sigma nought. The MODEX data products will not be commercially available since the MTI capability is experimental in nature.

BLANK PAGE

# 3 Anticipated Applications Potential

In this chapter we address how and why the new capabilities of RADARSAT-2 are expected to enhance the potential of its data for applications in the fields of agriculture, cartography, disaster management, forestry, geology, hydrology, oceans, and sea and land ice. In evaluating the application potential of RADARSAT-2, the focus is on the information content of the images and not on, for example, the economic viability of the use of the images in a particular application. The assessments are based on results of our ongoing applications development work and on results that have been published in literature by other researchers. The applications potential as demonstrated in connection with RADARSAT-1 image products will often be used as a starting-point for our discussions.

## 3.1 Agriculture

In agriculture, the condition of the soil and the crops changes diurnally, from day to day, and throughout the growing season. Agricultural targets also vary spatially with differences observed from field to field, as well as within individual fields. Consequently, mapping and monitoring soil and crop characteristics presents an enormous challenge. Imagery acquired from orbiting satellites offers a tremendous opportunity to track temporal changes in soil and crop conditions and to map crop characteristics over large areas.

Crop information includes both crop type and crop condition. In addition to identifying crop type and variety, identifying crop growth stage can be of value. Growth stage is important relative to moisture and temperature conditions during key crop development stages. Crop condition is loosely defined as the vigor or health of a crop. Crop condition is often related to crop productivity and yield, but this relationship is complex. Crop condition indicators can include biomass, height, leaf area, plant water content, chlorophyll and nitrogen, among others. These indicators must be linked to crop growth stage, and thus it is necessary to monitor these indicators over the entire growing season. As well, crop productivity and yield can be detrimentally affected by growth detractants. These detractants include infestations of weeds, fungus and insects, as well as damage that can result from major storm events.

Knowledge of crop acreage as well as crop condition throughout the growing season can be used in applications spanning from global to local scales. Crop information is important in the marketing of agricultural products both nationally and internationally, in validating crop claims, in enforcing agricultural practices, and in site specific crop management. Marketing agencies like the Canadian Wheat Board use acreage and predicted productivity to set marketing strategies for Canadian wheat. In the major rice growing regions of the world, predictions of rice production help marketing agencies and local governments to gain advantage in the import and export of this commodity. Suppliers and manufacturers of agricultural commodities, including seeds, fertilizers, herbicides and implements, benefit from knowledge of current crop acreages and farming practices, and trends in these practices. Crop insurance agencies require acreage estimates of crop damage, and a method to validate insurance claims. In countries with agricultural subsidies, crop information is used to verify subsidy claims. Concern over environmental contamination of surface and ground water from agricultural sources is growing. Monitoring and enforcing controls on agricultural practices requires a capability to map large agricultural regions repeatedly throughout the growing season. At the farm level, crop and soil information help producers manage their fields on a site specific scale. With this information producers can

plan the amount and spatial distribution of inputs such as fertilizers, herbicides and pesticides. If the information is provided in a timely fashion, the producer can take steps to mitigate fertility, water or infestation problems.

There is no easy solution to gathering crop information. The area coverages are often too large for ground surveys, particularly at the regional and national scales. When temporal information is required, as is the case for predicting crop productivity, ground surveys are equally prohibitive. In instances where regional yield data are collected, as is the case in rice production in China, farmers are required to report acreage and production information. Remote sensing is an obvious tool to replace or verify this self-reporting approach. Many agricultural service providers offer crop scouting services. These scouts visit or "scout" client fields periodically throughout the growing season. Scouts watch for infestations of weeds, insects and fungus, and provide recommendations on treating detected infestations. These service providers also recommend fertility treatments. However, with the huge acreages involved, scouts rarely walk the entire field and only periodically re-visit any particular field. Satellite optical imagery like SPOT and IRS are now being used to supplement crop scouting by directing scouting activities to areas of the field where a problem is suspected.

Visible, infrared and microwave wavelengths are sensitive to very different soil and crop characteristics. Data from optical and radar sensors are thus complementary. Synthetic Aperture Radar (SAR) responds to the large scale crop structure (size, shape and orientation of leaves, stalks, and fruit) and the dielectric properties of the crop canopy. Crop structure and plant water content vary as a function of crop type, growth stage and crop condition. Reflectance in the visible-infrared spectral region depends primarily on the plant pigmentation and internal leaf structure.

With these sensitivities, information derived from satellite-based sensors has enormous potential for mapping and monitoring of soils and crops. However, Brown (2000) outlined barriers to the successful adoption of future remote sensing products and services in the agri-business community. The timely acquisition and distribution of remote sensing products and services was identified as one of these barriers. Clearly, the value of the information provided by remote sensing significantly diminishes over time, when producers are seeking real time mitigation of infestations and fertility problems. Although visible and infrared wavelengths are sensitive to changes in crop condition, timely acquisition of optical imagery can be problematic due to cloud cover. This suggests that if remote sensing is to be used in operational site specific crop monitoring, radar must be used to supplement acquisitions of optical imagery. Crop classification also depends on image acquisitions during key stages of crop growth development. McNairn *et al*. (2001a) reported poor crop classification results with SPOT imagery due to the late acquisition of the image in the growing season. However, no cloud-free optical imagery was available earlier in the season. Yield prediction also requires data throughout the season and thus acquisition of imagery must be assured. Acquisition of cloud-free optical imagery in temperate regions cannot be guaranteed and thus operational applications will not rely solely on optical sensors. In tropical and sub-tropical regions, SAR is very often the only option.

### 3.1.1 Crop type

The increased resolution of the RADARSAT-2 Ultra-Fine mode will not significantly improve the capability of SAR for crop type mapping. The resolution of the fine and standard modes is adequate for field-based information, in most regions of the world. Crop type information is

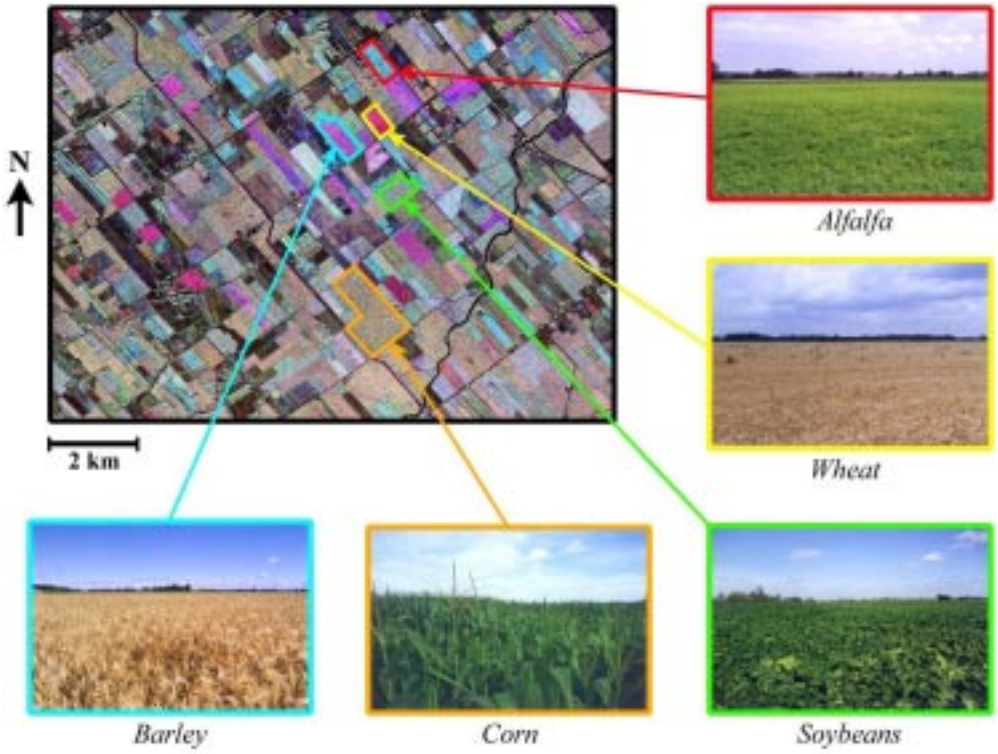


**Figure 3.1.1-1** Crop type classification with multi-polarized C-Band SAR. These airborne CV-580 data were acquired just south of Ottawa (Canada) on July 9, 1998. This composite includes the three linear polarizations displayed in red (HH), green (HV) and blue (VV). All five major crop types in this region are clearly identified using these three polarizations.

often required at a regional scale and these imaging modes provide a good compromise between resolution and swath coverage.

The single most important new capability of RADARSAT-2 will be the simultaneous acquisition of multiple polarizations. Scattering from a target is a function of the illuminating wave polarization. Agricultural crops that have linear features of length comparable to the incident wavelength tend to cause larger reflections when the polarization alignment agrees with their structural alignment (Raney, 1998). This is because the electric fields couple to the structure of the target. The polarization of the transmitted microwave (horizontal (H) or vertical (V)) also dictates which components of the vegetation and soil contribute to the total amount of energy scattered back to the SAR sensor. Vertically-polarized microwaves (V) couple with the predominant vertical structure of most vegetation and as a result, penetration of the signal through the canopy is reduced. VV-polarized radar returns thus provide good contrast among vegetation types that have different vertical canopy structures. Differences in this vertical structure that result from changes in the vegetation growth stage or the health of the vegetation may also be detected in VV-polarized images. At steep incidence angles, horizontally-polarized microwaves (H) tend to penetrate the canopy to a greater extent than vertically-polarized waves and hence HH images tend to provide more information about the underlying soil condition. However, the “coupling” of both soil and vegetation information in the total C-HH backscatter can make the extraction of information about the vegetation itself difficult. Cross-polarized radar returns (HV or VH) result from

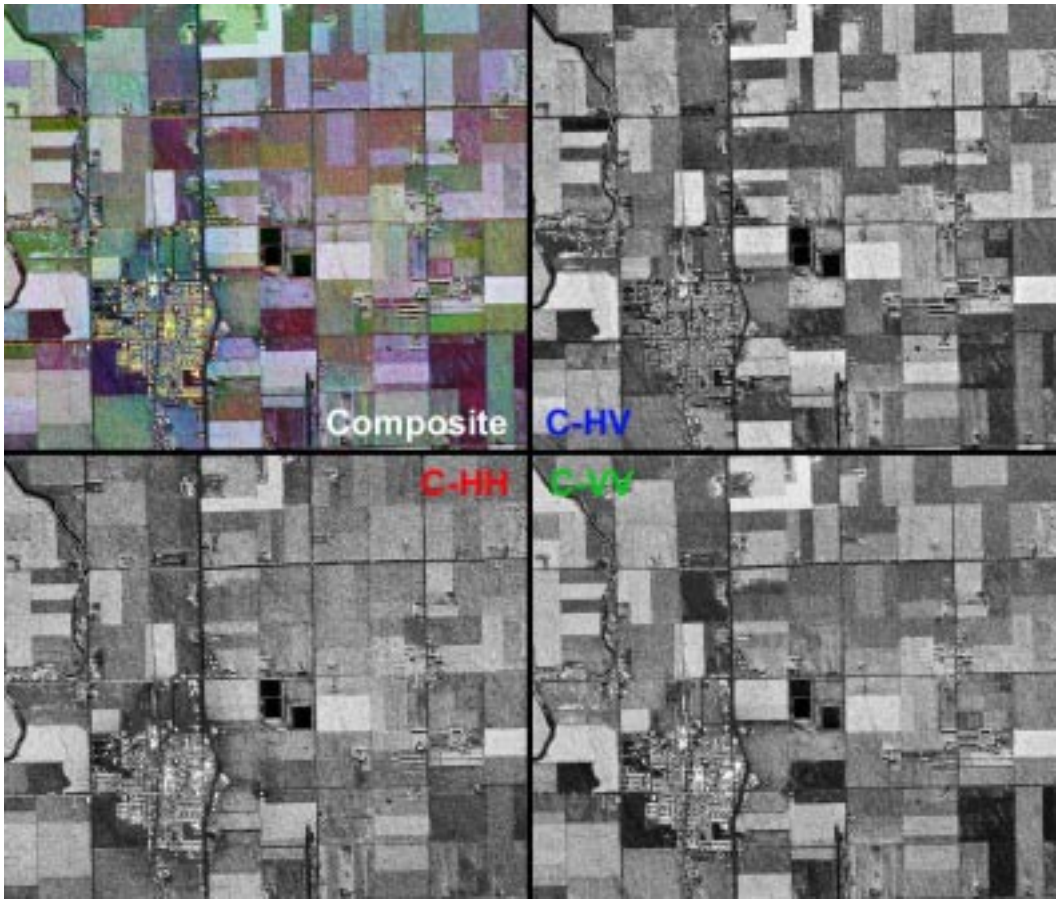


**Figure 3.1.1-2** Sensitivity of C-Band linear polarizations to different crop types. Of all three polarizations, the cross-polarization appears to be most sensitive to differences in crop type from field to field. However, each polarization provides some unique information and a three-band composite is required to separate all crop types. These data were acquired with the airborne CV-580 SAR over Altona, Manitoba (Canada) on July 26, 1995.

multiple reflections within the vegetation volume. C-HV and C-VH images are sensitive to crop structure within the total canopy volume and thus provide information that is complementary to HH and VV imagery.

SAR sensors that acquire imagery at a single transmit-receive polarization, like RADARSAT-1, provide one-dimensional data sets. Consequently, more than one date of imagery is usually required to provide meaningful crop information (McNairn *et al*., 2001a). Timing of acquisition is still important. The greatest success at separating crop types with RADARSAT-1 is achieved with imagery gathered during the period of seed development (McNairn *et al*., 2001a). In contrast, similar crop type information can be provided by a single date image, if the sensor acquires information at multiple polarizations (Figures 3.1.1-1 and 3.1.1-2) (McNairn *et al*., 2000a). From CV-580 airborne imagery acquired near Ottawa (Canada), classification results clearly demonstrated the advantage of multi-polarized data sets for crop type mapping (Table 3.1.1-1). The HH-HV-LL 3-polarization combination had the highest Kappa coefficient (0.92). However, the most significant conclusion is drawn from the relative classification accuracies of the multi-polarized and single polarization

**Table 3.1.1-1** Gaussian maximum-likelihood crop classification results based on multiple polarizations. These C-Band data were acquired over Ottawa (Canada) with the airborne CV-580 (incidence angles of 46º-57º) on July 9, 1998.

| | | | Percent correctly classified | | | | |
|---|---|---|---|---|---|---|---|
| **Polarization** | **Kappa** | **Var. Kappa** | **Overall** | **Alfalfa** | **Corn** | **Soybean** | **Grains** |
| HH, HV, LL | 0.9171 | 0.0012 | 94 | 90 | 95 | 96 | 93 |
| HH, HV, RR | 0.9008 | 0.0014 | 93 | 90 | 95 | 96 | 87 |
| HV, VV, RL | 0.8514 | 0.0020 | 90 | 90 | 97 | 78 | 87 |
| HH, RL, LL | 0.8496 | 0.0022 | 90 | 80 | 92 | 91 | 87 |
| HH, RR, RL | 0.8485 | 0.0022 | 90 | 80 | 95 | 91 | 80 |
| HV, RR, RL | 0.8309 | 0.0026 | 88 | 100 | 92 | 74 | 93 |
| HH, HV, VV | 0.8177 | 0.0027 | 87 | 90 | 82 | 91 | 93 |
| HH, VV, RR | 0.8145 | 0.0026 | 87 | 80 | 95 | 91 | 67 |
| HV, RL, LL | 0.8134 | 0.0028 | 87 | 100 | 92 | 70 | 93 |
| HH, HV, RL | 0.7997 | 0.0029 | 86 | 80 | 84 | 87 | 93 |
| HH, VV, LL | 0.7980 | 0.0027 | 86 | 70 | 95 | 91 | 67 |
| HH, VV, RL | 0.7976 | 0.0027 | 86 | 60 | 95 | 87 | 80 |
| HH, RR | 0.7827 | 0.0028 | 85 | 80 | 92 | 96 | 53 |
| HH, LL | 0.7491 | 0.0031 | 83 | 60 | 92 | 96 | 53 |
| HH, RR, LL | 0.7331 | 0.0033 | 81 | 70 | 89 | 91 | 53 |
| VV, RL, LL | 0.7299 | 0.0033 | 81 | 30 | 95 | 83 | 80 |
| VV, RR, RL | 0.7120 | 0.0034 | 80 | 20 | 95 | 83 | 80 |
| HH, HV | 0.6870 | 0.0041 | 78 | 80 | 71 | 78 | 93 |
| HV, VV, RR | 0.6155 | 0.0047 | 73 | 70 | 76 | 65 | 80 |
| HV, RL | 0.6071 | 0.0046 | 72 | 80 | 74 | 57 | 87 |
| HV, VV, LL | 0.6009 | 0.0048 | 72 | 70 | 74 | 65 | 80 |
| VV, RL | 0.5973 | 0.0036 | 72 | 20 | 95 | 83 | 33 |
| RR, RL, LL | 0.5855 | 0.0048 | 71 | 70 | 76 | 61 | 73 |
| HV, VV | 0.5822 | 0.0050 | 71 | 70 | 76 | 57 | 80 |
| HH, VV | 0.5086 | 0.0049 | 66 | 50 | 79 | 74 | 33 |
| RR, RL | 0.5070 | 0.0049 | 66 | 10 | 82 | 61 | 73 |
| RL, LL | 0.5070 | 0.0049 | 66 | 10 | 82 | 61 | 73 |
| HV, RR, LL | 0.4761 | 0.0053 | 63 | 80 | 66 | 35 | 87 |
| HV, RR | 0.4760 | 0.0057 | 64 | 70 | 71 | 35 | 87 |
| HV, LL | 0.4436 | 0.0059 | 62 | 70 | 68 | 30 | 87 |
| HH, RL | 0.3923 | 0.0059 | 57 | 50 | 55 | 48 | 80 |
| VV, RR, LL | 0.3681 | 0.0050 | 53 | 80 | 50 | 52 | 47 |
| VV, RR | 0.2929 | 0.0058 | 50 | 30 | 50 | 52 | 60 |
| VV, LL | 0.2716 | 0.0060 | 49 | 30 | 50 | 48 | 60 |
| HV | 0.2508 | 0.0056 | 45 | 30 | 26 | 61 | 80 |
| RR, LL | 0.2439 | 0.0054 | 45 | 70 | 45 | 43 | 33 |
| VV | 0.2317 | 0.0056 | 47 | 0 | 47 | 52 | 67 |
| RR | 0.2305 | 0.0055 | 47 | 0 | 50 | 52 | 60 |
| LL | 0.2252 | 0.0056 | 47 | 0 | 53 | 48 | 60 |
| RL | 0.2242 | 0.0054 | 45 | 0 | 47 | 52 | 60 |
| HH | 0.2127 | 0.0050 | 44 | 60 | 50 | 52 | 7 |

configurations. These results suggest that the choice of polarizations within the 3-band combination is less important. All three linear and all three circular polarizations appear in one of the top three band combinations. The values in Table 3.1.1-1 also indicate that the greatest difference in accuracy is observed when comparing the single and dual-polarization results. In comparing results using a single polarization, the highest Kappa coefficient was associated with C-HV. The cross-polarization did particularly well at separating small grain crops from other crops, relative to the other single polarizations.

The cross-polarization could be particularly interesting for general land cover applications. Several researchers have indicated that cross-polarizations are useful for differentiating vegetative surfaces from bare surfaces (Baronti *et al*., 1995; de Matthaeis *et al*., 1992) as well as for differentiating among vegetation canopies such as agricultural crops and forested areas (Lemoine *et al*., 1991). Cross-polarizations may also be less sensitive to the effects of row direction. Row direction effects refer to the direction of planting, tillage or harvesting relative to the look direction of the sensor. These effects are less pronounced at larger incidence angles, but can be significant at smaller angles. Row direction effects can cause a "bow-tie" effect within an individual field following harvesting or tillage, or can cause

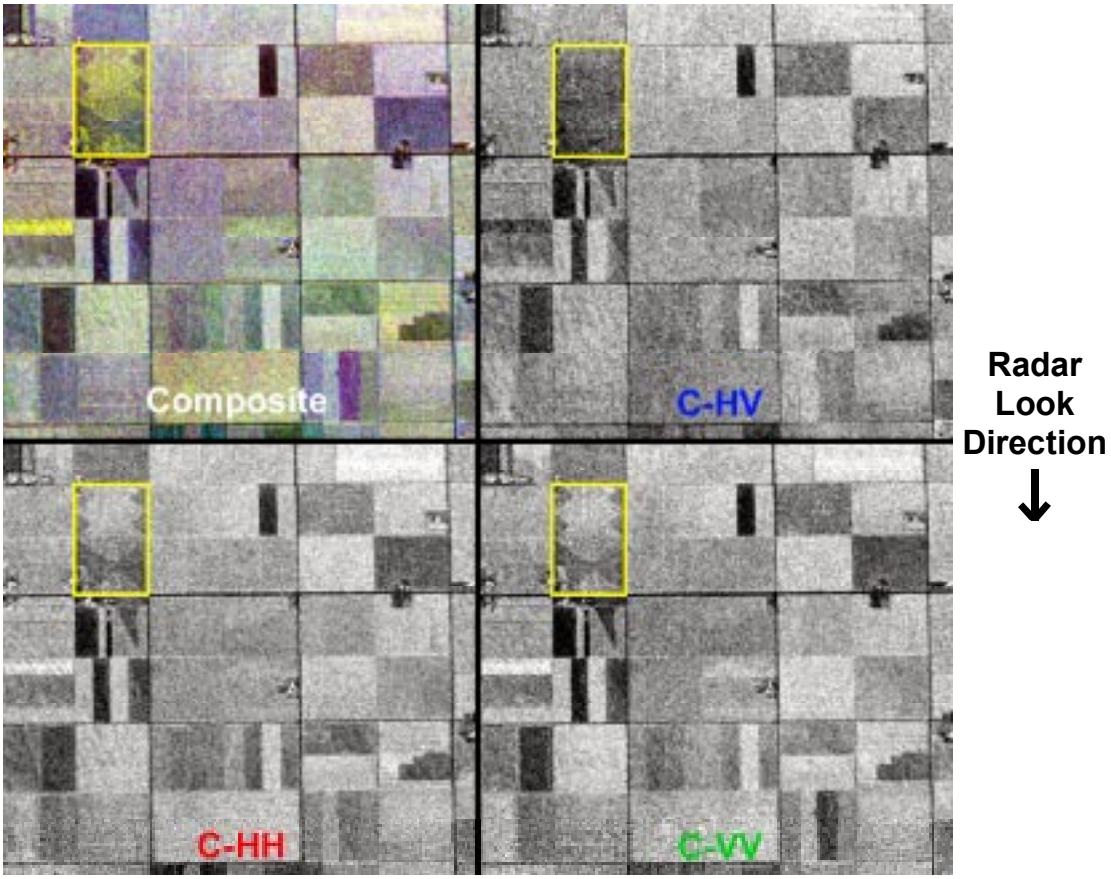


**Figure 3.1.1-3** Row direction effects as a function of polarization. In this image, both the C-HH and C-VV polarizations are sensitive to the direction in which this crop was harvested. Where the row direction if perpendicular to the radar look direction, backscatter is significantly higher. In the HV polarization, the look direction effect is virtually eliminated. This image was acquired with the airborne JPL AIRSAR over Altona, Manitoba (Canada) on October 8, 1994.

significant backscatter differences between fields with the same crop type and crop condition. In Figure 3.1.1-3, this effect is visible in both the HH and VV polarizations. In these like-polarizations, backscatter is significantly higher when the row direction is perpendicular to the radar look direction. The effect disappears in the cross-polarization. This lack of sensitivity with the cross-polarization was quantitatively verified in McNairn *et al*. (2001b). These results suggest that the linear cross-polarization has an advantage over the linear like-polarizations, for operational mapping.

RADARSAT-2 will also have the capability of acquiring fully polarimetric data in some imaging modes. The importance of this additional polarimetric information is still unclear. Studies published in the open literature have not rigorously addressed the role of polarimetric data sets in agricultural applications. Most published studies have explored scattering mechanisms (single, double, diffuse) and have demonstrated the use of scattering parameters for general land cover classification (urban, wetland, bare soil, crops, forests etc.) (Evans *et al*., 1988; van Zyl, 1989; Hoekman *et al*., 1992; de Matthaeis *et al*., 1992). These classes can, however, be derived from multi-temporal RADARSAT-1 or multi-polarized SAR imagery. This review of the literature suggests that significant research is still required to understand the application potential of these complex data.

The Canada Centre for Remote Sensing (CCRS) has acquired three fully polarimetric CV-580 data sets at various Canadian agricultural sites, to study this capability. These campaigns include Ottawa (Ontario) in 1998, Clinton (Ontario) in 1999 and Indian Head (Saskatchewan) in 2000. Work to date has focussed on both the linear and circular polarizations. Further analysis will explore various polarimetric parameters including phase differences, power extrema, polarimetric signatures, pedestal height and the unpolarized component. However, since multiple polarizations (either linear or circular) are clearly adequate for crop type classification (Table 3.1.1-1), most of the analysis of these polarimetric parameters will deal with detecting and mapping crop condition. With respect to the circular polarizations, preliminary results suggest a potential advantage of applying these polarizations to crop type mapping. In Figure 3.1.1-4, field average sigma nought is plotted as a function of incidence angle, for corn fields at a similar growth stage. These plots indicate that although linear polarizations, and in particular C-HH, are quite sensitive to the effect of incidence angle, the circular cross-polarization (RL) configuration has a reduced sensitivity. Although these results must be further explored, this reduced sensitivity would be a significant advantage for crop monitoring where various beams must be combined.

There are a few publications that provide results from analysis of polarimetric data sets. These studies are limited, but do further our understanding of these data. Groot *et al*. (1992) generated information on the degree of polarization for various land cover classes (Table 3.1.1-2). Degree of polarization is a measure of how much the polarization of the wave backscattered by a distributed target varies from point to point within that target. These results demonstrated that smooth bare surfaces result in strongly polarized returns (degree of polarization close to 1). A mixture of scattering mechanisms or “diffuse” scattering (from thick vegetation canopies) will have almost completely unpolarized returns (d close to 0). Evans and Smith (1991) suggest that the degree of polarization could be used for vegetation discrimination. In research with Ku-Band, Hinds (1989) discovered that the degree of polarization varied as a function of crop type, growth stage and polarization. Cereal crops (wheat and barley) all exhibited unpolarization effects primarily for vertically oriented transmit polarizations with only minor unpolarization occurring for horizontally oriented states. The degree of polarization also varied through the growth cycle of crops, decreasing as the crop canopy developed and increasing as the crops matured and dried out. For crops

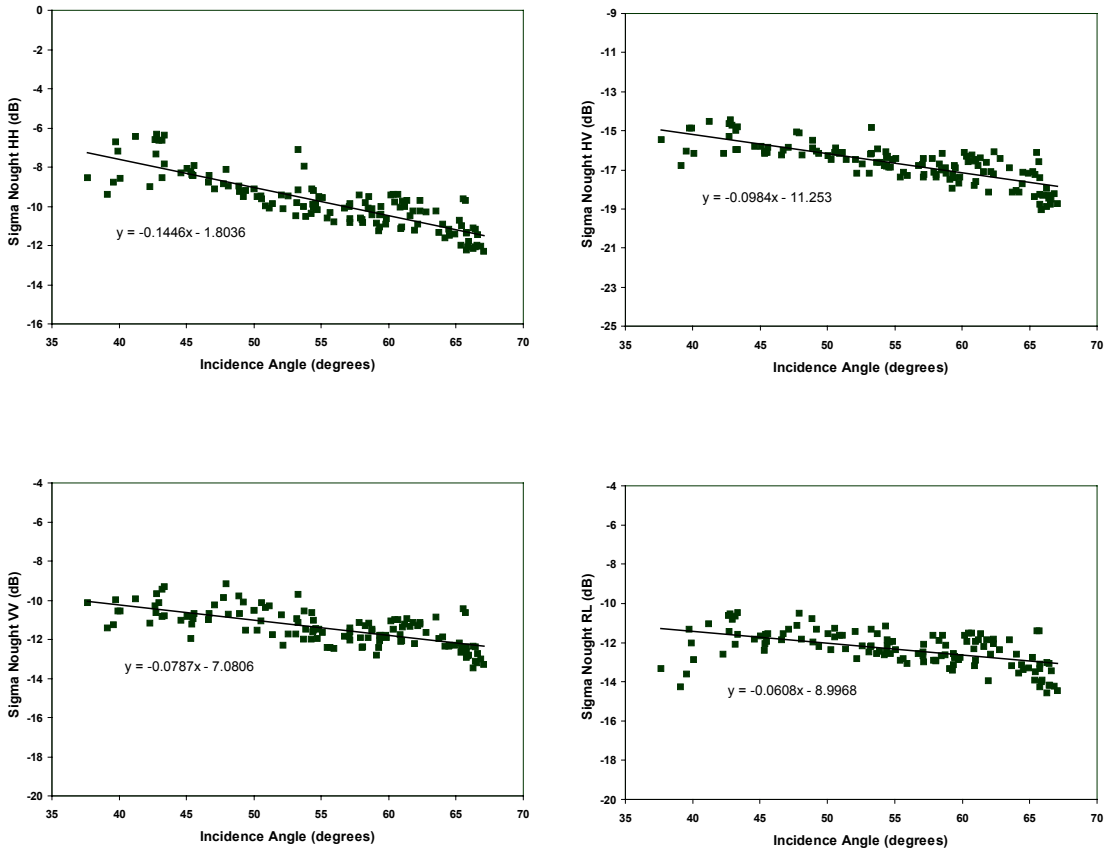


**Figure 3.1.1-4** Backscatter as a function of incidence angle. In these graphs, backscatter from a number of cornfields is plotted as a function of incidence angle, for each linear polarization as well as the RL circular polarization. As demonstrated in this figure, RL is least sensitive to variations in incidence angle.

with a random, chaotic structure like canola the unpolarization signature was much less sensitive to the orientation of the transmit waves.

Groot *et al* (1992) also examined land cover classifications based on the minimum and maximum linear polarization orientations. Signatures with a minimum at 90$^{o}$ were mostly generated by crops like wheat with elongated stems that couple with the vertically transmitted waves. There was no preference for orientation angle from canopies with randomly oriented leaves such as potato and sugar beet that scatter the radiation independent of orientation angle. Signatures with a maximum at 90 $^{o}$ were typical of bare soil surfaces that are flat relative to the wavelength. Polarimetric plots generated from SIR-C data demonstrate these differences in minimum and maximum backscatter as a function of polarization, for bare fields and standing senesced crops (Figure 3.1.1-5) (McNairn *et al.*, 1998). These plots clearly indicate that the scattering mechanisms for these surfaces are very different. As well, the pedestal height is significantly higher for fields with vegetation, even though in this particular example, the vegetation is senesced. Pedestal height is low (around 0.20) for bare fields. The pedestal height, as well as the shape of the plot, is wavelength dependent. Groot *et al*. (1992) reported that signatures that are not symmetric and that have a minimum that does not coincide with an orientation angle of 90$^{o}$ were

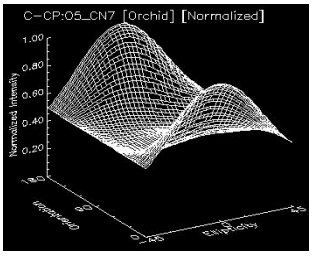


a) Standing Senesced Corn (October 5) C-Band

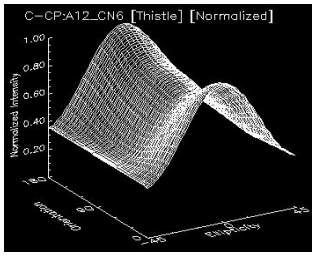


b) Corn Residue (April 12) C-Band

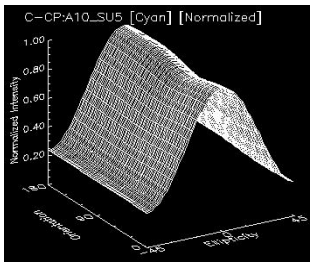


c) Bare Soil (April 10) C-Band

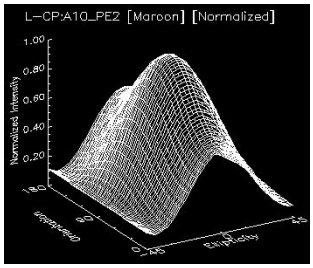


d) Bare Soil (April 10) L-Band

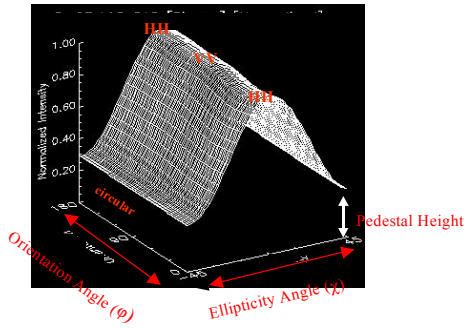


e) An example polarization plot indicating the location of the linear co-polarizations and the pedestal height

**Figure 3.1.1-5 (a-e)** Co-polarization plots generated for bare soil, standing senesced vegetation and crop residue. In these plots, the maximum backscatter response from fields with senesced vegetation is at the HH-polarization. For the bare field, C-Band backscatter response is about equal for all linear polarizations. However, at L-Band the maximum response is at VV, suggesting that this bare field appears smooth relative to the L-Band wavelength. Notice as well the difference in the pedestal height among the various land covers. These data are from SIR-C and were acquired over Altona, Manitoba (Canada) in 1994.

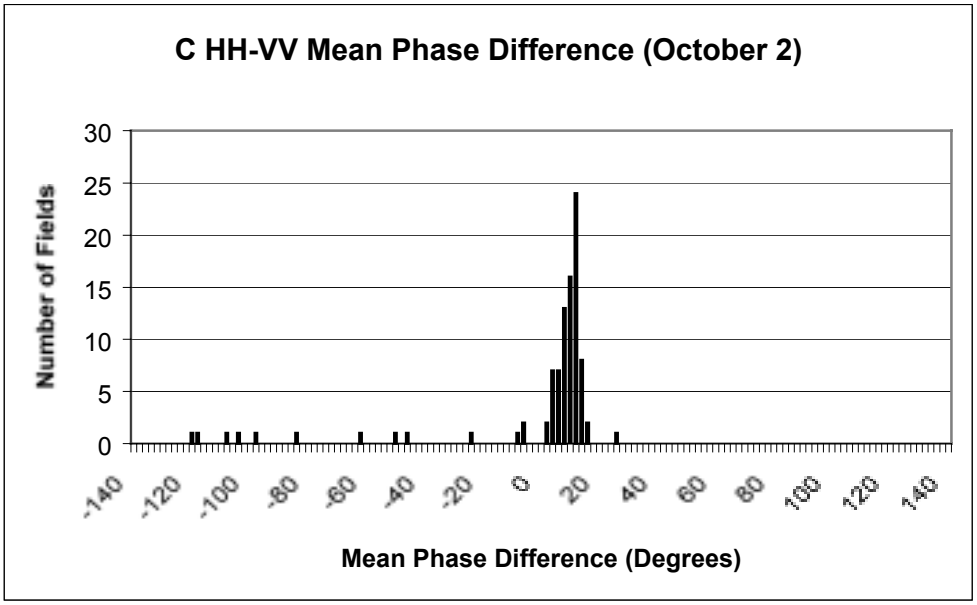


**Figure 3.1.1-6** A frequency distribution for field average co-polarized phase differences. In general, bare fields have average co-polarized phase differences close to zero degrees. Only fields with standing senesced vegetation have significant co-polarized phase differences. These data are from SIR-C and were acquired over Altona, Manitoba (Canada) in 1994.

recorded for crops with a non-random orientation caused for example, by prevailing winds where the crop stems are tilted. The minimum is then found at polarizations that are aligned with the tilted stems.

Co-polarized phase differences originate from different electrical path lengths between the H and V polarized waves. Hoekman *et al* (1992) hypothesized that bare fields, stubble fields and senesced cereals should have a phase difference close to zero, green crops of intermediate height a small phase difference, while for thick canopies like corn, phase differences would be appreciable. This hypothesis was supported by work by Wang and Mo (1990) and Ulaby *et al* (1987). Mean co-polarized phase differences for several agricultural fields are presented in Figure 3.1.1-6 (McNairn, 1999). In this example, bare fields without vegetation cover have mean co-polarized phase differences close to 0 ($0^o$ ± $20^o$). The fields that have mean phase differences greater than $40^o$ have a standing senesced corn crop. Ulaby *et al* (1987) also discovered that although mean phase difference may be equal, the standard deviations associated with phase differences can provide meaningful information. The information contained in the phase difference distribution was confirmed by McNairn (1999). Some typical distribution plots are given in Figure 3.1.1-7

## C-BAND

**Fields With Low Residue (< 30%)**

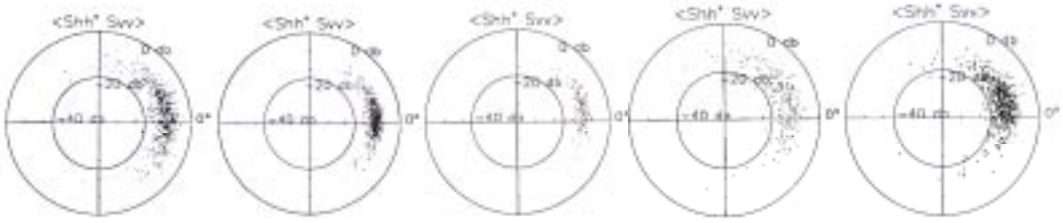

| | | | | | |
|---|---|---|---|---|---|
| **(a)** | Wheat/Barley | Wheat/Barley | Wheat/Barley | Lentil | Canola |
| **(b)** | 7.22° | 5.65° | 11.05° | 17.77° | 13.84° |
| **(c)** | 27.75° | 16.16° | 15.42° | 30.29° | 26.30° |

**Minimum Till and No-till Fields**

| | | | | | |
|---|---|---|---|---|---|
| **(a)** | Wheat/Barley | Wheat/Barley | Corn | Corn | Canola |
| **(b)** | 12.66° | 17.00° | 3.00° | 3.09° | 14.14° |
| **(c)** | 67.22° | 82.25° | 55.22° | 47.47° | 50.17° |

**Senesced Crops Before and After Harvest**

| | | | |
|---|---|---|---|
| **(a)** | Harvest Sunflowers | Standing Senesced Sunflowers | Standing Senesced Corn |
| **(b)** | 9.54° | -65.53° | -101.63° |
| **(c)** | 26.11° | 92.56° | 96.09° |

**(a) Residue type**
**(b) Field average co-polarized phase difference**
**(c) Standard deviation associated with co-polarized phase difference, on a field basis**

**Figure 3.1.1-7** Co-polarized phase difference distribution plots. These plots demonstrate the distribution of phase differences for individual fields. The accompanying labels provide the field average co-polarized phase distribution, as well as the standard deviation of the phase difference distribution. In general, standing senesced vegetation and no-till fields exhibit broader or noise-like distributions. Smoother surfaces have small phase differences and narrow distributions. These data are from SIR-C and were acquired over Altona, Manitoba (Canada) in 1994.

### 3.1.2 Crop condition

In contrast to field-based crop type mapping, RADARSAT-2's Ultra-Fine mode could prove interesting for within field zonal mapping of crop condition. Polarization diversity will also be very important for deriving condition information. Results to date clearly indicate that a single polarization is limited in terms of information content. However, the optimal polarization for mapping crop condition varies depending on the crop growth stage and crop type (Figure 3.1.2-1).

For crops with very significant biomass, the information on crop condition provided by C-band is limited due to signal saturation. McNairn *et al*. (2000a) reported that once a corn canopy reaches a height of about one metre, the SAR signal saturates. Signal saturation appears to be a problem for all the linear polarization (HH, VV, HV). The circular (RR, RL) polarizations may be less sensitive and this possibility must be further explored. Although saturation is problematic once corn canopies acquire significant biomass, information on the soil and corn conditions is still available early in the season. From the 1998 Ottawa data set, zonal patterns are visible in an early season SAR image and these zones can be easily classified (Figures 3.1.2-2 a,b). Although these patterns are present in all polarizations, the best contrast (greater than 3 dB) between zones of high and low backscatter is observed for the linear and circular cross-polarizations (HV and RL) (Figure 3.1.2-2 c). The growth patterns for this cornfield are clearly linked to underlying soil and field characteristics

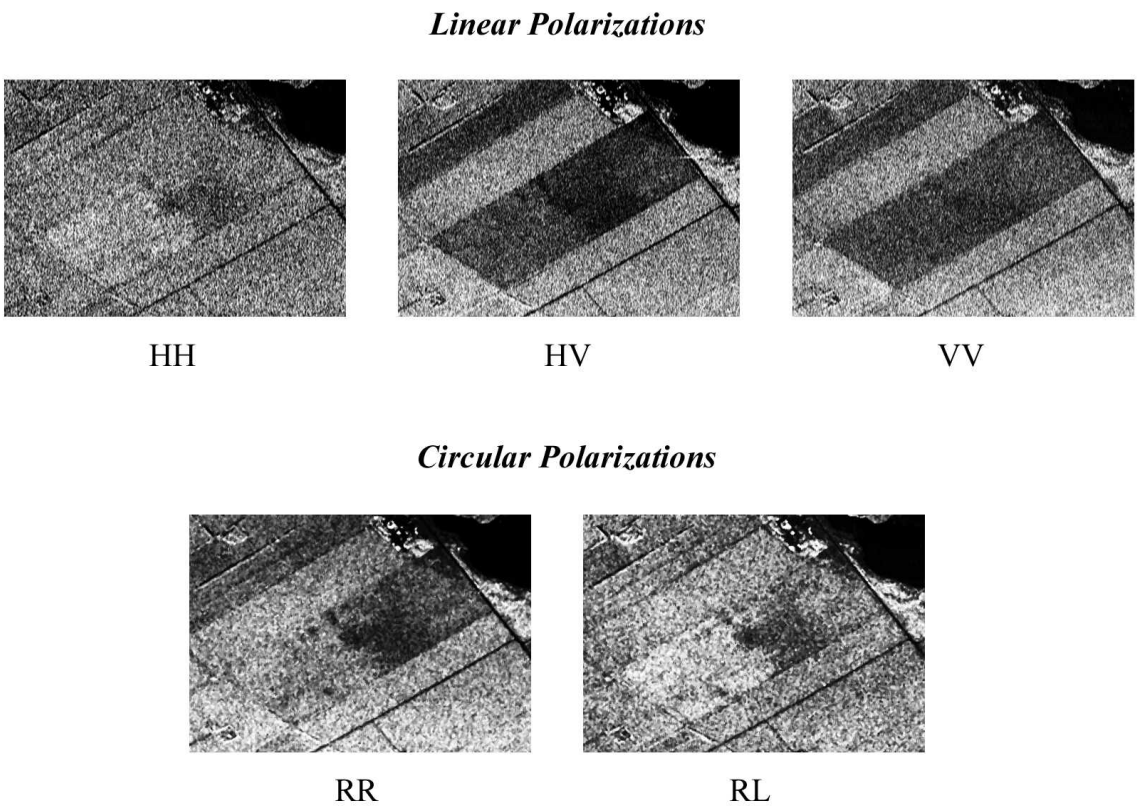


**Figure 3.1.2-1** Crop condition information provided by linear and circular polarizations. Each polarization provides different information on crop growth across this wheat field. Imagery was acquired with the CV-580 south of Ottawa (Canada) on July 9, 1998.

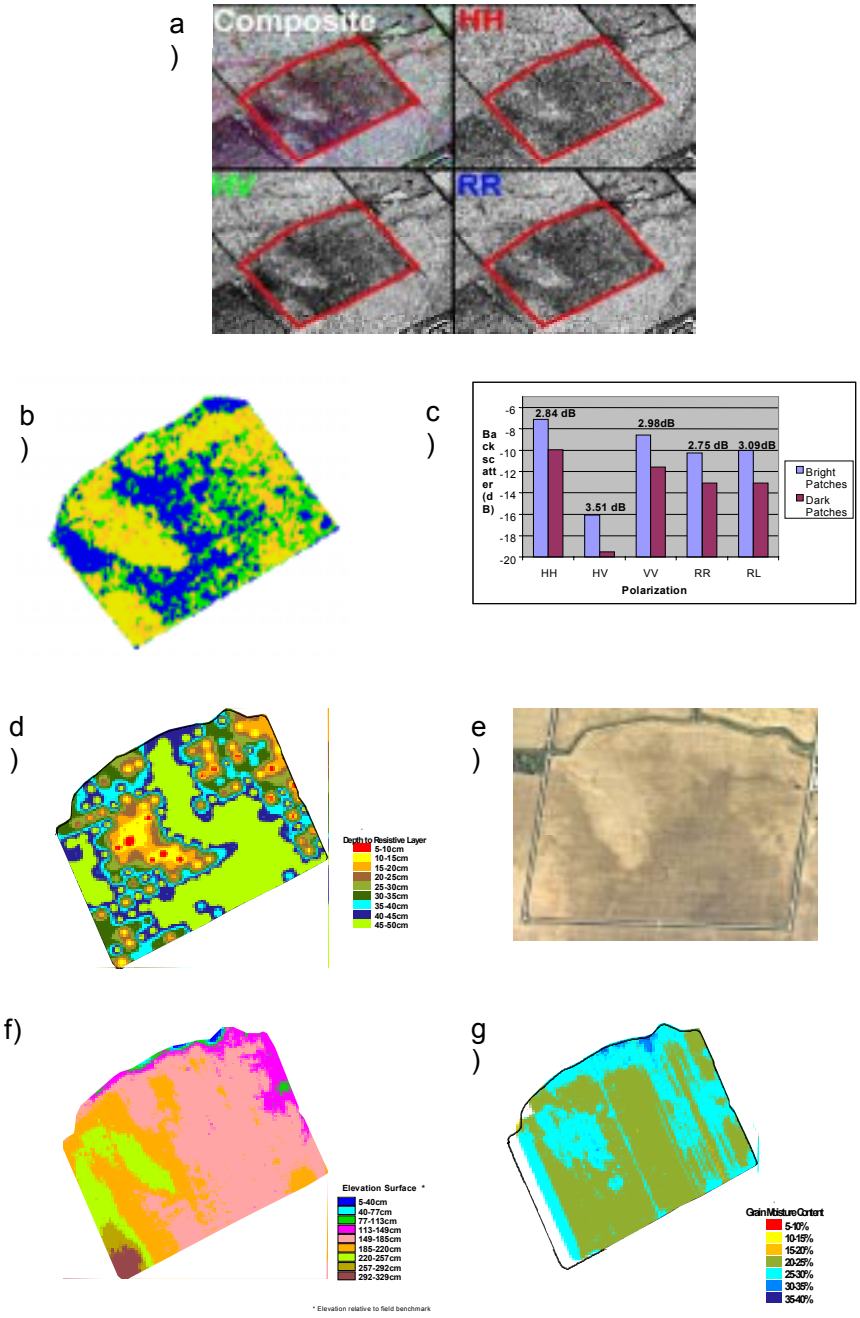


**Figure 3.1.2-2 (a-g)** Detecting variable corn growth: (**a**) a composite of two linear and one circular polarization shows variability in soil and crop conditions within this corn field; (**b**) an unsupervised classification using the VV, HV and RR polarizations; (**c**) differences in backscatter between the bright and dark patches in this field, as a function of polarization; (**d**) soil penetrometer map indicating zones of soil compaction; (**e**) colour air photo of field taken prior to planting, indicating variations in soil characteristics across the field; (**f**) elevation map; (**g**) map of corn grain moisture at harvest. The imagery was acquired with the CV-580 south of Ottawa (Canada) on June 19, 1998. GIS coverages were provided by Agriculture and Agri-food Canada.

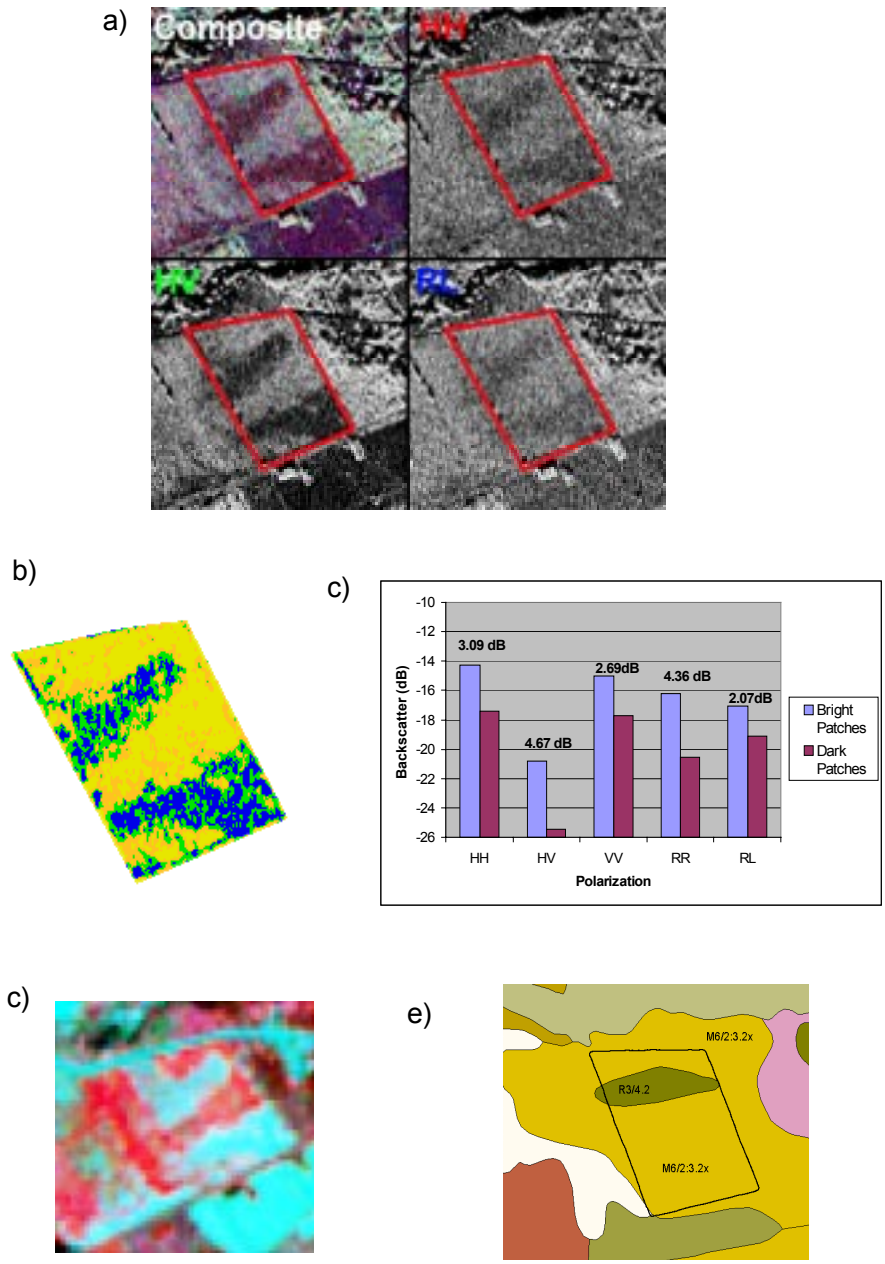


**Figure 3.1.2-3 (a-e)** Detecting variable soybean growth: (**a**) a composite of two linear and one circular polarization indicating variable soybean growth resulting from soil moisture and texture differences; (**b**) an unsupervised classification using the VV, HV and RL polarizations; (**c**) differences in backscatter between the bright and dark patches in this field, as a function of polarization; (**d**) IRS-1C image acquired over this field on July 18, 1998; (**e**) the regional soil map. The imagery was acquired with the CV-580 south of Ottawa (Canada) on June 19, 1998.

a

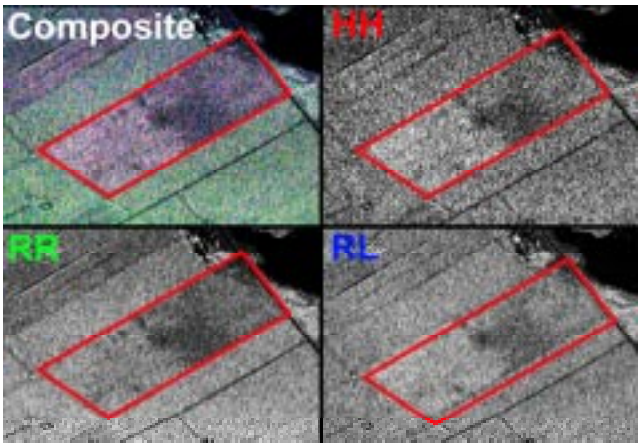


b

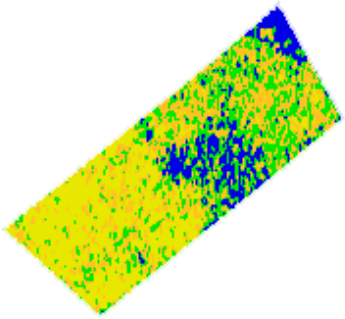

c

| | HH | HV | VV | RR | RL |
|---|---|---|---|---|---|
| Dark-Bright | 4.34 | 2.78 | 0.90 | 3.91 | 3.43 |
| Dark-Medium | 1.93 | 1.85 | 1.29 | 1.91 | 1.75 |
| Bright-Medium | 2.41 | 0.93 | 0.39 | 2.00 | 1.68 |

d

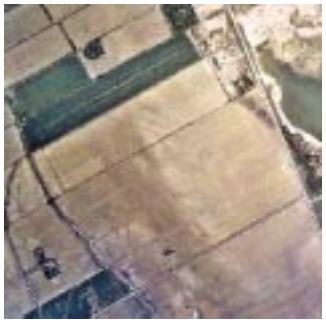

e

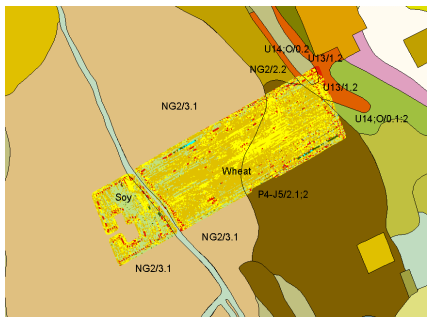


**Figure 3.1.2-4 (a-e)** Detecting variable wheat growth: (**a**) a composite of one linear and two circular polarizations indicating difference in senescence rates in a wheat crop resulting from soil moisture and texture differences; (**b**) an unsupervised classification using the HH, RR and RL polarizations; (**c**) differences in backscatter between the classified zones, as a function of polarization; (**d**) colour air photo of field taken prior to planting, indicating variations in soil characteristics across the field; (**e**) yield map overlaid on the regional soil map. The imagery was acquired with the CV-580 south of Ottawa (Canada) on July 9, 1998. GIS coverages were provided by Agriculture and Agri-food Canada.

including soil compaction, soil colour and elevation (McNairn *et al.*, 2000b) (Figures 3.1.2-2 d,e,f). Of significant interest is the correlation between zones detected in this SAR image and corn grain moisture at harvest (Figure 3.1.2-2 g). This correlation suggests a link between conditions early in the season, as detected on the SAR image, and grain quality at harvest.

For crops with less biomass, zonal information can be provided by SAR imagery throughout the crop growth cycle. On a soybean field from the Ottawa data set, the HV and RR polarizations prove to be the best at discriminating zonal patterns (Figures 3.1.2-3 a,b). With these polarizations, more than 4 dB separates zones of high and low backscatter (Figure 3.1.2-3 c). Both of these polarizations are sensitive to canopy volume scattering. These zones also appear on a mid-season colour-infrared image with regions of poor growth corresponding to regions of low backscatter (Figure 3.1.2-3 d). These zones of poor crop vigor occur where soils are finer textured and where drainage is poor (McNairn *et al.*, 2000b) (Figure 3.1.2-3 e). As the crop grows the contrast between these zones of crop vigor is reduced and is only detectable with the HV polarization.

SAR backscatter appears to be particularly sensitive to crop condition in small grain crops, such as wheat and barley. In many cases, zones of crop condition are most obvious in the weeks just prior to crop harvest (Figures 3.1.2-4 a,b). In the example presented in Figure 3.1.2-4, HH distinguishes the best between zones in this wheat field, although the circular polarizations also provide good contrast. During this acquisition, the wheat crop across the entire field was undergoing senescence. Backscatter is lower on the sandier, well-drained areas of the field. This suggests that in these well-drained regions the wheat crop was drying down faster (McNairn *et al.*, 2000b). With reduced crop moisture, backscatter decreases. The sensitivity of the HH polarization also suggests that with less crop moisture, the signal may be penetrating the canopy and responding to the underlying soil characteristics. The soil patterns visible on the bare soil air photo, and the regional soils map, both follow the pattern on the SAR image (Figures 3.1.2-4 d,e). What is particularly interesting is the correspondence between the wheat yield map and the patterns visible on SAR imagery (Figure 3.1.2-4 e).

Imagery acquired over Indian Head (Saskatchewan) provides many good examples of sensitivity to crop conditions (Figure 3.1.2-5). In this image, regions of poor crop vigor and crop stress are clearly visible. In most instances, stress is related to excessive soil moisture early in the growing season. Although field conditions had dried significantly by the time of the image acquisition, the stress on the crops is still evident. Crops in these zones tended to be shorter, sparser and nitrogen stressed. The link to final yield has yet to be determined.

In terms of crop condition mapping with polarimetric parameters, very little can be found in the literature. In one study by Kharuk and Yedgrov (1990) water stress in vegetation could be diagnosed early as a result of the alteration of the polarization characteristics of the reflected radiation. This alteration was due to the improper orientation of foliage in the crown. As a result of water stress, vegetation deviates from its initial spatial orientation altering the crown architecture. The researchers discovered that a 30-40% decrease in foliage moisture was accompanied by a considerable decrease in the degree of polarization.

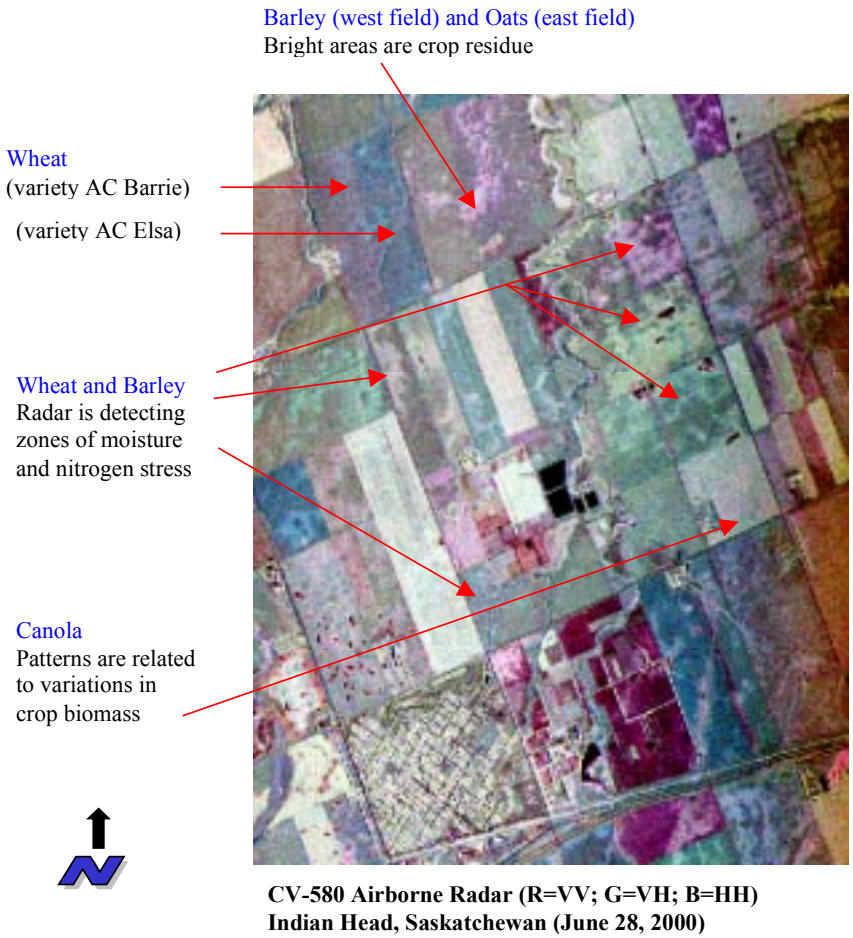


**Figure 3.1.2-5** Airborne CV-580 imagery acquired over Indian Head, Saskatchewan (Canada) on June 28, 2000. In this multi-polarization composite, areas of crop stress related to excess soil moisture earlier in the season are clearly evident.

### 3.1.3 Crop yield

Crop productivity estimation and yield prediction is difficult, regardless of crop type. Many variables influence productivity including soil characteristics, meteorological conditions and management approaches. Even if information on all of these variables is collected, models may not accurately predict yield. However, predictions are usually more accurate if this information is gathered continuously throughout the growing season. In particular, meteorological conditions, management applications and growth detractants during key growth stages can significantly alter the amount and quality of fruit development. With this requirement for large temporal data sets, acquisition of data via in-situ sensors is key. These sensors can provide a great deal of quantitative data on parameters such as incoming solar radiation, air temperature and precipitation. The role of remote sensing in crop productivity modelling is two-fold. Images can provide a method to monitor crops for infestations and fertility problems. In addition, products derived from multi-spectral, hyper-spectral and radar can supply some of the data inputs to yield models.

**R = HH**
**G = HV**
**B = VV**

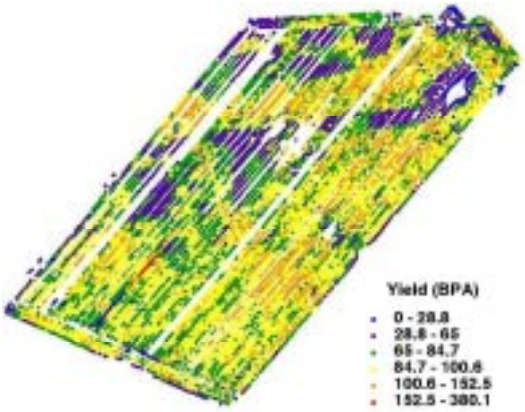


**Figure 3.1.3-1** Airborne CV-580 imagery acquired near Clinton, Ontario (Canada) on June 30, 1999. An accompanying yield map demonstrates that the SAR is detecting variability in the condition of this wheat crop. The yield map displays crop productivity in bushels per acre.

Although some of these remote sensing products have been developed, integration of in-situ and remote sensing information in yield models is still being explored. Data from the Ottawa campaign has demonstrated that SAR imagery, even if acquired early in the season, does detect zones related to the amount and quality of the harvest (Figures 3.1.2-2 and 3.1.2-4).

A similar correlation is detected on some of the wheat fields covered in the Clinton 1999 campaign. In this example (Figure 3.1.3-1) yield visually correlates with zones detected by the SAR sensor.

Multi-frequency SAR acquisitions could significantly improve the information content related to crop condition and crop yield. Using data acquired at different frequencies could be used to separate soil contributions from contributions originating from the vegetation. Longer wavelengths could also be advantageous in reducing the saturation effects observed for larger biomass crops.

## 3.2 Cartography

With the advent of instruments that produce images from electromagnetic radiation beyond wavelengths to which the human eye and cameras are responsive, human “vision and perception” has been greatly extended. Remote sensing has evolved into an important supplement to ground observations and aerial images in the study of terrain features, such as ground elevation. Digital Elevation Models (DEMs) are currently one of the most important data used for geo-spatial analysis. Unfortunately, DEMs of sufficient point density

are still not available for many parts of the Earth, and when available they do not always have sufficient accuracy. Since a DEM enables easy derivation of subsequent information for various applications, elevation modelling has become an important part of the international research and development (R&D) programs related to geo-spatial data.

Due to high spatial resolution of civilian satellite synthetic aperture radar (SAR) sensors since the 1980s with the Shuttle Imaging Radar (SIR), a large number of researchers around the world have investigated elevation modelling and the production of DEMs. Recent discussions on different aspects of radar for radargrammetry and for cartography can be found in Leberl (1990) and Polidori (1997), respectively. Furthermore, the recent research in computer vision to model human vision has led to the advent of new alternatives applied to satellite imagery. Elevation extraction is becoming a more active R&D topic since the launch of the Canadian RADARSAT-1 in 1995. However, an update of the previous research studies for cartography is then useful for predicting RADARSAT-2 potential in relation to its new capabilities useful for cartography (Ultra-Fine mode, better orbit-control and polarimetry).

### 3.2.1 Interferometry for DEM generation

Spaceborne Interferometric SAR (InSAR) generated DEMs can offer a cost-competitive alternative for DEM production. There are two techniques that could be used with RADARSAT-2:

- Data acquired on repeat passes over the same terrain, in the same imaging mode, can be combined interferometrically to produce a DEM and an associated geocoded ortho-image. As the two acquisitions would be separated in time by 24 days, there are some restrictions associated with this approach, these are discussed further below.
- The second technique depends on the launch of RADARSAT-3 around 2 years after the launch of RADARSAT-2, and the simultaneous operation of the two satellites in a tandem configuration. If this is possible, then there are exciting possibilities to create a 'bistatic' mission with even stronger DEM capabilities than the repeat-pass option above. Again, this is outlined below although the option depends completely on the existence of RADARSAT-3 in a close orbit to RADARSAT-2. This option is currently under study by MDA and CSA.

*DEMs from repeat-pass InSAR with* RADARSAT-2*.*
The repeat-pass interferometric SAR concept for DEMs is now well established (Gabriel and Goldstein, 1988; Li and Goldstein, 1990; Prati and Rocca, 1990; Massonet and Raboute, 1993; Zebker *et al.*, 1994; Vachon *et al.*, 1995). While a great deal of work has been done with ERS data, particularly ERS 1/2 tandem data, there are advantages, and one disadvantage, in using RADARSAT-1 data. The disadvantage is simply that there is no possibility in reducing the 24-day repeat cycle and therefore the revisit time for the interferometric pair. As a result this option is not viable for those regions of the world with heavy vegetation, for example the world's rain forests, because of the inevitable changes in backscatter and associated loss of coherence. However, there are many areas in the world where repeat-pass InSAR is viable with a 24-day separation in data acquisition.

The imaging geometry of the first pass must be repeated almost exactly on the second pass. The concept of the critical baseline was introduced (Gabriel and Goldstein, 1988; Massonnet and Raboute, 1993) to describe the maximum separation of the satellite orbits in the cross-azimuth, cross-range direction (usually referred to as the perpendicular baseline).

If this value is exceeded one would not expect clear phase fringes or adequate "phase coherence". The sensitivity to terrain topography increases with the perpendicular baseline so that there is an optimum baseline for DEM generation. In practice, the optimum baseline is terrain dependent as moderate to large slopes can generate an aliased phase rate or a phase, which can be difficult to process in subsequent stages, e.g. phase unwrapping. Normally, a baseline between one third and one half of the critical baseline (i.e. around 300 to 500m for ERS data) is good for DEM generation if the slopes are moderate. In mountainous regions a smaller baseline would be more appropriate. RADARSAT-1 has three options for the slant range resolution which are changed for the various modes (Raney *et al.*, 1991; Parashar *et al.*, 1993). In particular, use of the fine resolution mode relaxes the criterion for the critical baseline and it is possible to use baselines of 1 km or larger. This increases the sensitivity to topography and can lead to a more accurate DEM product than with the lower resolution modes of RADARSAT or ERS (Vachon *et al.*, 1995; Armenakis *et al.*, 2000). The height accuracies of spaceborne InSAR derived DEMs for an Arctic test site were compared by Armenakis *et al.* (2000) to reference data derived from airborne optical stereo and airborne InSAR derived DEM data. Overall the accuracy was estimated to be in the order of ±10m (1 Std.dev.) based on quantitative methodology and data visualization. However, by subtracting the RADARSAT and ERS 1/2 DEMs from the airborne DEM, the lower noise in the RADARSAT DEM was apparent. The standard deviation of the difference data was ~ 4.3 m for RADARSAT and ~ 8.8 m for the ERS tandem mode data. The advantage of the RADARSAT data derived from the larger baseline and resulting better sensitivity to topography.

Use of a larger baseline also reduces the sensitivity to changes in atmospheric propagation conditions (Mattar *et al.* 1999). Various propagation effects can corrupt the differential phase and create errors in an interferometric product. These have been described by Goldstein (1995), Massonet and Feigl (1995), and Tarayre and Massonet (1996). The usual culprit is variations in atmospheric water vapour in the troposphere, which retards the propagation and leads to an additional phase variation which corrupts interpretation of the differential phase in terms of topography or surface motion. Tests of interferometric mapping in the high Arctic in winter have revealed modulations in a height error map (a comparison of airborne and spaceborne InSAR derived DEMs) which appeared to be related to variations in atmospheric water vapour (Mattar *et al.*, 1999). Ionospheric effects can also lead to InSAR errors (Gray *et al.*, 2000) although these effects are more probable near the equator and in polar regions.

There are a number of approaches to both recognizing these effects and in adopting a strategy to minimize the errors. Ferretti *et al.* (1999a) show that combining multiple interferograms can improve the quality of a DEM product, as well as simplify phase unwrapping. By looking for time coincident weather data it may also be possible to exclude passes which include heavy cumulo-nimbus clouds or rain. Another simple strategy is to work with as large a baseline as possible. In this way the phase error associated with the propagation inhomogeneity leads to a smaller error in elevation. This strategy was used to show the strength of RADARSAT Fine mode InSAR in a dry Arctic environment in comparison to some ERS tandem modes pairs with much smaller baselines (Mattar *et al.*, 1999).

As RADARSAT-2 will have an even higher bandwidth mode (up to 100 MHz), it is tempting to suggest that even larger baselines (5 or even 10 km) could be used with this satellite. If successful, this approach would lead to a very sensitive topographic mapping system. However, there may be practical limitations to the magnitude of the baseline. As the

baseline increases so the vertical distance over which the phase changes by 2 pi radians gets smaller and smaller. Eventually the phase unwrapping stage will become difficult for some types of terrain, for example, treed or possibly urban areas, in which there are real, relatively sudden, variations in topography which are a significant fraction of the '2 pi altitude of ambiguity'. More work is required to understand and predict exactly what the limitations on practical baselines will be for different terrain types. This is in contrast to the use of InSAR for terrain movement in which a very small baseline is clearly optimum to avoid problems with topography.

*DEMs from a* RADARSAT-2*/3 'bistatic' mode of operation*
Two of the major problems with using repeat-pass interferometry for DEMs, loss of coherence and propagation problems, can be avoided by collecting the data from the two offset antennas at the same time. This would be possible if the RADARSAT-2/3 system was designed such that only one satellite was transmitting but both were receiving. This would require careful satellite orbit control and also receive window synchronization. The latter could be done by using GPS time on both satellites. The option, which could be used to map most the world, is currently under study by MDA and CSA (Reeves, 2000).

### 3.2.2 Stereoscopy for DEM generation

Since the launch of different satellite sensors (Almaz, ERS, JERS, etc.) in the beginning of the 1990s, radargrammetry has re-emerged as a hot R&D topic. The Russian Almaz-1 SAR system acquired images with different angles to obtain stereo images in the latitude range from 0º to 72º. Yelizavetin (1993) digitally processed two images with 38º and 59º look-angles over a mountainous area of Nevada, USA. No quantitative results were given. Stereoscopy with ERS-SAR data has been done using an image with its normal look-angle (23º) and a second image with the Roll-Tilt Mode (RTM) angle (35º) to generate a same-side stereo pair (Raggam *et al.*, 1993). However, this ERS stereo configuration is very rare due to the limited amount of SAR data acquired in RTM. Another ERS stereo configuration can also be used with two normal look-angle (23º) images from ascending and descending orbits to generate an opposite-side stereo pair (Toutin, 1996). Comparison of these research results (20 m versus 40 m) confirmed the superiority of the opposite-side stereo pair. With the JERS-SAR, stereoscopy can only be obtained with adjacent orbits generating a small overlap with a weak stereo configuration (ray intersection angle less than 4°) that cannot be used in a low-to-moderate relief terrain.

Evaluation of DEM generation results is limited due to the small amount of SAR stereo data at suitable configurations. However, the launch of RADARSAT-1, with various SAR operating modes has changed this limitation. In fact, it is the first commercial SAR system, which can generate various stereo configurations using images from a broad range of look directions, beam positions and modes at different resolutions (Parashar *et al.*, 1993). Under the Applications Development and Research Opportunity (ADRO) program sponsored by the Canadian Space Agency, researchers around the world have undertaken studies on RADARSAT-1 stereoscopic capabilities by varying the geometric parameters (look and intersection angles, resolution, etc.). Most of the results were presented at the final RADARSAT-1 ADRO Symposium "Bringing Radar Application Down to Earth" held in Montreal, Canada in 1998 (CSA, 1998). There was a general consensus on the achieved DEM extraction accuracy: a little more (12 m) for the Fine mode, and a little less (20 m) than the image resolution for the Standard mode, independently of the method used (digital stereo plotter or image matching). Relative elevation extraction from a Fine mode

**Table 3.2.2-1** General results of radargrammetric-DEM accuracy.

| Satellite | SAR band - polarization | Resolution (m) | Relief type | Accuracy (m) | |
|---|---|---|---|---|---|
| | | | | Same-side | Opposite-side |
| SIR-A | L-HH | 25 | High | 100 | |
| SIR-B | L-HH | 40 | Medium | 25 | |
| | | | High | 60 | 36 |
| ERS-1/2 | C-VV | 24 | Medium | 20 | 20 |
| | | | High | 45 | |
| JERS | L-VV | 18 | High | 75 | |
| Almaz | S-HH | 15 | High | 30-50 | |
| RADARSAT-1 | C-HH | 7-9 (Fine) | Low | 10 | 10 |
| | | 20-29 (Stand.) | Medium | 15-20 | 40 |
| | | 20-40 (Wide) | High | 25-30 | |

RADARSAT-1 stereo pair for the measurement of canopy heights in the tropical forest of Brazil was also addressed (Toutin and Amaral, 2000). Table 3.2.2-1 summarises the general results of DEM generation for different satellites and terrain relief (Toutin and Gray, 2000).

However, there were no significant correlations between DEM accuracy and intersection angle in ADRO experiment results. The greater the difference between two look-angles (large intersection angle), the more the quality of the stereoscopic fusion deteriorated. This cancels out the advantage obtained from the stronger stereo geometry, and this is more pronounced with high-relief terrain.

On the other hand, although a higher resolution (Fine mode) produced a better quality image, it does not change the stereo acuity for a given configuration (e.g. intersection angle), and it does not improve significantly the DEM accuracy. Furthermore, although speckle creates some confusion in stereo plotting, it does not degrade the DEM accuracy because the matching methods or the human stereo viewing "behave like a filter". Preprocessing the images with adaptive speckle filtering does not improve the DEM accuracy with a multi-scale matching method (Dowman *et al.*, 1997); it can slightly reduce the image contrast and smoothes the relief (Toutin, 1999). In fact, most of the experiments showed that the principal parameter that has a significant impact on the accuracy of the DEM is the type of the relief and its slope. Figure 3.2.2-1 is an example of DEM accuracy as a function of the terrain relief and its slopes (Toutin, 2000).

The two characteristics of RADARSAT-2, which could improve DEM generation, are the Ultra-Fine mode (3 m by 3 m; 1 look) and better-orbit knowledge (15-20 m in each axis). According to theoretical error propagation modeling, an estimation of error in the elevation coordinate, $E_h$, due to an error in range, $E_r$, for the measurement of a target in the stereo image can be computed (Leberl, 1990):

$$E_h = [(\sin^2\theta_L + \sin^2\theta_R)^{1/2} / \sin\Delta\theta] \, E_r \qquad (3.2.2\text{-}1)$$

Where $\theta_L$ and $\theta_R$ are the look angle of the left and right images respectively, and $\Delta\theta$ is the intersection angle as the difference between the two look angles.

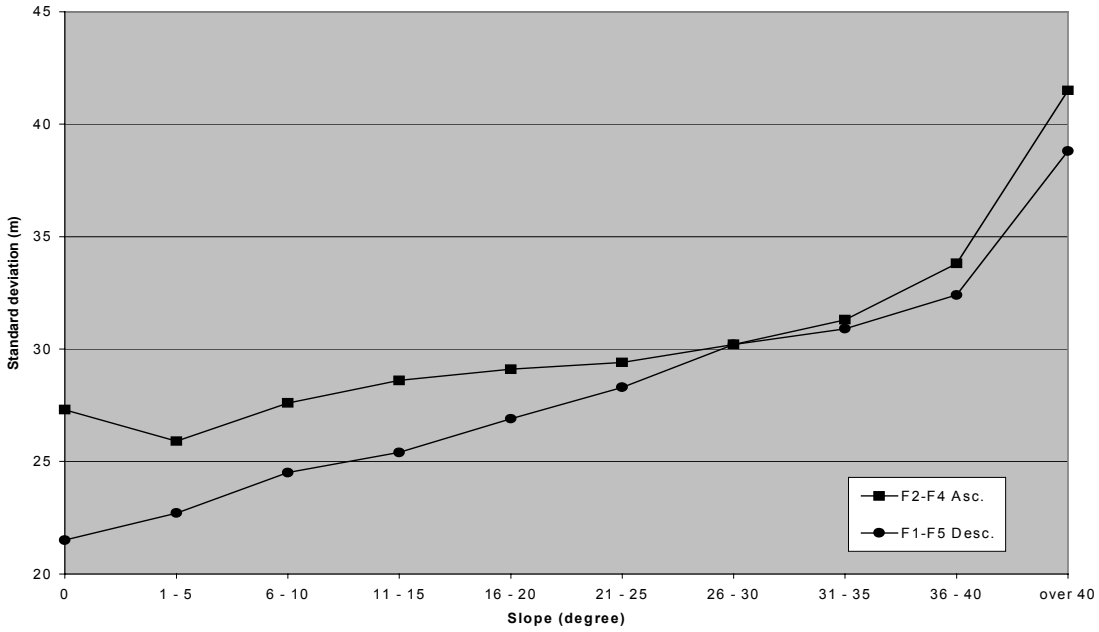


**Figure 3.2.2-1** DEM accuracy with 73% level of confidence (in metres) generated from two stereo pairs (F2-F4 and F1-F5) as a function of the terrain slopes (in degrees).

Based on this modeling, the ultra-fine mode should enable to generate DEM with accuracy better than 5 m using ground control points. However, it is more conservative to expect accuracy between 5-10 m. The previous experiments and results (Table 3.2.2-1) with RADARSAT-1 standard and fine modes demonstrate a degradation of the DEM accuracy relative to the SAR resolution: a little more (12 m) for the Fine mode, and a little less (20 m) than the image resolution for the Standard mode.

In areas without control data, better-orbit knowledge will be a key point to achieve much better results than with RADARSAT-1. However, the absolute accuracy will be degraded to about 20 m. As mentioned before, the speckle of this one-look mode should not have a large impact on the accuracy, such it has been demonstrated with the one-look Fine mode of RADARSAT-1. The type of relief will still be the most important parameter influencing the DEM accuracy.

### 3.2.3 Polarimetry for DEM generation

SAR polarimetry has been used with success for thematic classification studies involving natural scenes and man-made targets. A recently developed application of SAR polarimetry involves both a direct measure of terrain azimuthal slopes and a derived estimate of the terrain elevations (Schuler *et al.*, 1996). The method is mainly based on empirical comparisons, supported by preliminary theoretical analysis between the terrain local slope and the co-polarised signature maximum shift. This has been validated over different geographical areas and different types of natural targets using different DEMs as reference. Although it was only tested with airborne P- and L-band SAR platforms, it is worth mentioning since RADARSAT-2 will generate full polarimetric SAR data.

**Table 3.2.3-1** Results of polarimetric-DEM accuracy with NASA/JPL's AIRSAR data.

| Study site | SAR band | Resolution (m) | Relief type | Accuracy (m) | |
|---|---|---|---|---|---|
| | | | | One pass | Two passes |
| Forested area | P | 6.6 x 12.1 | Low-Medium | 10-20 | N.A. |
| | | | High | 30-40 | N.A. |
| | | | Whole area | 20-30 | 36 |
| Desert area | L (1 pass) P (2 passes) | 6.6 x 12.1 | Low-Medium | 6 | 6 |
| | | | High | 24 | 18 |
| | | | Whole area | N.A. | 29 |

Polarimetric SAR measures the amplitude and phase terms of the complex scattering matrix. Based on a theoretical scattering model for tilted, slightly-rough dielectric surfaces (Valenzuela, 1968), azimuthal surface slope angles and signature-peak orientation displacements produced by such slopes are proportional over a range of azimuthal slopes. Schuler *et al.* (1993) first demonstrated that the resolved azimuthal wave-tilts produced significant and predictable displacements in the location of the maxima of the co-polarised signature of ocean backscatter. They then hypothesised that an azimuthal angle of an open-field terrain caused a proportional shift of the co-polarised polarimetric signature maximum from its flat position by an angle almost equal to the terrain slope. Azimuthal direction slopes can then be computed from the polarimetric SAR data without any prior knowledge of the terrain. By integrating the slope profiles in the azimuthal direction relative terrain elevation can be derived. To obtain absolute elevation, one elevation point must be known along each slope profile.

Since one elevation point along each slope profile is not normally available in an operational environment, sets of elevation profiles spaced throughout the range direction have to be available to obtain two-dimensional topographic elevations maps. Two orthogonal-pass SAR data is thus a solution to generate an elevation surface with only one elevation point (Schuler *et al.*, 1998). The elevation surface may be generated as an iterative solution of a Poison-type differential equation.

Furthermore, attempts to use shorter wavelength radars (C- or L-band) yielded larger errors for forested terrain, mainly for the C-band (Schuler *et al.*, 1996). The larger slope error indicates that canopy and/or branch scattering is then dominant over the terrain relief scattering. Table 3.2.3-1 summarises the general results of elevation extraction or DEM generation with polarimetry from airborne SAR data (Toutin and Gray, 2000). There was no test realised with two passes over forested area. There was no accuracy evaluation for the whole desert area with one pass technique (Schuler *et al.*, 1996). There was also no explanation why with the two-pass technique over the desert area, the accuracy for the whole area (29 m) is worse than the accuracy of the other relief classes (6 m and 18 m) (Schuler *et al.*, 1998).

However, with spaceborne platforms, parallel or orthogonal flights (from opposite or same side) are very rare. Even sun-synchronous satellite orbits are parallel only near the Equator. Elsewhere, crossing orbits or convergent configurations must be considered. If rigorous intersection geometry is applied, no differences exist between computations for parallel orbits and those for crossing orbits. The left and right looking capabilities of RADARSAT-2 combined with ascending and descending orbits could give quasi-orthogonal pass SAR data to apply this method.

The main difficulty to apply this technique (one pass or two quasi-orthogonal passes) with RADARSAT-2 SAR C-band data is the more complex radiative transfer models or discrete scatter formulations (Durden *et al.*, 1989) of forest backscatter from a sloping terrain than with the open-terrain algorithm using P-band data. Future work should be directed towards an analysis based on a volume scattering to take into account the more complicated situation of the SAR backscattering in forested or agricultural areas. With such scattering models, quantitative slope and elevation values could be derived from the relationship between radiation frequency, incidence angle and type of scatterer. However, the main drawbacks of this emergent technique are the volume scattering models, and also the limited availability of polarimetric data to evaluate the robustness of the technique with different topographic and land-cover situations. RADARSAT-2 should be a good candidate to look at some of these drawbacks.

### 3.2.4 Cartographic feature extraction

Few qualitative and quantitative results have been published on cartographic feature extraction from RADARSAT-1 images. Sempere (1998) made a quantitative evaluation of the image content of ortho-rectified RADARSAT-1 images in a French operational context for topographic mapping and digital data base updating. He noticed a small potential for mapping planimetric features (roads, railroads) at 1:100,000-map scale in developed countries due to the high density of communications network. Although the ortho-rectified RADARSAT-1 images are compatible with the planimetric precision at this scale, important fieldwork should be required to resolve the omission and commission errors. Nevertheless, such mapping applications remain possible for developing countries, which are often difficult to survey with optical sensors due to perennial cloud cover. However, the SAR ortho-rectification process requires precise DEMs, which are rarely available in these countries. Figure 3.2.4-1 shows the relationship between the DEM accuracy, the viewing angle of the SAR image, and the resulting error generated on the ortho-image (Toutin and Rivard, 1997). As an example, a 20-m elevation error due to the DEM accuracy and the interpolation into the DEM generates a positioning error of 60 m and 20 m on the standard-1 (S1) and fine-5 (F5) ortho-images, respectively.

Some studies related to the detectability of trail and road in rainforests with no significant topographic relief, as a function of the SAR parameters and trail (or road) shape were also addressed (Touzi and Sasitiwarih, 1998). It is shown that the visibility of these features on SAR images depend mainly on the SAR resolution, trail (or road) width and their orientation relative to the SAR viewing direction. The results are confirmed experimentally on the dense forest site in the south of Sumatra, Indonesia, using the multi-resolution capability of RADARSAT-1. The best trail detectability is obtained with the Fine modes at the highest incidence angle. This permits even the detection of 5 to 6 m width trails under particular conditions. The use of the ascending and descending modes is ideal. It permits trail imaging with different orientation, and as such increases trail detectability. Finally, the effect of speckle on trail and road visibility is discussed, as well as the speckle reduction of SAR images for trail and road enhancement.

Even if stereo-radargrammetry is generally used for DEM extraction in the international research communities, it also could be used by analogy with photogrammetric stereoscopic methods to extract cartographic features from a digital stereo workstation without *a priori* existing elevation information. The “naturalness” of a 3D representation of reality enhances our ability to interpret two-dimensional imagery. Cartographers, engineers, geologists,

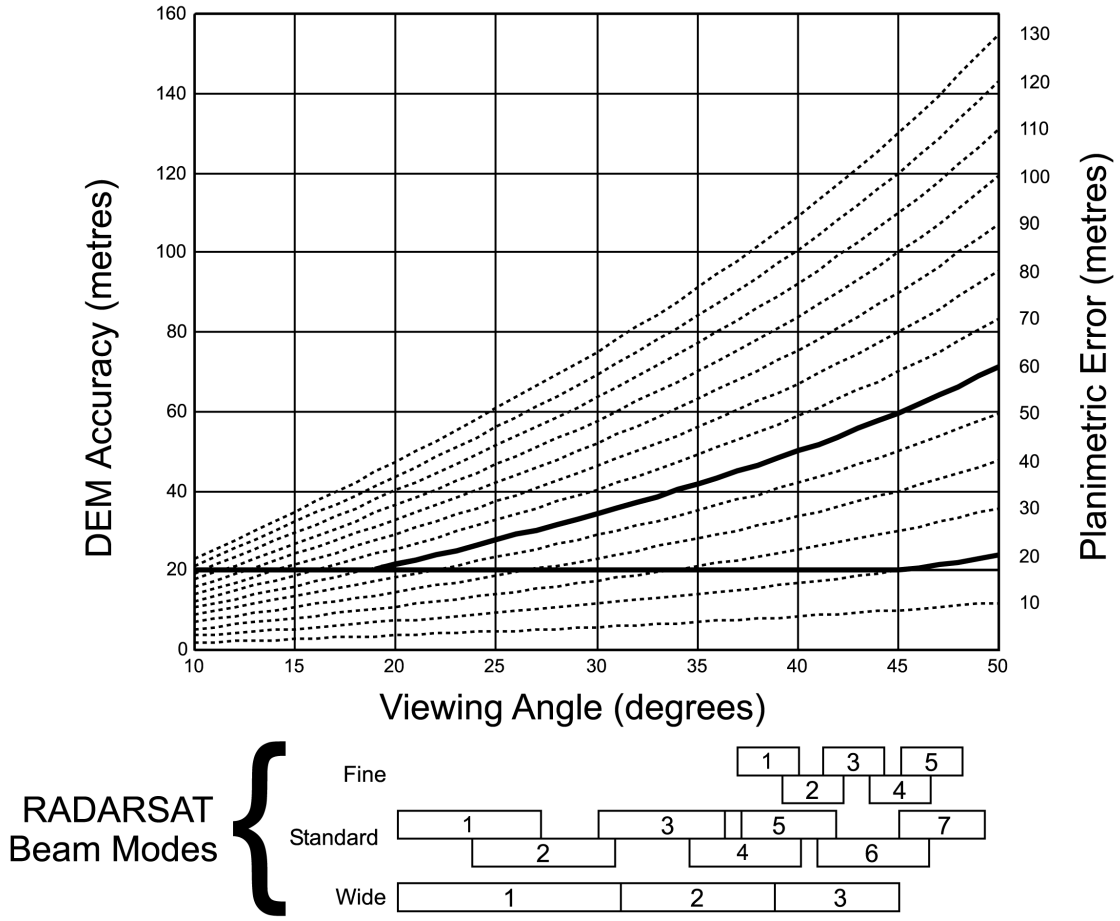


**Figure 3.2.4-1** Relationship between the DEM accuracy, the viewing angle of the SAR image, and the resulting error generated on the ortho-image.

hydrologists, and other geo-scientists, use different three-dimensional viewing methods to perceive the ground elevation and better understand the Earth's surface. Representation of the third dimension of the terrain relief supplies important information about the relationship between land shape and structure, slopes and waterways, surface material and vegetative growth. Consequently, subtle features not discernible in a single SAR image are often recognized in stereo images combining the radiometry of the two images and the relief perception.

Stereoscopy is thus an important issue in countries where precise DEM and maps are not available. Stereo-radargrammetry has been proven to be more accurate for planimetric feature extraction because the feature positioning is not affected by any elevation error in the stereo compilation (the operator plots at the vertical of the point) (Toutin, 2001). Furthermore, since the stereo-restitution is directly done on the raw images, no resampling, such as in the ortho-rectification process degrades the image radiometry, geometry and interpretability. Few researchers have addressed these stereo-radargrammetry capabilities and results are limited to those done at CCRS (Toutin, 2001) to evaluate the potential of RADARSAT-2 for cartographic feature extraction.

Planimetric features such as roads were interactively stereo extracted by an operator on a PC-based stereo workstation from stereo pairs generated with Standard mode images (S1-

S7 and S4-S7) and Fine mode images (F1-F5). The omission errors and positioning accuracy depend mainly on the definition, the visibility of each road category by itself and with its surrounding element (forest, bare soil, agricultural fields, houses, etc.) and the backscatter related to SAR and surface interaction. The omission errors vary from 0% for the highways extracted from F1-F5 stereo pair to 73% for the city streets extracted from S1-S7 or S4-S7 stereo pairs. Completeness needs to be assessed based on density of the communication network and the map scale. Positioning accuracies with 68% and 90% confidence level of about one resolution cell and two to three resolution cells respectively, were obtained. The stereo configurations (e.g., the intersection angles) do not have an impact on this accuracy.

Even if the omission errors are presently not acceptable for the mapping community, the road accuracy results obtained from the stereo compilation of fine and Standard mode RADARSAT-1 images are encouraging since they correspond to the positional accuracy standard of 1 : 50,000 and 1 : 100,000 paper maps, respectively. The Ultra-Fine mode of RADARSAT-2 could thus reduce the omission error, mainly in the dense communication network to better fulfil the mapping requirements. If the two to three resolution cell accuracy with 90% confidence level obtained with RADARSAT-1 Fine mode images can be extrapolated to RADARSAT-2 Ultra-Fine mode images (6-9 m), it should then meet the accuracy for the 1 : 50,000 paper maps and also for the digital maps, such as the Canadian National Data Base (NTDB) which has more severe standards (about 10 m with 90% confidence level).

## 3.3 Disaster Management

Disasters around the world result in more than 150,000 deaths per year and adversely impact another 120 million people, as well as cause damages in excess of $500 billion annually. Remote sensing and its application to disaster prediction, response and mitigation are at a crossroads. Over the next few years there could be dramatic changes leading to wider acceptance and use of remotely sensed data by the disaster management users.

Spaceborne SAR sensors hold excellent possibilities for operational use in a variety of disaster management scenarios. They make very reliable sources of information in the sense that they can image independent of solar illumination and under adverse atmospheric conditions. To date, RADARSAT-1 data have been used effectively in support of the management of disasters such as floods and oil spills. Thanks to certain technical enhancements the future RADARSAT-2 satellite is likely to offer improved potential for application to disaster management. In this section we deliberate upon the value of RADARSAT-2 data as a source of information for search and rescue activities and for the mapping and monitoring of floods, geological hazards, hurricanes and oil spills.

### 3.3.1 Floods

In a disaster situation, the ability to obtain timely information is crucial to the success of saving lives and reducing property damage. For flood mapping, remote sensing can assist in all phases of the disaster management cycle; quick flood products are important for the response phase as well as the recovery phase, by assisting in damage assessment and change detection. Timely information is not the concern in the mitigation and preparation phases, however remote sensing is used to gather information layers to feed into predictive

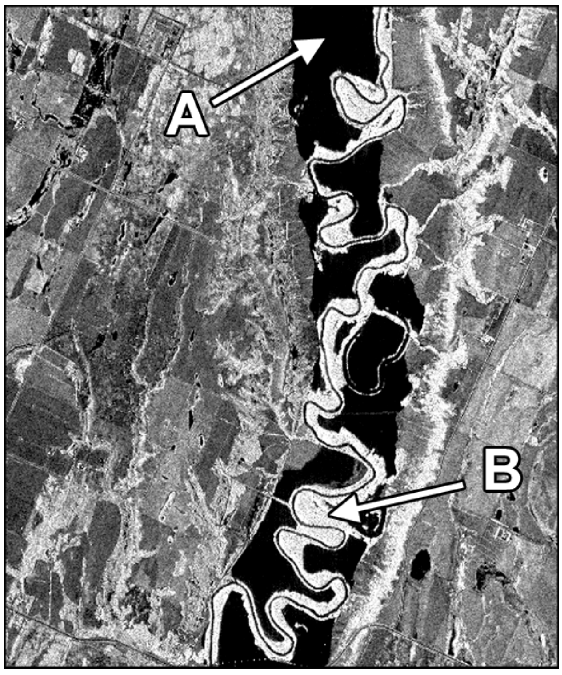


**Figure 3.3.1-1** Airborne polarimetric radar data (C-HH Convair-580) of the Assiniboine River, Manitoba on April 22, 1995. A) represents an area of flooded land, dark tones result from specular reflection, B) represents an area of flooded forest, bright returns result from the double bounce effect off the tree trucks and underlying water surface.

models and landcover information. SAR data is well suited for mapping flooded regions, as cloud cover is often associated with weather systems that deliver heavy rains, and radar can penetrate though vegetation giving an indication of the underlying ground conditions. The differences in roughness of land (diffuse scattering), water (specular scattering) and flooded vegetation (double bounce) is quite evident on radar imagery, which allows easy interpretation of flooding extent (Figure 3.3.1-1).

Due to the advantages of using SAR systems for flood mapping, airborne and satellite platforms have been used extensively in flooded environments, both flat open areas and forested regions. Conflicting results have been published as to the optimal SAR configurations for flood mapping. ERS-1 has been used with successful results as a stand-alone data source (Brakenridge *et al*., 1994) and also as part of a data fusion exercise (Pohl *et al*., 1995). However, Pultz *et al*. (1991) and Barber *et al*. (1996) stated that the optimal configurations for flood mapping are HH polarization and large incidence angles ($\theta > 45°$), not those found on the ERS-1 satellite (Crevier and Pultz, 1996).

Detecting flooding underneath a substantial amount of vegetation or forest cover is possible using certain polarizations and system configurations. For flooded forests, it was shown that the differences in backscatter returns between flooded and non-flooded areas are greatest at HH and lower at HV and VV (Crevier and Pultz, 1996). This is due to the strong double bounce effect (the interaction of the radar with the tree trunks and the ground surface) in the HH polarization. The majority of research indicates that incidence angles also affect the returns from flooded land and flooded forests, however some studies reported no differences in detecting the flood boundary with incidence angle (Ormsby *et al*., 1985; Imhoff *et al*., 1986). Most studies found the contrast between flooded and non-flooded forest stands

at HH polarizations decrease with increasing incidence angles, as the radar interaction is occurring more with the forest canopy than the underlying flooded area (Richards, 1987).

RADARSAT-1 has proven to be an excellent source of data for flood mapping. Not only is the system configurations ideal for mapping flooded areas, but the stearable beam and choice of beam modes (resolution and incidence angle) allows the flexibility required for emergency situations. RADARSAT-2 will increase the availability of optimal data for flood mapping as a result of the right and left looking modes, the continuation of the RADARSAT-1 configuration, and fully polarimetric capability. Hess *et al*. (1990) and Pope *et al*. (1994) concluded that polarimetric radar (with various look angles, frequencies, polarizations and temporal sequence) provided enhanced flood information for over land floods and flooded forest regions. RADARSAT-2's fully polarimetric data are not likely to significantly enhance the flood mapping application, since single-channel HH polarized data are already an excellent source of information. However, the application would benefit considerably from the introduction of a SAR satellite that operates in a frequency band lower than C-band, e.g. L-band. This would enhance the capability to map floods in forested areas, in particular.

### 3.3.2 Geological hazards

The geological hazards discussed in this section include landslides, volcanic events and earthquakes. The uses of Earth Observation systems for geological hazards include geologic, geomorphologic and land use mapping of the hazard prone areas, the monitoring of processes (e.g. movement and deformation), and the assessment of damages after the event.

Landslides pose serious threats to settlements, and structures that support transportation, natural resources management and tourism. They do considerable damage to highways, railways, waterways and pipelines. They commonly occur with other major natural disasters such as earthquakes (Keefer, 1984 and 1994), volcanic activity (Kimura and Yamaguchi, 2000), and floods caused by heavy rainfall, like the Venezuela landslide in December 2000 which killed 50000. Recent scientific publications address the application of SAR to the morphological characterization of landslides (Soeters and van Westen, 1996; Singhroy *et al.*, 1998 and 2000a,b) and the measurement of slow slope movements (Refice *et al.,* 2000; Fruneau *et al.*, 1996; Ferretti *et al.*, 1999b; Rott and Siegel, 1999).

Volcanoes pose a serious threat to population and infrastructure near erupting volcanoes, due to hazards such as lava flows, mudflows and ash falls. Many volcanic phenomena are detected and partly quantifiable using remote sensing information. This includes the monitoring of deformation, thermal and gas emissions, and processes during eruptions (Francis *et al.,* 1996; CEOS, 2000a). The high resolution mapping of topographic and geomorphic changes are important since they influence the direction of lava and pyroclastic flows and lahars.

Remote sensing systems have some limited use in the mitigation and response phases of earthquake risk management, but not the warning phase. They are usually used for geological base mapping (lithology and faults), and earthquake damage assessments (CEOS, 2000b). The following section discusses the potential uses of RADARSAT-2 for geological hazard investigations.

*Morphological analysis of landslide and volcanic areas*

Landslide inventory maps are the primary planning tool for assessing risk. They show the landslide distribution based on type, activity, dimensions, and the analysis of the most relevant terrain parameters related to the occurrence of landslides. Currently, landslide inventory mapping uses stereo 1:25,000 aerial photographs, ground surveys, and historical occurrences of landslides. SAR images are particularly useful when high-resolution stereo images are used to map the morphological features of landslides, the type of movement and the overall terrain condition. From this information, the susceptibility of a site to sliding can be interpreted. There are two aspects where RADARSAT-2 data will be useful for landslide mitigation. First, the multi-temporal images can be used to map changes in landslide distribution, vegetation and land use to update existing landslide inventory maps. Second, images acquired in the Ultra-Fine mode (3 m by 3 m resolution) will facilitate more accurate mapping of the geomorphology of landslides and related slope characteristics including lithology, and faults. Using the Ultra-Fine mode data, landslide mapping at a scale of 1:25,000 to 1:50,000 should be feasible. It is important to have the capability to map small landslides since these slides often cause considerable property damage.

Effective volcanic hazard monitoring and mitigation requires access to high quality geomorphic and topographic data to predict the direction of lava or pyroclastic flows and lahars. In addition, the mapping of young volcanic deposits is essential to the evaluation of volcanic hazards. It gives insight into the style of recent activity, and offers the best and often the only basis for planning for future events (CEOS, 2000b). Results of a study by CCRS, the Geological Survey of Japan, and the National Institute for Earth Sciences and Disaster Prevention in Japan show that the stereo Fine mode capability of RADARSAT-1 can be used to delineate different types and ages of pyroclastic flows at the Unzen Volcano (see Figure 3.3.2-1). This delineation is based on their characteristic SAR backscatter and

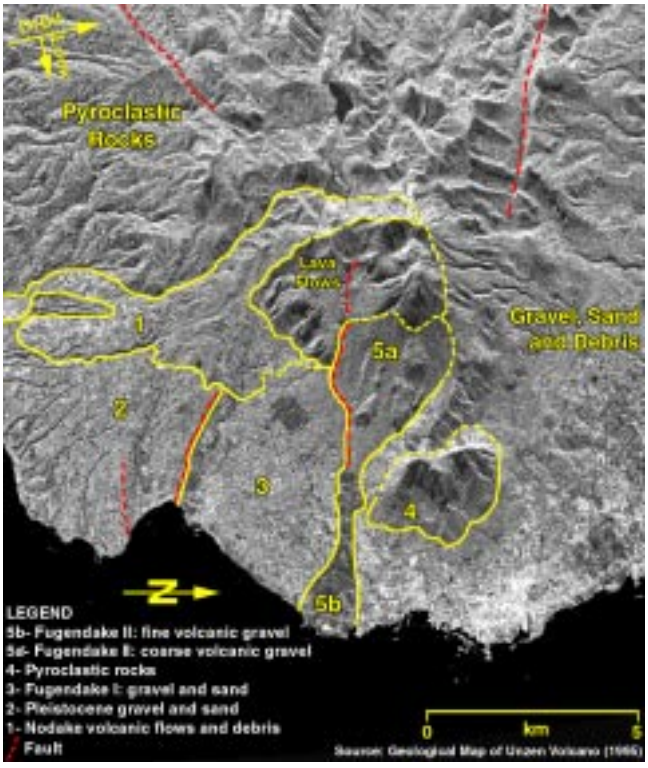


**Figure 3.3.2-1** RADARSAT-1 C-HH image showing types of pyroclastic flows of the Unzen Volcano, Japan. The ultrafine and polarimetric images of Radarsat-2 will improve volcanic terrain mapping.

morphology. RADARSAT-2's Ultra-Fine imaging mode and polarimetric capability are expected to improve the potential for the mapping of volcanic areas.

Interferometric techniques have been used to observe motion related to earthquakes, volcanic deformation and subsidence. However, its use for detecting landslide motion is difficult. This is because mass movements are small in size and typically occur on steep slopes in high-relief vegetated terrain like the Canadian Rockies. In addition, atmospheric effects introduce coherence loss and resolution problems in the analysis of interferometric pairs. When the conditions are suitable SAR interferometry can produce coherence maps, which could indicate subtle changes in the microscopic soil structure, which could in turn be a hint for failures. ERS-1 and -2 InSAR was applied to monitor slow movements in Alpine areas over annual and monthly intervals, with typical displacements of the order of a few millimetres to several centimetres within these time periods. The standard method of InSAR analysis is applicable over areas with sparse or no vegetation. However, studies that make use of the permanent scatter processing technique show that motion in vegetated landslide areas can be measured as long as a few stable scatterers (houses, roads, etc.) are present (Fruneau *et al.,* 1996; Ferretti *et al.,* 1999b; Rott and Siegel, 1999; Singhroy, 2000c). This technique promises to be a good tool for precise and frequent monitoring of small precursory movements of buildings and structures associated with landslide, volcanic and earthquake reactivation. The technique will benefit from RADARSAT-2's improved orbit control and knowledge.

*Tectonic Mapping*

The regional tectonic setting of an area forms the basis for assessing its vulnerability to earthquakes, landslides and volcanic eruptions. Early results by Saint-Jean *et al*. (1999) have shown that fault mapping can be improved using suitable polarimetric composites. This has potential to improve our current SAR structural mapping techniques, particularly if the images are fused with other optical, topographic and geophysical images (See also section 3.5.2). In addition, the ultra-high resolution and dual viewing capabilities of RADARSAT-2 will further improve fault identification in areas of earthquakes, volcanoes and landslides, and significantly contribute to our understanding of regional tectonics.

*Damage Assessment*

Disaster response comprises the rapid damage assessment, and relief operations, once the disaster has occurred. Currently, damage assessment is done using aerial photography, videography and ground checks. In order to be able to use remote sensing data for damage assessment, two criteria should be met, that is, reliable high temporal and high spatial resolution. In cases where the damage is extensive, either as a single large event, or many small events covering a large area, there is a need for high-resolution images (> 5 m), before and after event. RADARSAT –2 can be used to supplement airborne and ground techniques for local and regional damage assessment. The capability of mapping damage in near real time is of prime concern to relief agencies that require images to locate victims and structures at risk, and to assess loses for future planning. The CEOS earthquake hazard team recommended 2 m or better to assess damage to infrastructure based on the Kobe earthquake estimates (CEOS, 2000a). Although RADARSAT-2 will not be able to meet this resolution requirement, the system certainly has the advantage to be able to acquire data under adverse atmospheric conditions. This shortens the (average) response time and increases the revisit frequency.

### 3.3.3 Hurricanes

Section 3.7.1 discusses the estimation of wind fields from SAR images of the ocean's surface. SAR ocean images often show the imprints of marine atmospheric boundary layer (MABL) processes that modulate the near surface wind field. Rougher areas corresponding to higher wind speeds appear bright, while smoother areas corresponding to lower wind speeds appear relatively dark. The RADARSAT-1 SAR's ScanSAR wide mode, with a swath width of 500 km and a spatial resolution of 100 m, has recently provided some striking images of mesoscale cyclones, including polar lows (Chunchuzov *et al.*, 2000) and hurricanes (Katsaros *et al.,* 2000). The SAR images of these important disturbances are a unique sea surface view that is complementary to conventional remote sensing observations (e.g., lower resolution cloud top images from GOES and AVHRR). An example RADARSAT-1 SAR image showing a portion of a recent hurricane, including MABL processes such as convective cells, precipitation, and boundary layer rolls is shown in Figure 3.3.3-1.

Hurricanes are tropical cyclones that have winds that reach sustained speeds of 64 knots (33 m/s) or more. Hurricane winds blow in a spiral pattern around a relatively calm "eye". The "eye" may be 30 to 50 km in diameter and the storm may extend outward from the "eye" for more than 500 km. As hurricanes move towards land, their trajectories can be difficult to predict and they can bring torrential rains, high winds, and storm surges; their effects may be devastating and can last several weeks. The Atlantic Basin hurricane season lasts from August through October.

Although initial RADARSAT-1 observations dating from the 1998 hurricane season were

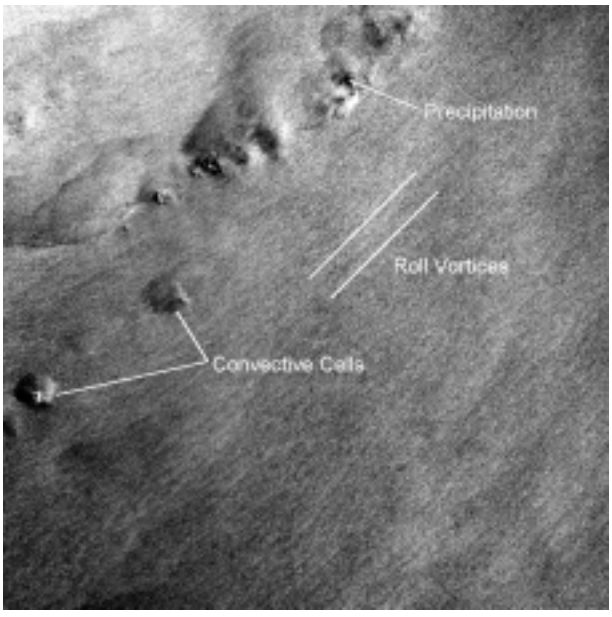


**Figure 3.3.3-1** A portion of a RADARSAT-1 ScanSAR wide mode image of Hurricane Florence when the storm was off the US East Coast and to north of the Bahamas on 13 September 2000. The image covers a 150 km by 150 km region located to the south-east of the storm's eye. Readily apparent are local regions of intense precipitation (appearing dark) as well as cells of intense convection. The clearly visible streaks on the image are aligned with the local wind direction (from the lower-left towards the upper right) and are thought to be associated with organized boundary layer structures such as roll vortices. The roll vortices have a spacing of about 3 km in this case. (© CSA 2000)

largely serendipitous, “Hurricane Watch”, a collaboration between the Canada Centre for Remote Sensing (CCRS), the Canadian Space Agency (CSA), and the National Oceanic and Atmospheric Administration’s (NOAA) Hurricane Research Division (HRD), routinely acquired RADARSAT-1 ScanSAR wide mode imagery of hurricanes during the 1999 and 2000 Atlantic Basin hurricane seasons. The CSA’s Disaster Watch Program and Background Mission Program submitted imagery requests in support of this project. Disaster Watch made manual requests as late as 25 hours in advance of the pass time that were fewer in number but more accurate than those of the Background Mission. NOAA/HRD attempted to co-ordinate their WP-3D hurricane penetration flights with the RADARSAT pass times. This effort has resulted in 10 images of hurricane eyes, and numerous images of the peripheral regions of these storms.

These images provide exceptional detail and can offer information on the structure and distribution of rain cells and rain bands as well as a direct measure of the storm’s wind field at the ocean’s surface. These observations have provided new insights to storm morphology, storm dynamics, and SAR ocean imaging. For example, the wide extent of organized boundary layer structures between rain bands was first revealed by RADARSAT-1 SAR images. The presence and extent of these structures could have bearing on our understanding of hurricane dynamics and intensity change. They will be the focus of a detailed in situ study during the 2001 version of the Hurricane Watch activity.

With RADARSAT-1 alone, the available repeat coverage of storms such as hurricanes is rather limited due to the available swath coverage, the size of the storm, and the repeat cycle of the satellite. In principle, additional scheduling opportunities will be possible with RADARSAT-2 if left or right looking geometry can be made available to this application. Furthermore, reductions in the ordering lead-time will improve the scheduling accuracy. This suggests that RADARSAT-2 data could be used for storm tracking and could contribute to landfall predictions, particularly if used in conjunction with other wide swath SARs such as ENVISAT’s ASAR. VV acquisitions may provide better quantitative wind field information since the available wind retrieval model functions are better developed for VV polarization.

Polarimetric and dual polarization data, as will be available from RADARSAT-2, also provides intriguing new opportunities for the observation of severe storms. Although the mechanisms are not yet understood, recent wind/rain tank observations (supported by SIR-C data) suggest that co- and cross-polarization ratios (CCP-ratios) at C-band may provide a mechanism to estimate the rain rate (Braun et al., 2000). This would represent important additional quantitative information on hurricane state and evolution when the storms are offshore and beyond the range of coastal weather radar. Of course, access to CCP-ratios suggests that ScanSAR could not be used. The use of narrower swath polarimetric modes would significantly reduce the probability of obtaining a hurricane image. Nevertheless, RADARSAT-2 will provide an important validation opportunity for the development of a rain rate information product for hurricanes and other convective storms.

### 3.3.4 Oil spills

Spillage of oil in coastal waters is one of the most hazardous events to occur. The potential damage to the natural and economic health of the area at stake requires that agencies be prepared to detect, monitor and clean up any large spill in a rapid manner. The capability of radar remote sensing systems to locate mineral oil spills and map their extent is well known and was first reported in the early 1970’s (e.g. Guinard and Purves, 1970; Krishen, 1973;

van Kuilenburg, 1975). To date, combinations of airborne and satellite radar systems are applied routinely to fight oil pollution in European waters, in particular (e.g. Lankester, 1998; Pedersen *et al.*, 1995; Pellemans *et al.*, 1995; Gade *et al.*, 2000). In a market assessment for RADARSAT 3, oil spill detection and monitoring was projected as the fourth highest ranked application (Radarsat International and Spot Image, 1995).

The detection of oil spills by radar systems is based on the dampening effect oil has on the capillary surface waves. At intermediate incidence angles (between 20º and 75º), these waves govern the backscattering of radar waves of comparable wavelengths (Bragg scattering mechanism). Hence, wave dampening in the presence of oil results in a localised reduction of the measured radar backscatter. In SAR images, the darker oil-covered areas are often clearly visible among the rougher, and hence brighter, oil-free water surfaces. Unfortunately, oil spills are not the only phenomena known to cause locally reduced radar return signals. Features that present themselves in a similar fashion include low wind areas, grease ice, rain cells, natural surfactant slicks, and polluted or fresh water slicks. Clearly, the sensitivity of SAR to such oil look-alikes complicates its application. The variable most critical to the visibility of oil in radar images is wind speed. Winds ranging from 3 m $s^{-1}$ to 10 m $s^{-1}$ may be considered optimal since they generate a good oil-water backscatter contrast. At lower wind speeds, the return signal of oil-free water will approach that of oil-covered water while at higher wind speeds the backscatter of both oil-covered and oil-free water will be governed by large scale wind induced waves.

Evidently, the potential to detect oil spills in radar images is a function of the observed backscatter contrast. Various authors report that the oil-water backscatter contrast decreases with an increase in radar wavelength (e.g. Neville *et al.*, 1984; Wismann *et al.*, 1998; Gade *et al.*, 1998a). Also, there is agreement in the literature that VV polarised images provide better contrast than either HH or HV polarised images (e.g. Guinard and Purves, 1970; Krishen, 1973; Neville *et al.*, 1984; Witte, 1985; Madsen, 1987; Wismann *et al.*, 1998). This holds true for most frequency bands, including C-band, and results from the greater vertical versus horizontal polarised radar cross-section for an oil-free sea surface when observed at intermediate incidence angles. For C-band this is illustrated in Figure 3.7.1-1. Studies concerning the potential of fully polarimetric radar systems are scarce. However, the one study found to evaluate the information contained in C-band co-polarisation signatures concludes that there are no distinct differences between slick-covered and slick-free areas (Gade *et al.*, 1998a). It follows that the capability of RADARSAT-2 to image in VV polarisation will enhance its potential for the detection and monitoring of oil spills. On the other hand, the satellite's full polarimetric capabilities can be expected to add little to its potential to support the oil spill application.

Hühnerfuss *et al.* (1996), Wismann *et al.* (1998) and Gade *et al.* (1998b) show that although the contrast in VV is better, the ratio of the mean backscatter from an oil-free and an oil-covered water surface (damping ratio) is polarisation independent. Wismann *et al.* (1998) report that relations between the damping ratio and Bragg wavenumber hold promise for discriminating mineral oil spills from natural surfactant slicks by means of multi-frequency radar systems. Similarly, the joint application of radar and optical sensor systems may be expected to improve the odds of distinguishing between oil and oil look-alikes. For example, thermal infrared images should provide a good basis for discriminating oil slicks from low wind areas. Compared to radar systems, certain optical systems also show more potential to map oil thickness (Brown and Fingas, 1998).

RADARSAT-2's Ultra-Fine resolution modes will enable the system to image an area at a spatial detail in excess of that provided by RADARSAT-1. This capability will enhance its potential for the tracking of identified oil slicks and the measurement of the extent of oil slicks, in particular. Finally, the oil spill application will benefit from the electronically steered antenna, which will allow RADARSAT-2 to image to either the left or the right of its ground track. This capability will reduce the time lapse between the occurrence of an oil spill and the first opportunity to image the area at stake. Moreover, it will reduce the time interval between subsequent data takes. Consequently, response teams will be able to obtain the necessary information sooner and more frequently.

### 3.3.5 Search and rescue

Most of the Canadian landmass is sparsely populated, and there are significant northern areas that are in darkness for prolonged periods each year. Airplane traffic over these areas continues to increase. The need to reach crash sites (often of airplanes carrying less than half a dozen passengers) and to assist the victims is served by Search and Rescue (SAR) in Canada, which is the responsibility of the Department of National Defence (Search, 2001).

A major improvement in capabilities to save lives of crash victims was the development of the COSPAS-SARSAT program (SARSAT, 2001) which makes it possible to detect Emergency Locator Transmitters (ELTs). The current Canadian Search and Rescue procedure, well detailed in the National Search and Rescue Manual (1998), involves listening for ELTs and visual searches from spotter aircraft. Unfortunately, although systems have been improving, the functioning of ELTs has been problematic. Statistics (obtained for the United States, and expected to be similar in Canada) indicate that ELTs function only about 25 percent of the time (Dreibelbis, 1999). In many cases, the ELT does not operate and other methods of finding the crash site are required.

The possibility of using imagery from space-borne systems to assist in search and rescue has been considered previously (e.g. Sivertson, 1976). The need to find such crash sites in inclement weather and darkness provides the opportunity for the development of techniques that make use of microwave remote sensing systems. These can provide imagery during periods when both visual searches and optical imaging systems are not able to help.

Synthetic Aperture Radar is particularly useful for the location of crashed airplanes because of the microwave scattering by the dihedrals formed by parts of the airplane structure. It has been found that these often survive the crash: If the orientation between the SAR system and the target makes it possible to image these dihedral structures, it can be easier to find the crashed aircraft (e.g. Jackson, 1998).

It is fortunate that in recent years, there have been active initiatives in this area, in particular at the Search and Rescue Mission at NASA Goddard Space Flight Center. The center launched a project in 1988 to investigate the feasibility of using space and airborne remote sensing technology to aid in beacon-less searches (Wallace, 1997). The $SAR^2$ Project, has carried out experiments beginning in 1989 with several systems for a variety of test targets and locales in the United States (NASA, 2001). A Canadian initiative at the Royal Military College examined the use of SAR and optical imaging (from space-borne and other systems) in search and rescue (e.g. Cunningham, 1994 and Creber, 1997)

**Table 3.3.5-1** Revisits of RADARSAT-1 and -2 during a 24-day cycle at various locations in Canada.

| | | RADARSAT-1 | RADARSAT-2 | | |
|---|---|---|---|---|---|
| **Location** | **Latitude / Longitude** | **S1-S7** | **S1-S7** | **Standard QP** | **Ultra-Fine** |
| Chibougamau, QC | 49° 55' N / 74° 22' W | 14 | 30 | 19 | 4 |
| Iqaluit, NT | 63° 45' N / 68° 31' W | 20 | 44 | 26 | 10 |
| Resolute, NT | 74° 42' N / 94° 50' W | 36 | 124 | 57 | 21 |
| Eureka, NT | 79° 59' N / 85° 57' W | 58 | 58 | 36 | 12 |

The search and rescue application in general will gain from RADARSAT-2's capability to image either to the right or the left of the sub-satellite track. This selective look direction option shortens the response time (on average) and increases the revisit frequency for most regions on Earth (see Table 3.3.5-1). In certain cases, the Ultra-Fine resolution modes are expected to be of assistance as well. However, this impact is diminished by the necessary trade-off against size of area that can be covered on a particular acquisition.

Research and development at CCRS focuses on the application of SAR to the location of crashed aircraft (Lukowski, 2001). Two case studies that address the use of interferometric coherence and polarimetric signatures for this purpose are described below. RADARSAT-2 is expected to assist in the further development and use of these methodologies (e.g. Gilliam, 1999).

*Interferometric Coherence*

Interferometric coherence can be used to locate non-changing, man-made objects within regions of natural targets. The location of crashed aircraft has been examined in coherence analyses performed with three RADARSAT-1 Fine Beam 5 images acquired in 1998 (July 4, July 28, and October 8). The target was a Fairchild-27 that crashed in Northern Canada in 1968 (Figure 3.3.5-1).

Figure 3.3.5-2 is a colour composite of two coherence pairs (July 28, 1998 – October 8, 1998 and July 4, 1998 – October 8, 1998) with the July 28 1998 intensity image as background. Close scrutiny of the colour version of the figure indicates that only one target was highlighted in white (i.e. the Fairchild-27). This is a consequence of the crashed aircraft having high backscatter and there being high coherence in both image pairs (resulting in a white composite sample). The number of false alarms detected would be less than 0.03 per square km.

**Figure 3.3.5-1** Photograph of crashed Fairchild-27, Cornwallis Island, Canada. (Courtesy of P. Budkewitsch, CCRS).

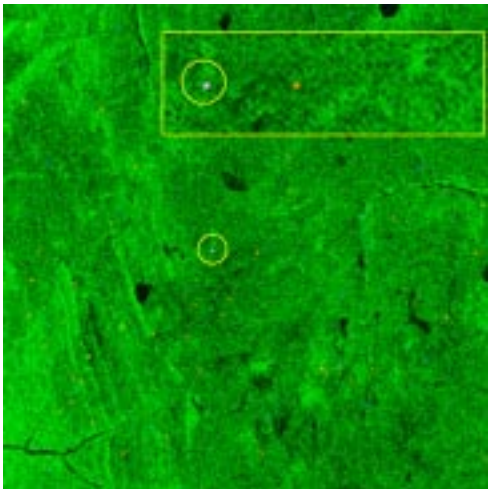

**Figure 3.3.5-2** Colour composite of RADARSAT-1 F5 images over the Fairchild-27 on Cornwallis Island. Red Channel: July 28,1998 – October 8, 1998 Coherence; Blue Channel: July 4, 1998 – October 8, 1998 Coherence; Green Channel July 28, 1998 Intensity. Circle indicates the airplane location. Inset shows enlargement in area of aircraft.

Thanks to a number of technical enhancements, the RADARSAT-2 orbit will be more stable and better known than the orbit of RADARSAT-1. This expected to improve the potential of the described interferometric coherence methodology for application to search and rescue.

*Polarimetry*

The distinctive polarimetric signatures of man-made targets provide an aircraft detection and classification opportunity. Studies at CCRS have employed a methodology based on work at NASA GSFC SAR[2] (Jackson, 1998). Our development and testing used data acquired by the C-SAR on board the Environment Canada Convair-580 operating in polarimetric mode (Livingstone, 1995; Brown, 1999)

A number of aircraft parked for the winter at the Carp, Ontario airport (Figure 3.3.5-3) were imaged on March 18, 1999. Signal data were processed at CCRS to calibrated imagery in each of the four polarimetric Scattering Matrix components ($S_{HH}$, $S_{HV}$, $S_{VH}$, and $S_{VV}$) at resolutions of 6 m (slant range) by 1 m (azimuth) (Hawkins, 1999).


**Figure 3.3.5-3** Parked aircraft at Carp Airport, March 19, 1999.

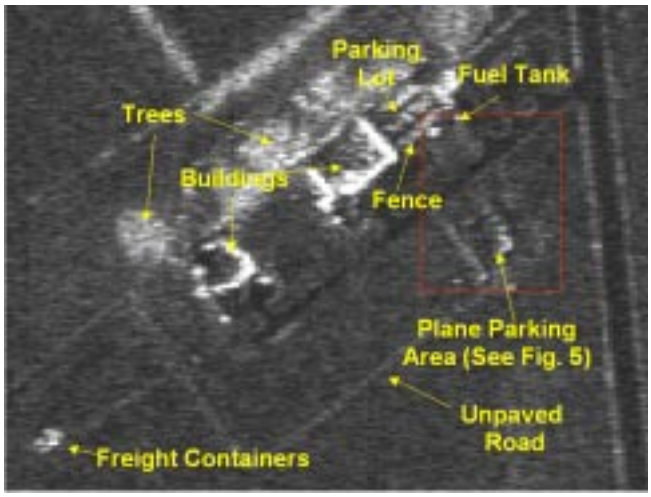


**Figure 3.3.5-4** Annotated SAR image of Carp Airport as at March 18, 1999.

Imagery annotated with ground truth information is presented in Figure 3.3.5-4. Corresponding results presented in Figure 3.3.5-5 show that man-made targets including the aircraft were detected. The small aircraft have been identified (as expected) and classified as aircraft based on their polarimetric signatures (dihedrals or narrow dihedrals). This study was complicated by the proximity of a number of other man-made targets (buildings) which are not expected to cause such difficulty in an actual search.

RADARSAT-2 will be the first operational system capable of acquiring full polarimetric radar image data from space. The results presented are promising and indicate that this capability will advance the use of SAR in support of search and rescue activities. However, the methodology will require further development.

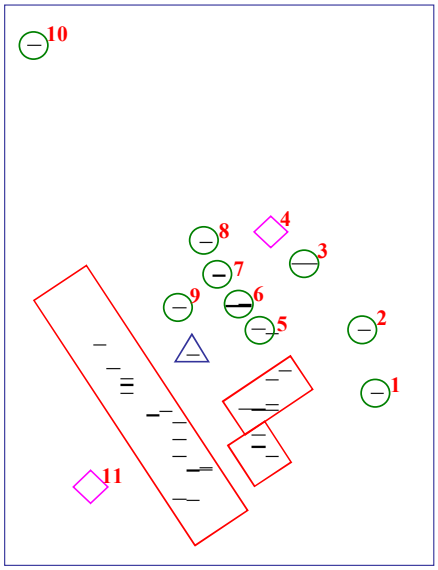


**Figure 3.3.5-5** Classification of area of Carp Airport, March 18, 1999 showing the 11 airplanes. O Detected and classified airplanes; ◇ Undetected airplanes; Δ Storage box; □ Buildings. Solid lines indicate locations of buildings.

## 3.4 Forestry

The applications in forestry can be grouped into two main categories:
- forest resource assessment applications which include the inversion of dendrometric or structural parameters at the stand level, such as biomass, forest species, and stand structural organisation
- forest resource monitoring applications which include, among others, the routine mapping of deforestation, clearcuts, fire (scars) and flooding.

To achieve the inversion of dendrometric characteristics such as biomass, the sensor requires, in most cases, measurement from the complete structure of the forest canopy or tree itself depending of the spatial resolution of the sensor. Also, the structural entities of interest must respond in a unique manner to the incoming radiation.

For RADARSAT-1 and –2, the frequency used allows for the measurement of structural elements in the upper portion of the majority of tree canopies. Results of modelling and field experiments confirm this and show that microwave-forest interaction is dominated by volume scattering. Because of the nature of this scattering mechanism, and the restricted portion of the canopy from where it originates, the effective dynamic range available for forest type discrimination is very low. Hence, variations in the backscatter behaviour of forest types are indicative of significant structural differences within the forest canopy. The polarization of the radar backscatter is well known to be sensitive to the orientation of the scattering elements. Consequently, RADARSAT-2 with its polarization diversity and polarimetric capabilities is likely to provide a significant step forward for the detection of structural differences between forests. Forest type mapping will certainly be the assessment application to benefit most from the polarization diversity offered.

Forest resource monitoring applications are of particular interest because they constitute the most promising and economically sustainable applications. RADARSAT-2's new imaging capabilities in the cross-polarization in particular will enable forestland managers to monitor forest change more accurately and timely. However, more efforts will have to be placed on investigating end-to-end solutions under specific environmental and ecological constraints. Ultimately, understanding of management practices, policies and regulations are also part of the equation for the success of RADARSAT-2. With the new technical capabilities of RADARSAT-2, tropical forest regions will constitute an even more promising market to develop. This will require additional application research and development.

The next sections will discuss the application of RADARSAT-2 type data to the mapping of forest types, clearcuts, fire-scars and timber yield.

### 3.4.1 Forest type

Previous research using images acquired by RADARSAT-1 and ERS-1 shows that single polarization C-band radar images offer little potential for forest type mapping during the spring and summer seasons (Proisy *et al.* 2000). Under leafy conditions, the radiometric information contained in this type of images does not even enable reliable discrimination of deciduous and coniferous species. In support of the RADARSAT-2 mission, CCRS has investigated the potential of fully polarimetric C-band SAR data for forest type discrimination

(Touzi *et al.*, 2001). Six forest areas in Eastern Ontario (Mer Bleu) with different species compositions were considered: deciduous / coniferous mixed forest, poplar, red pine, white pine, white spruce, and a red / white pine mixture (Figure 3.4.1-1).

A total of six C-band polarimetric Convair-580 SAR data sets was acquired over the study area, in December of 1997 and March, June, and July of 1998. During each flight corner reflectors and polarimetric ARCs were deployed for calibration purposes. The antenna bore-sight angle was at 58°, and the study site was illuminated at about 60°. Data within 20° from the bore-sight angle were calibrated with an accuracy of ± 1.5 dB and 5° for each of the four linear channels HH, HV, VH, and VV.

In addition to the conventional linear polarizations (HH, HV, VV) the following polarimetric variables were synthesised from the scattering matrix and investigated:
- circular polarizations RR, LL, and RL. These measurements should characterise backscattering dominated by a single or double bounce scattering mechanism
- the shape and pedestal of the co- and cross-polarized polarimetric signatures
- the extrema of the completely polarized and unpolarized wave components. These are indicative of the heterogeneity of the target's structure (Touzi *et al.*, 1993)

Figure 3.4.1-2 shows the HH, HV, and VV Sigma nought ($\sigma^o$) curves for the forest types studied on July 29 of 1998. The dynamic range of $\sigma^o$ is within 2 dB, and hence the forest types can hardly be discriminated. Notice that backscatter levels in the HH and VV polarizations are almost identical. Under leafy conditions, backscatter measurements in the

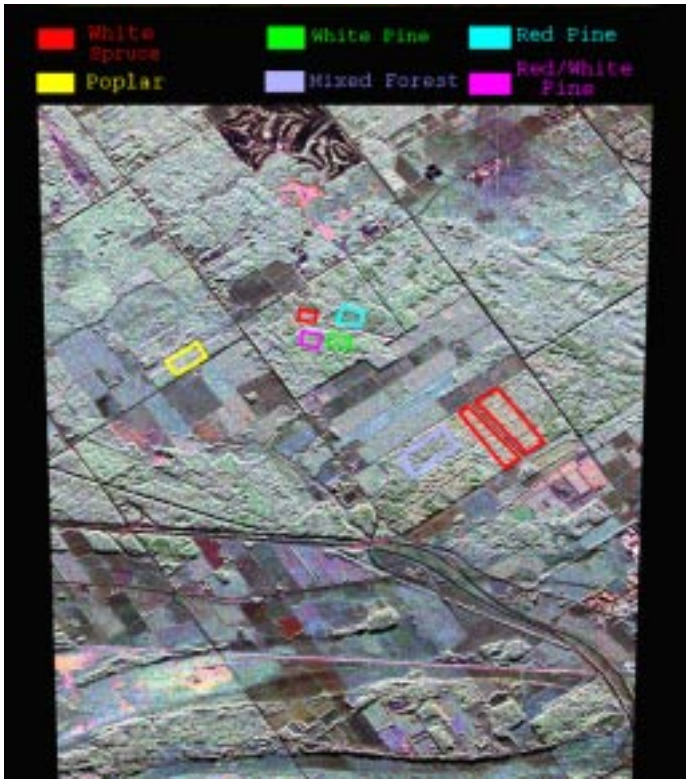


**Figure 3.4.1-1** Mer Bleue study site, showing six forest areas with different species compositions: deciduous / coniferous mixed forest, poplar, red pine, white pine, white spruce, and a red / white pine mixture.

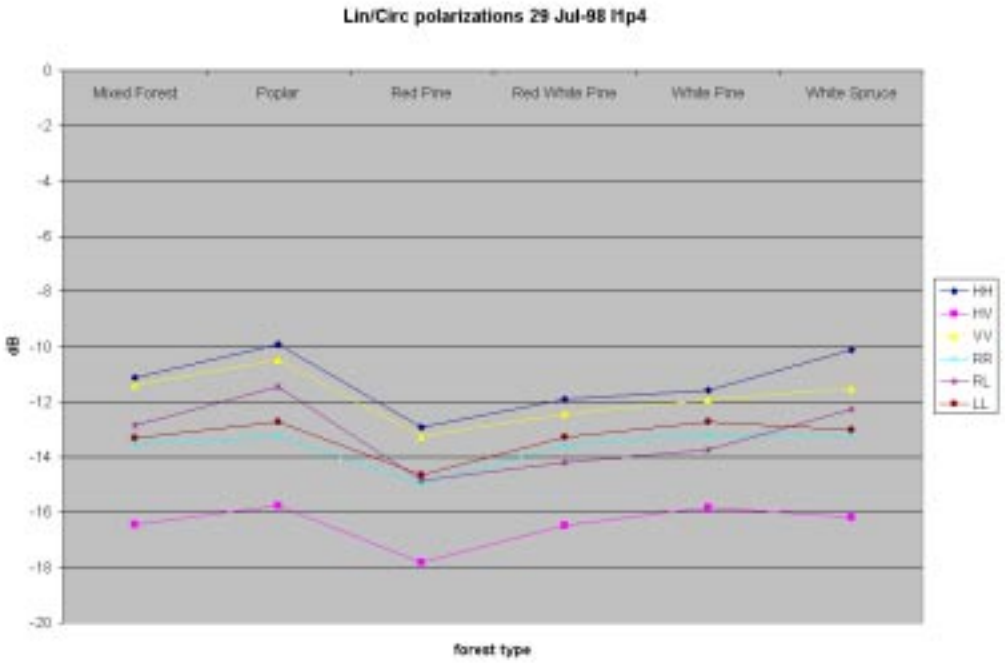


**Figure 3.4.1-2** Linearly and circularly polarized Sigma nought ($\sigma^o$) curves for the forest types studied. Data acquired during leaf-on conditions on July 29 of 1998.

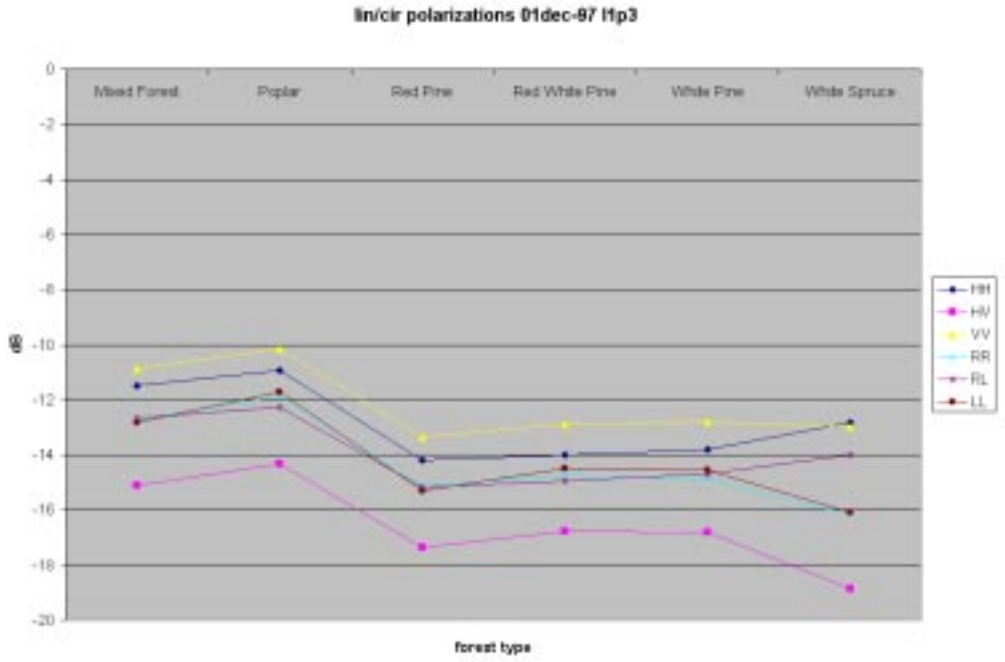


**Figure 3.4.1-3** Linearly and circularly polarized Sigma nought ($\sigma^o$) curves for the forest types studied. Data acquired during leaf-off conditions on December 1 of 1997.

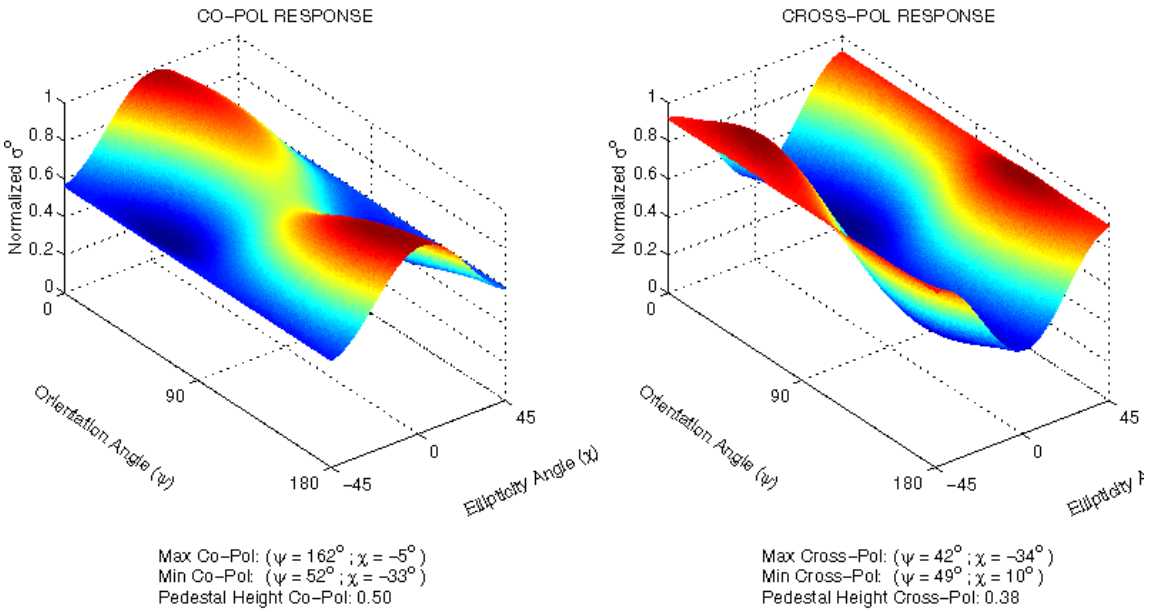


**Figure 3.4.1-4** Co- and cross-polarized polarimetric signatures of white spruce obtained from the data acquired on July 9, 1998.

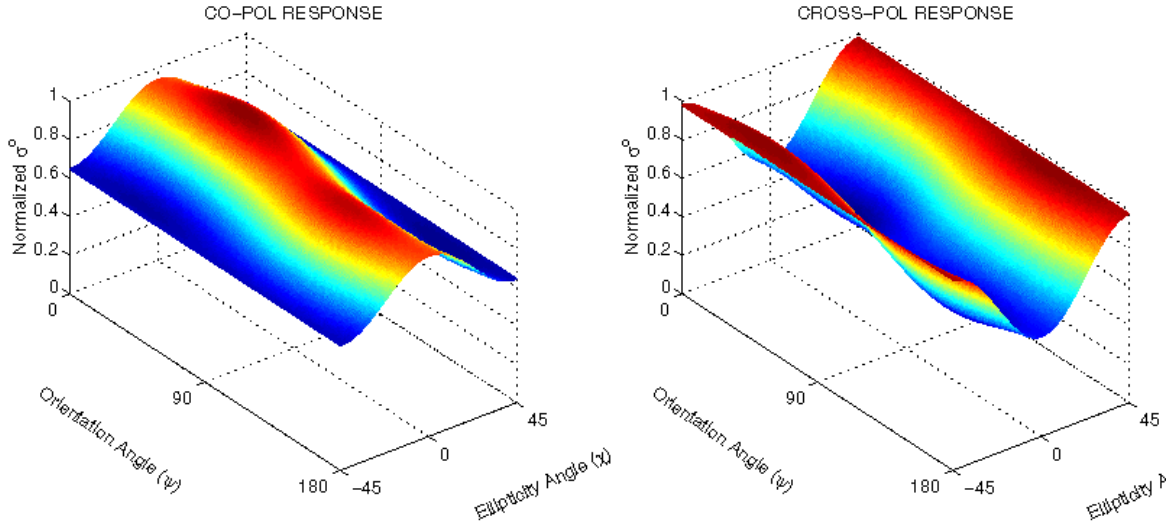


**Figure 3.4.1-5** Co- and cross-polarized polarimetric signatures red pine as obtained from the data acquired on July 9, 1998.

three linear polarizations cannot even be used to distinguish between poplar (broad leaf species) and coniferous species. As shown in Figure 3.4.1-3, linearly polarized images acquired during winter conditions do facilitate the discrimination of poplar and coniferous species. However, the dynamic range in backscatter remains small and other forest types can hardly be discriminated.

Figures 3.4.1-2 and 3.4.1-3 illustrate that the RR, RL and LL polarized radar return signals are also of little value for forest type discrimination. This can be explained from the fact that, in C-band, the backscatter of closed forests mainly results from volume scattering in the upper canopy and lacks significant single or double bounce components. Hence, the circular polarizations do not add to the information available in the linear polarizations. Notice the similarities in the curves for the like-circular (RR and LL) and cross-circular (RL) polarizations. This confirms the insignificance of the simple (single and double) scattering mechanisms.

Polarimetric signatures extracted from summer data show that, with the exception of the signatures for white spruce, the signatures for all other forests studied are largely identical both in shape and pedestal. The figures 3.4.1-4 and 3.4.1-5 present the co- and cross-polarized polarimetric signatures of white spruce and red pine as obtained from the data acquired on July 9, 1998. The signatures for the other forest types, poplar inclusive, resemble those as shown for red pine.

The information contained in the maximum of the completely polarized backscatter component is very similar to that contained in the minimum of the completely unpolarized backscatter component. This is expected, as the two variables, which are indicative of the structural properties of the target observed, are closely related (Touzi *et al.* 1992). The minimum of the completely polarized component for each of the stands studied ranges by

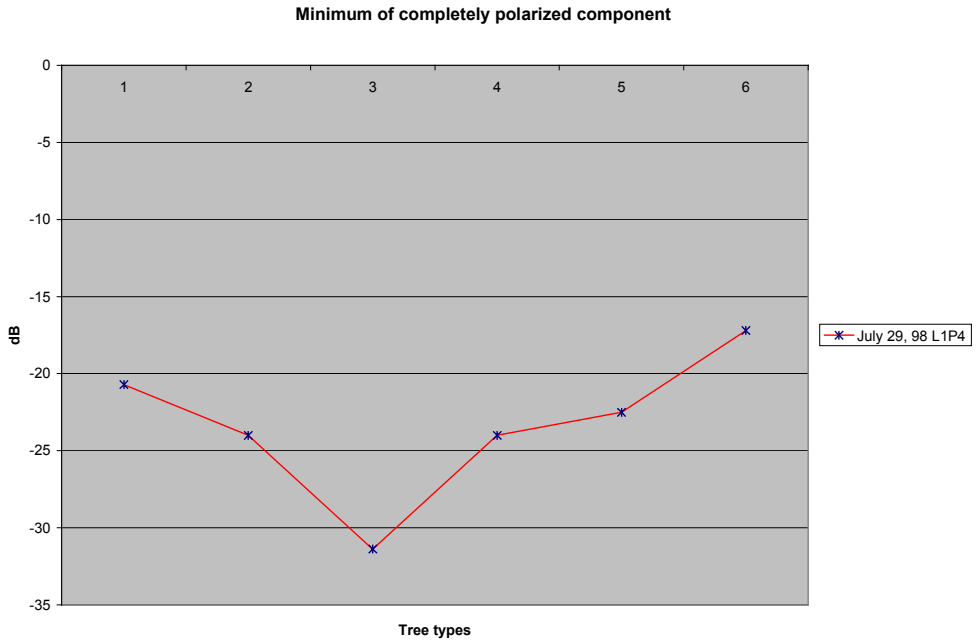


**Figure 3.4.1-6** Plot showing the minimum of the completely polarized component for the species studied.

about 15 dB for the data acquired in July of 1998 (see figure 3.4.1-6). Thanks to the large dynamic range, this variable offers good potential for forest type discrimination.

Several authors have illustrated the value of radar image texture for forest type discrimination (e.g. Hoekman, 1985; Ulaby *et al.*, 1986; Dams *et al.*, 1987; Edwards *et al.*, 1988; Luckman *et al.*, 1997b; van der Sanden and Hoekman, 1999). The new Ultra-Fine and Multi-Look Fine image modes of RADARSAT-2 will certainly add to its potential for forest type mapping by means of textural analysis.

### 3.4.2 Clearcuts

Clearcut mapping has been identified as the most promising application within the forestland application field. RADARSAT-1 has been used successfully to map clearcuts in a boreal environment, although the reported boundary errors are approximately 30 metres (Ahern *et al.*, 1997). The accuracy achieved under the best environmental conditions, that is, wet snow conditions is still considered too low for operational use of the images in the updating of forest inventories for logging activities. Next to the provincially legislated accuracy standards, the terrain relief is the most challenging element to deal with. The effects of the local incidence angle on the radiometry seriously limit the operational application of SAR data for clearcut mapping.

The Ultra-Fine mode data that will be provided by RADARSAT-2 may provide a significant increase on the achievable mapping accuracy of boundary placement. Though, the limited area coverage associated with this mode (20 km by 20 km) will probably cancel-out its gain in spatial resolution.

The clearcut mapping application will benefit most significantly from the added capability of RADARSAT-2 to image in the cross-polarization. Indeed, several studies have shown the advantage of cross-polarization over like-polarization for clearcut mapping (e.g. Ahern and Drieman, 1988; Ahern *et al.,* 1995; Morain and Simonett, 1996; Lee, 1981; Leckie, 1984; Kneppeck and Ahern, 1989). As a rule, the backscatter contrast between the clearcut and the forest is larger in HV than in HH or VV (Figure 3.4.2-1). Hence cross-polarized data make a better basis for the detection and delineation of clearcut areas. The option to acquire both cross- and like-polarized data in the SDP mode will further improve the satellite's potential for application to clearcut mapping.

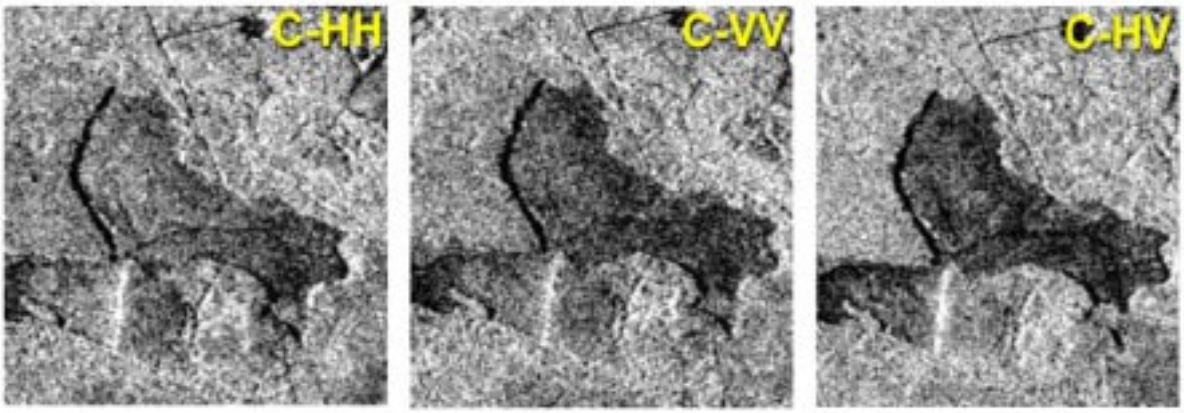


**Figure 3.4.2-1** Forest clearcut area seen in C-HH, C-VV and C-HV SAR imagery. Cross-polarized data provides the best detection and delineation of clearcut areas.

Few researchers appear to have investigated the use of C-band full polarimetric radar data for clearcut mapping. Consequently, it is not well known whether, in terms of information content, there will be any merit in applying this type of data. A definite disadvantage of the images acquired in the RADARSAT-2 QP mode is the limited coverage. There is evidence in literature that the clearcut mapping application would benefit greatly from the availability of SAR satellites that operate in frequencies lower than C-band (e.g. Cimino *et al.*, 1986; Drieman, 1987; Wu and Sader, 1987; Luckman *et al.*, 1997a; van der Sanden, 1997)

Deforestation mapping in dry and humid tropical environments is an application of considerable importance. The generally more relaxed accuracy standards for mapping in these regions facilitate the application of spaceborne SAR data. Then again the application is hampered by the complex and dynamic nature of the occurring forests and clearcuts.

### 3.4.3 Fire-scars

For fire-scar mapping, the single most important new feature of RADARSAT-2 will be the capability to simultaneously acquire data in multiple polarizations. Werle *et al.* (1991) and Landry *et al.* (1995) applied multi-polarized C-band Convair-580 SAR data to the mapping of recently burned boreal forests in northern Saskatchewan. Individual image channels, in particular those with like-polarizations, were found to offer little potential for the identification of recent burns. In fact, the HH-polarized image did not reveal any of the burned areas. It should be noted that these results were mainly based on shallow incidence angle configurations.

Other research has shown that wet soil conditions found at fire-disturbed sites in the boreal environment produce backscatter levels that are higher than those produced by the surrounding unburned forest. However, this holds true only when the data are acquired at steep incidence angles. In images acquired at shallower incidence angles, the contrast in the backscatter from the wet fire-scar and the forest is reversed (French *et al.*, 1998; Landry, 1998).

The increased spatial resolution of RADARSAT-2 is of little value for operational fire-scar mapping since the size of the areas burned will often exceed the 20 km wide swath as provided by the Ultra-Fine beam mode. Swath widths of the order of 50 km are generally required. Images acquired in the cross-polarization will most probably provide the best potential for burn mapping since this polarization is particularly sensitive to structural damage incurred by the forest canopy.

### 3.4.4 Biomass

The relationship between the radar backscatter and the biomass of forests has been studied widely (e.g. Sader, 1987; Dobson *et al.*, 1992; Le Toan *et al.*, 1992; Sun and Ranson, 1993; Beaudoin *et al.*, 1994; Rauste *et al.*, 1994; Skriver *et al.*, 1994).

Most studies reveal that the backscatter reaches a plateau and saturates once the biomass exceeds a certain threshold level. The sensitivity of radar waves to biomass increases with an increase in wavelength. Reported backscatter saturation points correspond to dry biomass levels of the order of 50 t $ha^{-1}$, 100 t $ha^{-1}$, and 200 t $ha^{-1}$ for C-, L- and P-band, respectively. Linear cross-polarized radar waves have often been found to be more sensitive

to biomass than linear like-polarized radar waves. Given this, RADARSAT-2's capability to acquire HV polarized data should be of advantage. Hence, it is expected that areas of low biomass can be monitored more effectively with RADARSAT-2 than with RADARSAT-1. It must be noted however that the use of SAR for biomass mapping is often complicated by factors that include the non-homogeneity of forest stands and relief induced backscatter variations.

There is no conclusive evidence in literature that full polarimetric data offer more potential for biomass estimation than linearly polarized data. Still full polarimetric data have the advantage that they provide information on the dominant scattering mechanisms and through this on the governing scattering sources.

## 3.5 Geology

Geological interpretations of terrestrial landforms are traditionally made using optical data sources, however where optical data is not available (regions with frequent cloud cover), SAR data has at first been used as a substitute. SAR data provides at once a synoptic perspective and great spatial detail in a consistent manner for almost anywhere on Earth. With increasing SAR application development, an appreciation of the information content of the data has grown among users as radar proves to provide geophysical terrain information that optical data cannot. In some cases, this includes surface roughness information that is useful for understanding processes of bedrock weathering and sorting of unconsolidated surface material. More sophisticated applications are involved with interferometric processing of SAR data pairs for precise mapping of terrain displacements.

Terrain mapping activities are related to the geology of surface, or unconsolidated deposits. Traditional geological mapping of bedrock is concerned with rock type identification, or lithological mapping, as well as understanding the three-dimensional geometrical arrangement and juxtaposition of different rock units that comprise the geology. Rock structures of importance that are mapped include the outline of the fold patterns of deformed rock layers and location and orientation of faults and fractures in the bedrock. Knowledge of geology is paramount for the assessment of a region's resource potential. Aerial photographs, geological maps and geophysical data are used together to assist the geologist to devise an exploration model in the search for non-renewable resources. Additional geologic information derived from remotely sensed SAR data can improve the chance of success and often the assimilation of SAR data into geological data sets for this purpose is accomplished through data fusion techniques.

### 3.5.1 Terrain mapping

The most significant improvements of RADARSAT-2 over other space-borne radar and optical systems for terrain mapping are its Ultra-Fine mode (spatial resolution 3 m by 3 m) and full polarimetric capability. The RADARSAT-2 Ultra-Fine mode data will permit detailed mapping of glacial terrain features, outcrops and fine geological structures. As such, its uses for terrain mapping will exceed those of RADARSAT-1 (Saint Jean *et al.*, 2000). Through fusion of Ultra-Fine mode RADARSAT-2 data (and high resolution optical data) with high resolution DEMs it should be possible to produce surficial geological maps at the scale of 1 : 20,000.

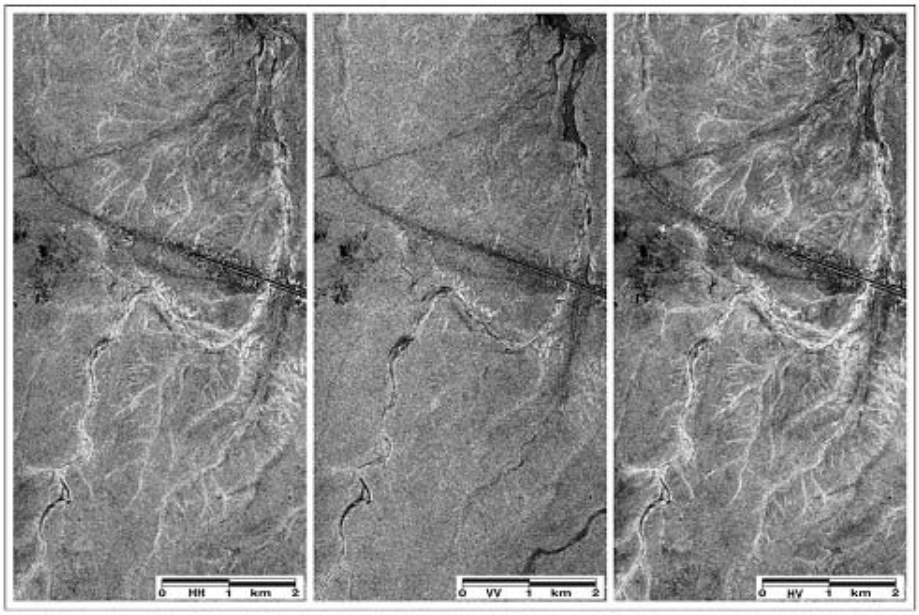


(a) (b) (c)

**Figure 3.5.1-1 (a-c)** Airborne SAR images showing the Azraq oasis in Eastern Jordan (**a**) C-HH image (**b**) C-VV image (**c**) C-HV image. The C-HV image makes the best basis for the delineation of surficial units and the distribution of wadis.

Thanks to geobotanical relationships the properties and extent of surficial deposits and rock units are often reflected in the nature and structure (e.g. architecture, density, distribution) of the overlying vegetation. Hence, these relationships allow for the mapping of surficial deposits and rock units based on vegetation characteristics. Singhroy (1996) reports on the correlations between outwash plains and vegetation types and ultra-mafic rocks and vegetation density. It is well known that the polarization of radar backscatter is primarily a function of the structural properties of the objects observed. Therefore, it is expected that the multi-polarized and fully polarimetric capabilities of RADARSAT-2 will improve its potential for the mapping of surficial deposits and rock units in vegetated terrains.

The mapping of recharge terrains in arid areas is fundamental for water harvesting and groundwater exploration. Figure 3.5.1-1 shows C-band HH, VV and HV images that were acquired by the Convair-580 SAR over the Azraq oasis in Eastern Jordan on December 8, 1993. Comparison of the three images clearly illustrates that the information content of the C-HV image exceeds that of the other two images. Hence, the C-band HV image offers the most potential for delineating surficial units and wadi distribution in recharge areas of sensitive surface aquifers (Singhroy *et al.* 1996; Saint Jean *et al.* 1996). Accordingly, RADARSAT-2 images are expected to make a better source of information for groundwater exploration than images from RADARSAT-1.

Interferometric synthetic aperture radar (InSAR) applications in the Earth Sciences have been on the increase since the seminal paper by Massonett *et al.* (1993) on the mapping and modelling of terrain displacement following the Landers Earthquake in California. Several research applications have since been published, including the mapping of the displacement field of the Kobe Earthquake in Japan using L-band (JERS) data. Other successful InSAR results have come from demonstrating terrain displacements around

volcanoes and land subsidence around underground mines and operating oil wells (e.g. Amelung *et al.* 1999, 2000; Fielding *et al.*, 1998; Lukowski *et al.* 2000). InSAR data provides quantitative, millimetre-scale estimates of terrain movements. For the Earth Sciences, InSAR applications hold great promise for monitoring of terrain movements of tectonic origin as well as those resulting from human activity (Armour *et al.*, 1998). Successes achieved with InSAR processing of data pairs over long intervals of time indicates that 24-day repeat-pass RADARSAT-2 data will be able to provide valuable future data sets for some applications. Thanks to improved orbit knowledge and control, RADARSAT-2 can be expected to offer more potential for InSAR based applications than RADARSAT-1.

### 3.5.2 Structure

Structures related to volcanic edifices, such as cones and calderas, have a morphological expression which stand out in relief. These topographic changes are easily mapped with SAR due to the changes in the average local slope (MacKay and Mouginis-Mark, 1997). Active volcanoes are difficult to monitor directly due to the extreme hazard and remote sensing with optical imaging systems is typically impeded by clouds of smoke and ash during eruptive cycles. SAR imaging is able to detect the changing morphology of the eruptive centre (Lukowski *et al.*, 2000).

Active faulting, differential erosion along ancient faults or along lithological boundaries exhibit some topographic expression which can be recognised in SAR images of almost any polarization provided the resolution is comparable to the features. Single polarized (HH or VV) SAR images have traditionally provided terrain information. Structural features with a subtle expression of topographic relief are enhanced due to the sensitivity of radar backscatter to the local incidence angle. Although incidence angle is significant, the most important parameter for this type of landform information is the resolution of the SAR imaging system.

For most land applications, like-polarized data (HH or VV) have very similar information content due to a similar backscatter response from rough surfaces or through volume scattering. Cross-polarized data (HV or VH) are more sensitive to the larger scale (larger than the radar wavelength) geometry of the surface or volume scatterers (Schaber *et al.*, 1997). The cross-polarized data is therefore sensitive to areas of extreme surface roughness or where abrupt changes in relief occur (escarpments) to cause depolarization of the radar return (Huadong, 1997; Schaber *et al.*, 1998). Bedrock fracture zones and fault scarps are typically highlighted by a much stronger contrast in backscatter returns relative to the surroundings in cross-polarized data than in like-polarized. In arid environments, at C-band, imaging depths are expected up to 0.5 m, thus permitting the recognition of bedrock structures beneath sand sheets (Schaber *et al.*, 1998).

### 3.5.3 Lithology

The wide range in surface roughness of volcanic lava flows often illustrates the best examples for discrimination of different flow units, however lithological discrimination among other rock types, such as sedimentary or metamorphic rock types, is considerably more challenging with a single polarization state and radar frequency. The advantages of multipolarized SAR, particularly the dual combination of a like- and cross- polarized data pair for discriminating different geologic units, has been endorsed by several researchers

(Dellwig and Moore, 1966; Daily *et al.*, 1978; Evans *et al.*, 1986; Schmullius and Evans, 1997). Most recent findings are based on studies using the JPL-AIRSAR system and the SIR-C/X-SAR experiment. Blom *et al.* (1987) recommend multifrequency and multipolarized SAR data to provide additional radar information to improve lithological discrimination.

Evans and van Zyl (1990) reviewed the important influence SAR wavelength has on radar backscatter characteristics and the advantages of simultaneous SAR data acquisitions at two or more wavelengths. For example, recent studies have shown that vegetated and barren geologic units are best discriminated at L-band, whereas distinguishing types of recent lava flows, such as smooth phahoehoe from rough a'a, are better determined at C- or X-band (Gaddis, 1992; MacKay and Mouginis-Mark, 1997). In many case studies, cross-polarized SAR yields a greater contrast than co-polarized data for mapping individual flow units or other geological units.

Most researchers conclude that at a minimum, dual-polarization radar is a requirement for single frequency (e.g. C-band) SAR systems and the addition of another radar frequency band (i.e., L-band) presides over polarimetric capability (see Schmullius and Evans, 1997). Evans *et al.* (1988) demonstrated that optimal polarization states can be determined from polarimetric SAR data to maximize the contrast between polarized or unpolarized returns. Better discrimination is possible between geologic materials (bedrock or surficial deposits) if the scattering mechanisms are different, although the new images derived from polarimetric data to maximize this do not appear to provide a significant increase in information content over standard like- or cross-polarized images. In arid environments, migrating and inactive sand dunes are best distinguished in cross-polarized data (Blumberg, 1998) whereas different types of dunes can be recognised from like-polarized SAR data. Investigations of dune fields illustrate the complementary value of dual-polarization data sets.

If a single radar frequency and polarization state must be chosen for geological applications, cross-polarized L-band has the greatest information content (Schaber *et al.*, 1997; Schmullius and Evans, 1997). However, for bedrock mapping applications, cross-polarized C-band images have a similar information content to like-polarized L-band (D'Iorio *et al.*, 1996; Huadong *et al.*, 1997) and cross-polarized data at all bands provides a strong contrast between vegetated and non-vegetated terrain types (Evans *et al.*, 1986; Blumberg, 1998).

## 3.6 Hydrology

Water is the most precious resource on the earth. It is a basic necessity and without it we would not survive, however it is also one of the most utilised and abused resources. Our global community will continue to experience increased pressure on our water resources, therefore the need to understand the hydrological processes that distribute water around the globe is more important than ever. Remote sensing offers the ability to derive hydrological parameters over a large spatial area, in a timely fashion, and less expensive relative to labour-intensive ground surveys. Furthermore, the area of coverage required for most hydrological parameters is quite large, as hydrological models are typically run at the sub-watershed or watershed basin scales, which requires regularly updated information at regional scales.

Radar imagery is well suited for hydrological applications as the scattering properties for water and land are extremely different, resulting in differences in radar return for both of these features. Water areas are associated with low radar returns due to specular

reflection, whereas land and vegetated areas are associated with medium to high returns due to diffuse scattering. Radar is extremely sensitive to changes in the dielectric constant which makes it a suitable choice for remote sensing of hydrological parameters such as soil moisture, snow studies, wetlands and for mapping watershed components. Cloud cover often occurs with hydrological events and in coastal regions thereby limiting the use of most remote sensing techniques except for SAR sensors. Due to the reliability of collecting SAR data in all weather conditions, a majority of remote sensing hydrological studies incorporates SAR imagery into their data sets.

RADARSAT-1 has demonstrated the ability of SAR spaceborne sensors for hydrological monitoring in many cases such as flooding events, wet snow mapping, and soil moisture. The ability to acquire timely images in all weather conditions have proven useful for the remote sensing community, resulting in many new radar users. The C-band HH configuration, with various beam modes (resolutions and incidence angles) have enabled clients to custom the radar images to their specific application. RADARSAT–2 will continue to operate using the same configurations as RADARSAT-1, with new choices of resolution, look direction and polarimetric capabilities. This will enhance the information available for hydrological studies by increasing the availability of data spatially and temporally, while providing even more choices for the end user.

### 3.6.1 Soil moisture

Soil moisture is an important parameter for many natural resource applications such as hydrological modelling, stream flow forecasting, agricultural practices, and flood forecasting. Decision makers and resource managers require timely, accurate measurements of soil moisture to manage the resources in watersheds and basins. The amount of moisture in the soil is dependent on a variety of elements including the amount of precipitation, temperature of air and soil, evaporation, soil type, slope/aspect, and land cover. Radar remote sensing is ideal for mapping soil moisture due to the sensitivity of radar to moisture (changes in the dielectric constant) and the ability to image through cloud cover, independent of sunlight. The radar response (tone and texture) of an image depends on the radar system parameters (wavelength, polarisation, incidence angle, viewing geometry) and the target parameters (dielectric constant, surface roughness, vegetation cover). An increase in either the dielectric constant, or the roughness of the surface will cause an increase in the amount of backscatter; it is this relationship between the dielectric constant and radar backscatter that enables measurements of soil moisture.

A linear relationship exists between volumetric surface soil moisture and radar backscatter for bare soil agricultural fields, however the difficulty arises when a vegetation cover is present (Moeremans and Dautrebande, 2000). Vegetation complicates the retrieval of soil moisture measurements from radar images, as the radar interacts with the vegetation and is affected by the physical structure and moisture within the biomass. The degree of radar interaction is dependant on the amount of penetration into the vegetation cover, which is determined by the wavelength employed in relation to the vegetation structure (the larger the wavelength the greater the penetration). Prevot *et al.* (1993) found that horizontally polarized radar are better than vertically polarized (VV) radar for vegetated soil due to the greater penetration into the vegetation cover, thereby increasing the interaction with the underlying soil surface.

In general, longer wavelengths are more useful for soil moisture studies, as the sensitivity to

surface roughness is decreased and the penetration depth is increased. Pultz *et al.* (1997) concluded that HH polarisation at C-Band is less sensitive to surface roughness than VV or HV. Soil moisture values can not be derived without accurate surface roughness measurements, as Altese *et al.* (1996) has reported the sensitivity to the roughness parameter is higher than the sensitivity to dielectric constant on bare agricultural fields. Many authors have noted that incidence angles between 20-50° are best for monitoring soil moisture (Oh *et al.*, 1992; Brown *et al.*, 1993). However, the decrease in radar backscatter as a function of incidence angle must be taken into consideration when comparing fields over a wide range of incidence angles. Pultz *et al.* (1997) noticed a decrease of 3 dB between incidence angles of 38 – 54, resulting in a change in backscatter of 0.2/degree (assuming a linear relationship). These studies developed relationships between soil moisture and radar backscatter using the top 10 cm of the soil profile on relatively flat land, although some studies stated that better correlations occurred when a smaller profile (closer to the air/soil interface) was used (Pultz *et al.*, 1997; Galarneau *et al.*, 1998).

Radar sensors have been used for soil moisture mapping for the past few years with varying success. Many studies have utilised space-borne satellites including ERS-1 & 2, J-ERS (Maxfield *et al.*, 1996; Taconet *et al.*, 1996; Wagner *et al.*, 1999; Quesney,*et al.*, 2000), RADARSAT-1 (Seglenieks *et al.*, 1998; Galarneau *et al.*, 1998) and other platforms such as space-borne shuttles (Pultz *et al.*, 1997; Shi *et al.*, 1996) and airborne systems like the Convair (Geng *et al.,* 1996) and AIRSAR (Shi *et al.,* 1996; Duncan *et al.*, 1994).

Extensive soil moisture research was conducted using the SIR-C/X-SAR instrument during the 1994 and 1996 space shuttle mission in southern Manitoba, surrounding the town of Altona, Manitoba. In one study published by Pultz *et al.* (1997), the authors examine temporal changes in C- and L-band radar for soil moisture on bare agricultural fields. Environmental factors such as frost and extremely high soil moisture measurements altered the radar backscatter, indicating the ability to monitor these conditions; however, under these conditions the accuracy of derived soil moisture values are affected. The results indicate a strong correlation of 0.84 for the 0-2.5 cm soil profile at C- and L-band HH, with decreasing soil moisture correlation as the soil profile increased (Table 3.6.1-1).

For the past several years, the Mississippi River watershed located immediately west of Ottawa, has been investigated by the Canada Centre for Remote Sensing, the Mississippi Valley Conservation Authority, and Kije Sipi Limited (a local water resources and

**Table 3.6.1-1** Multiple correlation statistics for radar backscatter and soil moisture and incidence angle. April and October data combined. All correlations significant >95% confidence level; n is # of observations, r is correlation coefficient, see is the standard estimation of error.

| | Profile depth (cm) | | | | | | | | | | | |
|---|---|---|---|---|---|---|---|---|---|---|---|---|
| | 0 – 2.5 | | | 0 - 5 | | | 0 -10 | | | 0 - 15 | | |
| **Band** | **n** | **r** | **see** | **n** | **r** | **see** | **n** | **r** | **see** | **n** | **r** | **see** |
| C-HH | 119 | .843 | 1.5794 | 116 | .799 | 1.6782 | 117 | .782 | 1.7509 | 117 | .771 | 1.7883 |
| C-HV | 119 | .537 | 1.5177 | 116 | .437 | 1.6296 | 117 | .424 | 1.6770 | 117 | .390 | 1.7051 |
| C-VV | 43 | .544 | 1.4326 | 46 | .527 | 1.4421 | 46 | .532 | 1.4371 | 46 | .529 | 1.4402 |
| L-HH | 119 | .833 | 2.2840 | 116 | .791 | 2.4837 | 117 | .787 | 2.4923 | 117 | .790 | 2.4752 |
| L-HV | 119 | .671 | 2.5397 | 116 | .594 | 2.6635 | 117 | .578 | 2.7114 | 117 | .580 | 2.7076 |
| L-VV | 43 | .526 | 2.5628 | 46 | .527 | 2.4855 | 46 | .505 | 2.5244 | 46 | .499 | 2.5337 |

environmental consulting company). Soil moisture research campaigns have been conducted on the Mississippi watershed and a sub-watershed of this basin, the Carp watershed (J.F. Sabourin and Associates Inc., 1998). The Mississippi Watershed basin encompasses over 4,000 km2 and is composed of a network or rivers, forest regions, urban areas and agriculture land (Figure 3.6.1-1). The study sites are distributed throughout the basin, and range from the forested Precambrian rock structures in the west to the agricultural Champlain Sea Clays in the east.

Previous soil moisture research in the Mississippi region was conducted on bare soil fields with successful results. Multi-date RADARSAT-1 images were correlated to field soil moisture data over a large range of incidence angles (18-28°) and soil moisture conditions (5 – 39%) in 1996/7. A correlation value of 0.95 was attained from averaged RADARSAT-1 backscatter and soil moisture when incidence angles were incorporated into the calculations (J.F. Sabourin and Associates Inc., 1998). Soil moisture maps were generated and compared to total antecedent precipitation maps, generated from ground based weather radar, which resulted in categorising soil moisture content into ranges of 5 classes from wet to dry soils. Currently, a soil moisture campaign is being conducted in the Carp sub-watershed for the fall/spring of 2000/01 which is aimed at assessing the capabilities of SAR data (both RADARSAT-1 and polarimetric airborne Convair-580 data) to retrieve soil moisture estimates over pasture lands. This collaborative effort has advanced the use of remotely sensed data in water resources management by demonstrating the integration of RADARSAT-1 data with *in-situ* data to derive soil moisture conditions to aid water management operations.

The extraction of soil moisture measurements from radar images requires substantial supporting information and parameters before algorithms can be utilised. Many of the parameters discussed previously affect the radar signals, independently of the moisture content, and must be account for. Authors have noted the importance of continued research

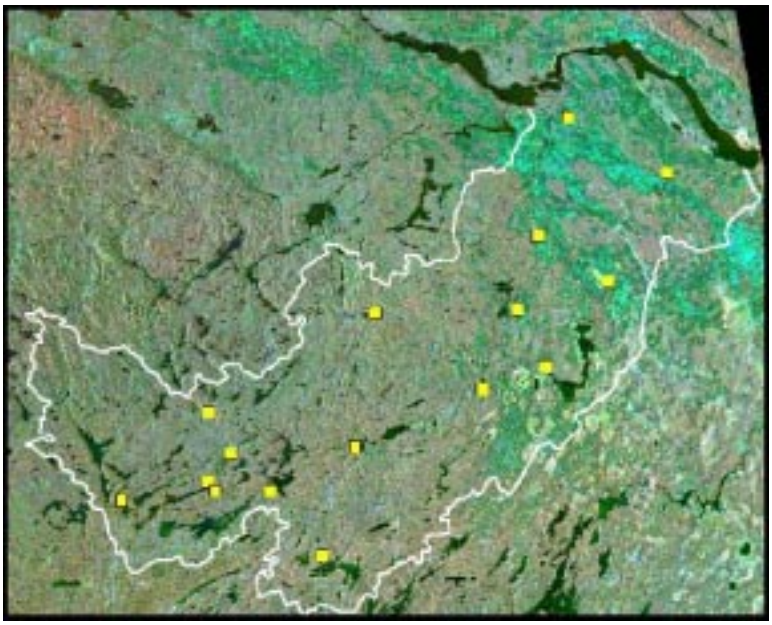

**Figure 3.6.1-1** Landsat-7 image of the Mississippi Watershed with sample sites identified in yellow and the watershed boundary in white.

on radar parameters affecting the retrieval of soil moisture measurements and algorithms (Engman and Chauhan, 1995; Wagner *et al.*, 1999). Although the procedure to generate soil moisture measurements from radar signals is quite complex, the benefits of having timely, regional coverage outweighs the complexity. Developing reliable and cost effective techniques to utilise remotely-sensed data in water resources management will assist water managers in overcoming current deficiencies in spatial coverage from just using in-situ monitoring methods. The launch of RADARSAT-2, with the varying beam modes (resolution and incidence angles) and polarimetric capabilities will provide increased data availability as well as enhanced information content for soil moisture activities.

### 3.6.2 Snow

Snow parameters are extremely important for input to hydrological models and for understanding changes in the climate system due to global warming. Remote sensing of snow parameters such as snow extent, snow water equivalent (SWE), and wet/dry state have been investigated by numerous researchers using various sensors, some to a greater degree of success than others (Goodison *et al.*, 1984; Shi, 1994; Pultz and Crevier, 1996; Bernier and Fortin, 1998). Ground-based observation stations are often very sparse and unevenly spatially distributed, while ground measurements are labour intensive, time consuming, and expensive compared to the regional coverage provided by remote sensing techniques. Microwave remote sensing techniques have an advantage over optical methods in that they have all-weather imaging capabilities, and are independent of sunlight, thus increasing image acquisition opportunities. Changes and complexities in the snow pack structure will alter radar scattering mechanisms and allow for estimates of snow parameters to be made.

SAR sensors are highly sensitive to changes in the dielectric constant and have a better spatial resolution than their passive counterparts. The relationships between snow pack characteristics and radar backscatter are quite complex. Many inconsistencies in the literature exist pertaining to the relationship between SWE and snow parameters to airborne and satellite SAR imagery (Bernier and Fortin, 1998; Leconte and Pultz, 1990). SAR backscatter is influenced by a number of parameters including surface roughness, topography, land cover, incidence angle and moisture content. Multi-polarized or polarization diversity SAR systems can transmit microwaves with either a horizontal (H) or vertical (V) polarization towards the target of interest. The scattered wave received at the sensor is a function of the geometric characteristics and physical properties of the ground target. Polarimetric SAR systems provide information on the complete scattering matrix of targets and permit the synthesis of all possible transmit-receive polarizations. By retaining the phase information, a number of other parameters can be generated to characterize the interaction of electromagnetic waves with targets of interest. For dry snow packs, at C-band wavelengths, the radar penetrates through the snow, where the dominant scattering occurs at the snow/ground interface (Leconte, 1996, Shi *et al.*, 1993). Reduced radar penetration occurs in a wet snow pack as the increase in dielectric constant results from the presence of liquid water (Sokol *et al.*, 1999)

One of the main obstacles in both passive microwave and polarimetric SAR remote sensing of snow cover are the complexities of the snow structure itself. As the snow pack ages, metamorphism occurs causing the snow structure to develop layers of various grain sizes, densities, bonding and textures. With passive microwave sensors, the energy is emitted from the soil layer and travels towards the air/snow interface; the entire snow pack structure

is relevant and must be accounted for. With radar remote sensing techniques, microwave energy is transmitted towards the snow surface, where this energy can penetrate into the snow structure, can be absorbed or scattered from the snow and/or ground surface or a combination of these processes can occur. Rott *et al*. (1992) concluded that at C-band frequencies, only the first few centimetres of the snow pack actually contributed to the backscattering, whereas at P-band the contribution included a few meters of the snow pack. A number of studies has been conducted to theoretically model the snow pack and understand the radar backscatter under different snow conditions (Leconte, 1996; Kendra *et al.*, 1998). These studies looked at soil state (frozen or not) as well as scattering mechanisms at the snow/soil interface and the snow/air interface, for varying snow depths and densities.

Surface roughness effects must not only be accounted for in soil moisture studies but also in snow research. Depending on the state of the snow, the radar may penetrate through the entire snow pack and interact with the snow/soil boundary. Surface roughness is measured on bare fields and values are represented as the standard deviation of the surface height variation (RMS) in millimetres. Rott *et al.* (1992) analyzed C-, L-, and P-band polarimetric AIRSAR data to investigate wet snow and the effect of surface roughness. This study notes the importance of surface roughness to C- and L-band data and the increasing importance of the volume contribution from C-band to P-band, where effects of incidence angles are most predominate at C-band.

Continuous monitoring of the snow conditions in mountainous regions is only possible with SAR imagery due to unstable weather conditions in these areas (Haefner and Piesbergen, 1998). A great deal of research on seasonal snow cover has been conducted in mountainous and alpine areas (Shi and Dozier, 1997). Geometric corrections of terrain distortions (using a DEM) are mandatory for quantitative analysis of SAR data in high relief areas. A variety of methods have been applied to geometrically and radiometriclly correct SAR data. Wet snow classifications were performed using ERS-1 data in the Swiss Alps by calculating the ratio between radar backscatter of a snow-free image and a snow covered scene (Haefner and Piesbergen, 1998)

Common snow parameters estimated by SAR techniques include SWE, snow extent, and snow wetness; although snow depth, grain size, and snow pack structure have also been investigated. Snow water equivalence is one of the most important parameters in snow hydrology, as it impacts most resource management activities including flood forecasting, agriculture, hydroelectric power, and storm water management. Researchers have used SAR data to estimate SWE, some with positive results and others unable to establish relationships. Bernier (1994) used ERS-1 data to estimate SWE values by using a ratio equation between snow images and no-snow images basing the relationship on the underlying soil temperature which is related to the thermal resistance of the snow pack. Ulaby and Stiles (1981) developed positive correlations between SWE and radar backscatter, whereas Leconte and Pultz (1990) established an inverse relationship with C-band radar and SWE. Mapping areal extent and the onset of snow melt (by mapping wetness) is helpful to resource managers, as information on the spatial pattern of spring melt is important for hydroelectric power and flood forecasting. This information is also beneficial to climate change research as the temporal pattern of the onset of snowmelt can indicate changes in climate. A number of classification algorithms have been developed to discriminate dry snow from wet snow.

In one study conducted by Sokol *et al.* (1999), coincident airborne polarimetric C-band SAR data were collected on December 1, 1997, March 6, 1998, and March 12, 1998, over two study areas in Eastern Ontario, Canada. Field measurements of snow pack properties and weather conditions were gathered along flight lines on bare agriculture fields during each airborne data acquisition. The multi-temporal, polarimetric data were analyzed with respect to changes in the SAR polarimetric signatures and microwave brightness temperatures as a function of changing snow pack parameters. Results indicate differences in radar backscatter from the three sampling dates, which represented distinct changes in snow conditions. Backscatter measurements in the HH, HV and VV polarizations show evidence of snow state; on March 6/98 (wet snow date) the measurements were up to 8 dB lower than the other two dates (dry snow). The pedestal height parameter also exhibited significant changes between dates, indicating a decrease in volume scattering on March 6$^{th}$ (wet snow date), and increasing values with increasing snow structure. Differences in total backscattered power appear to reflect the changes in dielectric constant over the three acquisition dates, showing similar values for December 1$^{st}$ and March 12$^{th}$ and significantly lower values for March 6$^{th}$. Co-polarized phase difference parameter and the linear ratio values did not exhibit substantial variations between sample dates, and therefore these parameters were not sensitive to the ground conditions investigated in this report.

Authors have noted that single frequency and polarization SAR data can be used to extract snow parameters, however better results can be found when using multi-frequency polarimetric SAR data (Haefner and Piesbergen, 1998; Sokol *et al.*, 1999).

### 3.6.3 Wetlands

Wetlands are an important component in the hydrological cycle and are involved in patterns of evaporation, transpiration, water distribution and flow. Wetlands can help control changes in water quality and quantity by lowering flood crests, reducing erosion, supporting ground water recharge and filtering toxins and sediments. They are also valuable from a biological point of view, supporting unique plants and animals, acting as carbon sinks, and producing organic matter, such as peat. The most commonly known benefits of wetlands are the recreational, educational, aesthetic and commercial aspects, which can often be in conflict with one another. Wetland classification and monitoring are the first steps to protecting these valuable resources.

Few research studies have been able to utilise fully polarimetric data to study wetland environments, as the sensor capabilities have not been easily accessible and the data not widely distributed. Many studies have used single channel linearly polarized data sets or at best have utilised two sensors with different wavelengths. The C-Band Shuttle Imaging Radar (SIR-C) experiments, Environment Canada's Convair-580 aircraft and JPL's AIRSAR are main sources of polarimetric data. C-band ERS-1 (VV) and RADARSAT-1 (HH) data are used extensively due to their long-term history and current availability for regions all over the world. JERS-1 data (L-HH) are also used in wetland studies and have been found to be more successful than other sensors for wetland mapping (Yamagata and Yasuoka, 1993). The Convair-580 data has been used in wetland studies (Sokol *et al.*, 1998), however due to the logistics and the cost of employing this airborne sensor the use of the data has been limited. SIR-C and airborne polarimetric systems (AIRSAR) collect data in specific bands, including P, L, and C. More commonly, C- and L-band frequencies with like polarizations (VV and HH) are collected on airborne systems due to the ability to use the results for space borne studies.

The best frequencies and polarisation for radar detection of wetlands depend on the type of wetland, water levels, vegetation structure, density and height (Sokol, *et al.*, 2000; Kasischke and Bourgeau-Chavez, 1997). P- and L-band (low frequency radars) are more suitable for detecting flooding under forests and dense vegetation types, whereas C-band data is better suited for herbaceous and sparse density wetlands (Kasischke *et al.*, 1997). Pope *et al.* (1997) reports that C-HH and C-VV are excellent at detecting flooding conditions in dense marsh communities and C-VV is superior to C-HH for detecting flooding in low density marsh sites. Yamagata and Yasuoka (1993) report that JERS-1 (L-HH) was superior over C-VV at distinguishing wetland classes, especially for bog and inundated vegetation sites. C-band HH shows some sensitivity in flooded forests only if little or no leaf structure exists, and C-band VV is even less sensitive in flooded forests. For X- and C-band, both VV and HH polarizations are good for non-woody wetlands and herbaceous wetlands (Kasischke and Bourgeau-Chavez, 1997). C-band HH (RADARSAT-1) and VV (ERS-2) multi-temporal data indicated minimal separability between bogs and fen wetlands in Atlantic Canada (Sokol *et al.*, 2000). The phase difference parameter increased significantly in all types of flooded marsh communities due to an absolute or relative increase in double-bounce compared with single-bounce interactions (Pope *et al.*, 1997). C-band phase difference was more sensitive to flooding conditions than L-band phase difference.

In one particular study, RADARSAT-1 C-Band HH and ERS-2 C-band VV data was used to investigate wetlands in Atlantic Canada during the summer of 1999 (Sokol *et al.*, 2000). As persistent cloud cover often limits the utility of optical data in Atlantic Canada, the value of using the all-weather capabilities of radar data is evident. Temporal sequences of RADARSAT-1 images were acquired in May, June and August 1999 (Figure 3.6.3-1), during which four RADARSAT-1 scenes, with incidence angles spanning 20-49° (Standard 1, 4, 7 and Fine 1) were acquired for each time period. Throughout the study period, 6 ERS-2 images were also acquired.

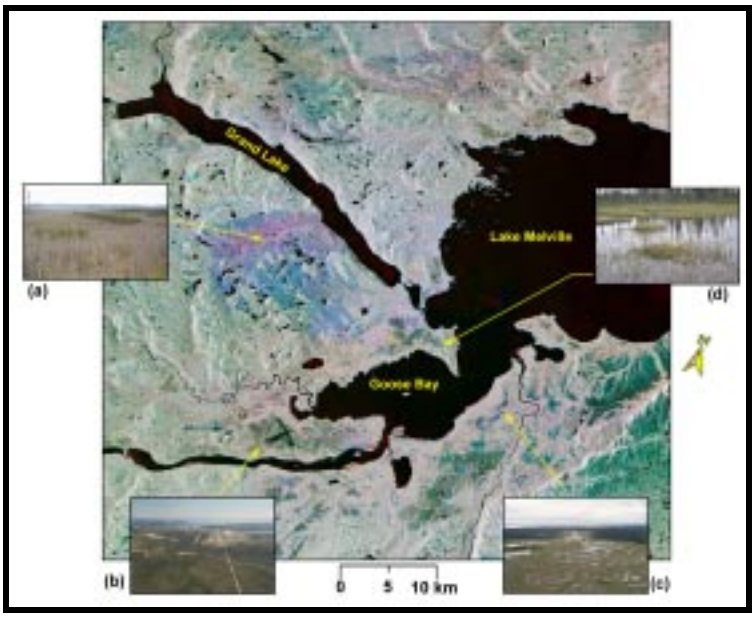


**Figure 3.6.3-1 (a-d)** Colour composite of Goose Bay, Labrador created from three 1999 RADARSAT-1 images (R=May 9, G= July 6, B= August 13). Ground photos of the region: (**a**) Grand Lake burn; (**b**) Happy Valley/Goose Bay Airport; (**c**) Wetland near Kenamu River; (**d**) Fen environment.

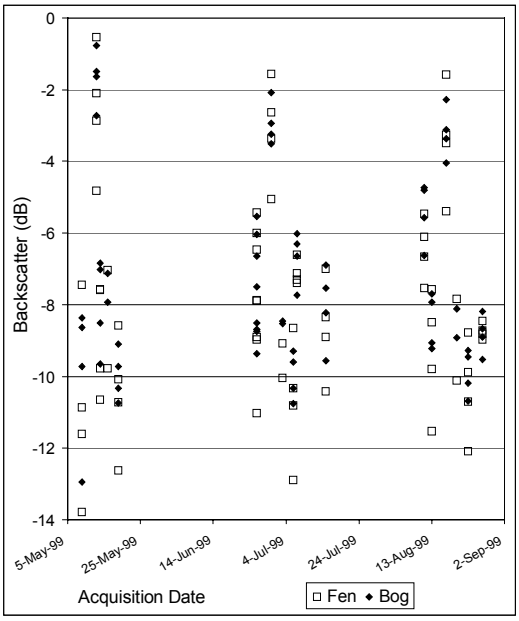


**Figure 3.6.3-2** Temporal sequence of Beta nought (β°) by wetland type.

Overall, little change in backscatter occurs temporally in these wetland targets, indicating the environments are not very dynamic from the May to August time period. ERS-2 values are only slightly more variable than RADARSAT-1 values, but could result from the mix of ascending and descending orbits, taken at different times during the day. For each beam mode, values for the wetland sites remain relatively unchanged over the temporal sequence. This may be due to the cool, short growing season in the Goose Bay region and the lack of nutrients in these wetlands (peat wetlands). No significant differences in backscatter values between bog and fen wetland classes are evident over the temporal sequence of images (Figure 3.6.3-2). The separability between these two wetland types, at all values from various beam modes and ERS-2 values, are minimal.

A research investigation along the shores of the St. Lawrence River utilised airborne fully polarimetric data collected by Environment Canada's Convair-580 aircraft. On September 1, 1997 C-band airborne polarimetric SAR imagery was acquired over wetland environments as coincident ground observations were taken. A total of five different wetland types were analyzed using polarimetric signatures, linear backscatter measurements, pedestal heights, total powers, co-polarized ratios, and cross-polarized ratios).

Preliminary analysis of the available variables enabled broad class discrimination of wetland vegetation. Co-polarisation signatures indicated a distinction among wetland sites with structural vegetation differences. Total power values were the best discriminator between wetland classes, while linearly polarized backscatter values agreed with the differences in vegetation density over the wetland sites. Pedestal height was able to discriminate sites with homogeneous and heterogeneous vegetation. The results suggest that the ability to fully discriminate wetland classes requires the use a combination of radar parameters. As the number of variables included in an analysis increases, the additional information gained about target scattering mechanisms is also enhanced. Hence, RADARSAT-2's polarimetric capabilities can be expected to improve its potential for application to wetland mapping relative to RADARSAT-1.

Further investigations, using polarimetric radar data acquired over a range of incidence angles, are necessary to gain a better understanding of the interaction of microwaves and wetlands. Environmental effects, including dew on vegetation must also be considered. The use of steeper incidence angles would likely contribute additional information on ground surface conditions. Numerous studies have indicated the need for continued research on SAR parameters and wetland characteristics (Brisco and Pultz, 1998; Sokol *et al*, 2000).

## 3.7 Oceans

The ability of countries to regulate marine activities within their respective Exclusive Economic Zones (EEZs) is directly related to their ability to monitor a diverse array of human activities and natural phenomena occurring over large expanses of open ocean. Increased consumption, a scarcity of resources, and technological advances have all led to an increase and intensification in offshore resource-based operations such as fishing, and oil and gas exploration and production. Although eager to maximise the benefits of such industry, countries are wary of any potential negative impacts on the natural ecosystems within their coastal areas. In order to develop and implement a sustainable approach to economic development in the EEZ, it is accepted that a concerted effort is needed to monitor these activities and their impacts on the coastal zone. Government and industry have looked towards satellite remote sensing as a potential monitoring tool. While visible and near-infrared imaging satellites have established a niche market in coastal zone applications, their relatively coarse resolution and susceptibility to cloud cover can limit their operational use. On the other hand, higher resolution SAR sensors can routinely return images of the coastal zone, in spite of cloud cover, whenever the satellite passes by.

SAR images of the ocean provide a unique view of many physical processes in the upper ocean and within the marine atmospheric boundary layer. The radar responds to ocean surface roughness with scales on the order of the radar wavelength through a Bragg scattering mechanism. Any physical process that modulates the ocean surface roughness at the scale of the radar wavelength may be imaged. Surface winds are the most important effect. Rougher areas corresponding to higher wind speeds appear bright in the radar images, while smoother areas corresponding to lower wind speeds appear relatively dark. The ocean surface imprint of many atmospheric phenomena, such as gravity waves, convective cells, and storms, may be seen in SAR ocean images. Surface currents can also modulate the roughness, providing imaging mechanisms for oceanic fronts, internal waves, and bottom topography. Surface films, naturally occurring, or as a result of oil spills, damp the roughness at the wavelength scale and appear dark. All of these processes are ambiguously combined in the images, often making ocean image interpretation difficult.

SAR images have advanced our ability to monitor the world's oceans, particularly for operational applications such as ship detection, oil spill monitoring, bottom topography change measurement, and wind field measurement. SAR is also of interest for ocean wave surveillance since it is the only spaceborne sensor that has adequate spatial resolution to provide a direct measurement of the surface wave field under all weather conditions. Operational demonstrations of several of these applications using RADARSAT-1 SAR data have already been carried out.

RADARSAT-2 will present new ocean application opportunities. In discussing RADARSAT-2, it is useful to make a distinction between wide area routine surveillance (*i.e.* if the location of the feature of interest is not known), versus tracking (*i.e.* if the location of the feature of

interest is known approximately). For surveillance applications, use of ScanSAR with its 500 km swath is imposed, and the issue then becomes to choose the single or pair of polarizations that will provide the most benefit. For tracking applications, the required area coverage may be significantly reduced, and advantage may be gained by acquiring polarimetric data. This is an important trade-off when considering the best RADARSAT-2 acquisition mode for a specific application.

In the subsequent sections, we will review the potential of RADARSAT-2 data for winds, ships, waves, currents, and coastal applications. The roles of RADARSAT-2 in the detection of oil spills and hurricanes are discussed elsewhere in this document.

### 3.7.1 Winds

SAR images of the ocean surface often show the imprint of atmospheric phenomena through their effects on the near surface wind field. The higher the near surface wind speed, the rougher the ocean's surface, and the larger the radar backscatter, defining one procedure for deriving wind information from SAR images.

Many possible roles for SAR-derived wind speed information have been proposed. For example:

- as additional information to aid the interpretation of SAR images acquired for other purposes such as ship detection, oil slick detection, or search and rescue operations;
- to improve site-specific weather forecasting in regions that are too small for relatively large (25 km to 50 km) scatterometer resolution cells, such as in the coastal or marginal ice zones, or in lakes or estuaries;
- as an approach to near-shore wind climatology over small spatial scales, information that could be used for coastal windmill placement, for example;
- for assimilation into coupled atmosphere-ocean models (possibly along with SAR-derived spectral ocean wave information); and
- to study atmospheric processes near the ocean surface such as related to atmospheric gravity waves, atmospheric wakes, hurricanes, cold air outbreaks, and polar lows.

There are several approaches to estimating wind speed from SAR ocean images. Here we focus mainly on the use of the normalized radar cross section, along with the wind direction and the SAR geometry (see Vachon and Dobson, 1996). This approach requires good absolute radiometric calibration of the radar images and a wind retrieval model function that relates the ocean wind speed to the normalized radar cross section, the relative wind direction, and the local incidence angle. Such models have been developed for ocean wind scatterometry. Although physics-based models are improving, the usual approach is to tune a semi-empirical model by using SAR observations that are collocated with *in situ* wind observations. For SAR, an approach to estimating the wind direction is to measure the orientation of low frequency coherent structures (*i.e.* boundary layer rolls that align with the nominal wind direction) in the SAR image. This is often carried out using an image spectral analysis (a wavelet-based approach might also be beneficial) and results in a 180° ambiguity in the estimated wind direction.

An alternate approach to estimating wind speed is to measure the degree of azimuthal cut-off that arises in SAR imaging of ocean waves. The wind speed affects the coherence time of the short scale waves, which in turn impacts the degree of azimuthal cut-off in the SAR image spectrum. Attempts have successfully been made to relate measures of the azimuth

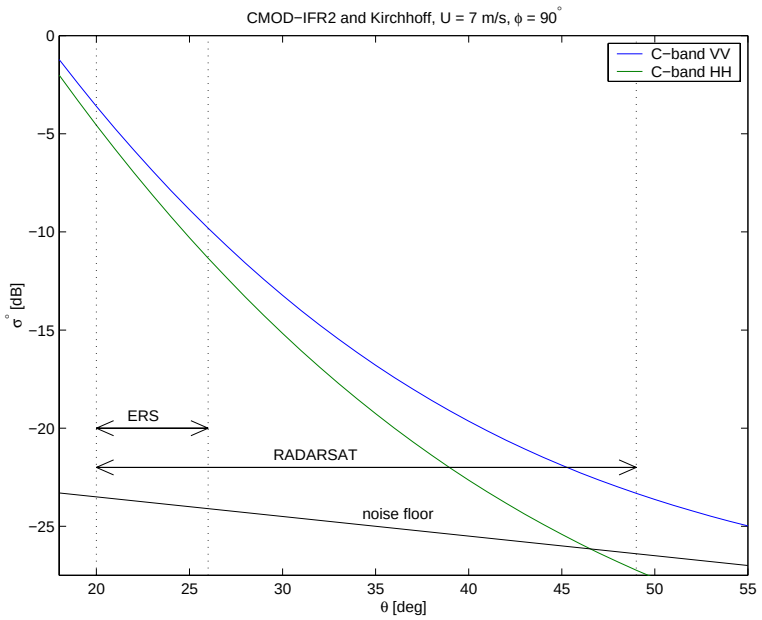


**Figure 3.7.1-1** Plot of normalized radar cross section σ° as a function of incidence angle for a 7 m/s wind speed blowing across the radar look direction for C-VV (CMOD_IFR2) and C-HH (hybrid model composed of CMOD_IFR2 and a Kirchhoff scattering polarization ratio). The nominal RADARSAT-1 noise floor, the ERS swath, and the accessible RADARSAT-1 swath are as indicated.

cut-off to the wind speed (see for example, Kerbaol *et al.*, 1998). This is a topic of ongoing research.

The potential of C-HH (C-band HH polarization) and C-VV (C-band VV polarization) images for the extraction of wind vectors has been demonstrated by Vachon and Dobson (2000). For C-VV radars such as the ERS SARs, there are several well-developed wind retrieval models to draw on. We have relied on the empirically derived CMOD_IFR2, which is used for the post processing of ERS Scatterometer data, achieving a root-mean-squared wind retrieval error of better than 2.0 m/s. For the C-HH RADARSAT-1 SAR, similarly well developed and validated wind retrieval models do not exist. Our approach has been to use a hybrid model that is composed of CMOD_IFR2 and a suitable C-band polarization ratio. We have shown that a polarization ratio based upon Kirchhoff scattering is appropriate, achieving a root-mean-squared wind retrieval error of better than 2.4 m/s. A plot of the C-VV and C-HH model functions (Figure 3.7.1-1) shows that, for incidence angles of relevance to RADARSAT-2, the C-HH cross section is always smaller than the C-VV cross section and decreases more rapidly with increasing incidence angle, all else equal. Note that the ERS SARs have a smaller incidence angle range (nominally 20º to 26º) than the RADARSAT-1 or RADARSAT-2 SARs (nominally 20º to 50º). These results suggest that C-VV will be the better choice for RADARSAT-2 wind field retrieval because:

- the wind retrieval model function, at least as the situation stands today, is more mature and does not require the use of an *ad hoc* polarization ratio; and
- there will be a better signal to noise ratio for higher incidence angles, which will be particularly beneficial for cases with lower wind speeds.

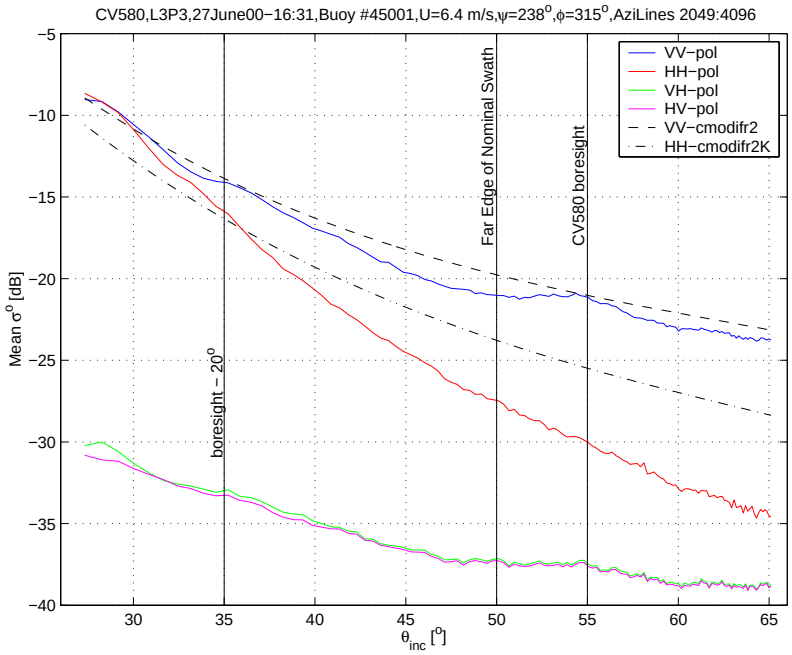


**Figure 3.7.1-2** Plot of normalized radar cross section σ° as a function of incidence angle derived from a CV-580 data set acquired over a NOAA buoy on Lake Superior in June 2000.

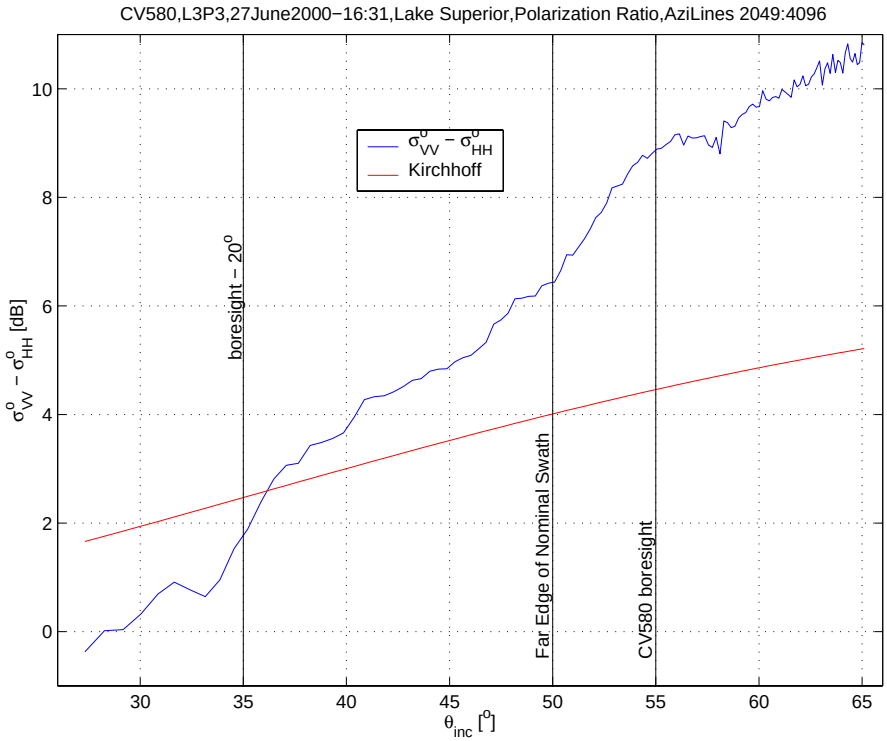


**Figure 3.7.1-3** Plot of C-band co-polarization ratio derived from the CV-580 data set acquired over a NOAA buoy on Lake Superior in June 2000, along with a Kirchhoff scattering polarization ratio.

ENVISAT's ASAR will present an important preparation opportunity for RADARSAT-2 since it will offer a dual polarization ScanSAR mode. In the meantime, there is some observational evidence from the CV-580 SAR that supports the validity of our hybrid model and provides some insight to the to cross polarization ocean responses, *i.e.*, C-HV (C-band HV polarization) and C-VH (C-band VH polarization). A polarimetric data set was acquired in June 2000 over an operational NOAA buoy moored in Lake Superior. Range-ward profiles of normalized radar cross section were derived and plotted against wind retrieval model function predictions, as driven by the wind vector measured by the buoy (see figure 3.7.1-2). The co-polarization ratio was also estimated and plotted, along with the prediction from Kirchhoff scattering (see figure 3.7.1-3).

The calibration of the CV-580 data are most reliable within ±20° of the bore-sight of the elevation antenna pattern, which was around 55° incidence angle in this case, well beyond the far edge of the nominal RADARSAT-2 swath (20° to 50°). That is, the radiometric calibration of the CV-580 SAR data is most reliable for incidence angles from 35° to 75°.

The results from this single line of CV-580 data show that the C-VV and C-HH model functions are in reasonable agreement over the applicable incidence angle range. In particular, the Kirchhoff-based co-polarization ratio agrees very well with the observed co-polarization ratio. The C-VH and C-HV results are also of interest and represent a rare measurement of the cross-polarization response of a water surface. With cross sections of –35 dB for these incidence angles, we expect that most cross-polarization returns will be below the RADARSAT-2 instrument noise floor, at least for larger incidence angles. However, C-HV or C-VH may provide a predictably low background for ship detection applications, for example.

### 3.7.2 Ships

Since the launch of RADARSAT-1 in 1995, we have investigated and validated the use of RADARSAT-1 SAR imagery for ship detection (see Vachon *et al.*, 1997b; Vachon *et al.*, 2000). It has been shown that RADARSAT-1 imagery in combination with an automated target detection system can provide up to 95% detection reliability for those beam modes that are best suited to ship detection. By building on these RADARSAT-1 successes, RADARSAT-2 will provide new opportunities for improved target detection with multiple and fully polarimetric data, higher resolution imagery, and an increased revisit schedule. These capabilities will provide users with the potential to classify ships and to better relate ship detection information to commercial needs such as the monitoring of offshore fishing activities.

There are two basic approaches to ship detection using SAR: detection of the ship wake signature, and detection of the ship target itself. Previous research using RADARSAT (C-HH) and ERS (C-VV) SAR data has shown that the ship-sea contrast is higher for HH polarizations, thus making RADARSAT-1 quite suitable for target detection. HH polarization clutter is smaller than VV polarization clutter and decreases more rapidly with increasing incidence angle. For this reason, signatures relating to ship wakes are rarely seen in HH polarization images, however VV polarization provides improved information on sea state and wake detectability. Figures 3.7.2-1 and 3.7.2-2 illustrate these generalities with a RADARSAT-1 (C-HH) image showing ship targets, and an ERS-2 (C-VV) image showing both ship targets and wakes.

**Figure 3.7.2-1** A RADARSAT-1 ScanSAR Narrow Far image of the Straits of Dover. The image covers 76 km from left-to-right. Many bright, point-like ship target signatures are visible in the busy shipping lanes. (©CSA 1997)

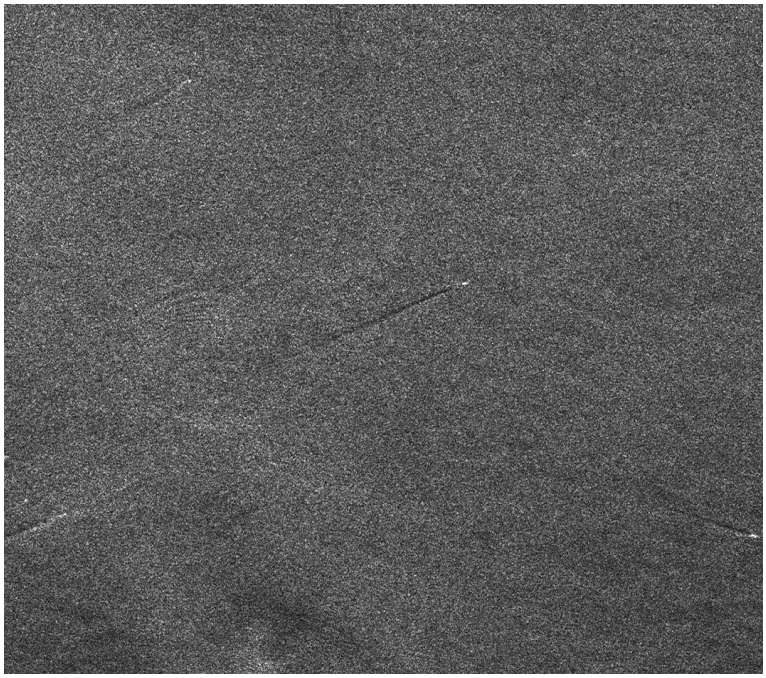

**Figure 3.7.2-2** An ERS-1 SAR image of Kattegat covering 17 km from left-to-right. Several bright ship targets that are offset from their wakes are apparent. Some dark, turbulent wakes are clearly visible. (©ESA 1991)

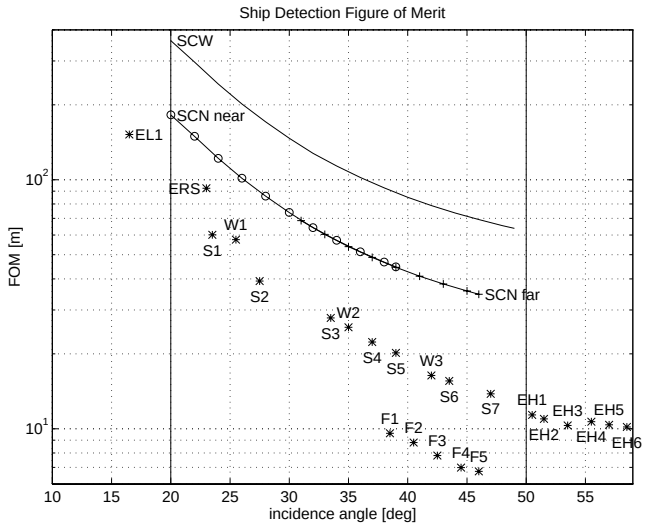


**Figure 3.7.2-3** Ship detection Figure-of-Merit (FOM) defined as the minimum detectable ship length for a 10 m/s wind blowing towards the radar, with assumptions about the wind direction, the clutter statistics, and the radar cross section of ships. All of RADARSAT-1's single beam modes and ERS are represented in this plot (for the nominal beam centre), as well as the range of values for RADARSAT-1's various ScanSAR modes. The FOM allows relative comparison of ship detection performance.

When selecting imaging modes for ship detection, it is essential to consider the trade-off between spatial coverage and spatial resolution. For the surveillance of large fishing ships in remote waters, the priority is usually for large area coverage. RADARSAT-1's ScanSAR wide mode has proven to be useful in this respect, providing an image swath of up to 500 km with a resolution of 100 m. For tracking known ship targets, higher resolution imagery may be useful, as is available from the standard and fine beam modes.

In order to quantify and compare the performance of the various beam modes for ship detection, Vachon *et al.* (1997b) introduced a Figure-of-Merit (FOM) that defines the minimum detectable ship size in the case of a 10 m/s wind blowing towards the radar, with a K-distribution defining the ocean clutter fluctuations, and a simple model relating the ship size to its radar cross section, see Figure 3.7.2-3. The FOM, which permits a relative assessment of ship detection performance, includes the radar's spatial and radiometric resolutions and is seen to be a strong function of incidence angle. This is caused by the reduction in background clutter with increasing incidence angle. As such, it is evident that large incidence angles are best for ship detection. Therefore, the best RADARSAT-1 SAR beam modes for ship detection are ScanSAR Narrow far, Wide 3, Standard 4 to 7, and all Fine modes. RADARSAT-2 will provide all of these imaging modes plus an ultra-fine mode with a resolution of 3 metres. Imagery from this new mode will allow a rather detailed analysis of ship structures and should permit estimation of ship type, size, and orientation.

Figure 3.7.2-4 shows a comparison of the FOM for RADARSAT-1's ScanSAR Narrow modes with ENVISAT's ASAR Wide Mode. These results indicate that RADARSAT ScanSAR Narrow Far mode is a good choice overall for ship detection (*i.e.* it allows detection of smaller ships across a 300 km image swath, all else equal), but that ENVISAT's Wide Mode with HH polarization will also support the detection of ocean going fishing

vessels. The principle difference between these two modes is the radar resolution (nominally 50 m for RADARSAT-1's ScanSAR Narrow Far mode and 150 m for ENVISAT's Wide Mode).

RADARSAT-2 will also provide dual polarization and fully polarimetric data, allowing the user to exploit various polarization combinations to optimise the detectability of specific target types. For ship surveillance, it is expected that a dual polarization ScanSAR wide mode data set composed of VV and VH channels will be optimal. The VH channel should provide point target information against a very dark clutter background (indeed, against the noise floor of the instrument for most wind conditions and incidence angles), while the VV channel should provide adequate ocean clutter signal to allow wake analysis for most accessible incidence angles. Furthermore, it is expected that fully polarimetric data will improve ship target detection and possibly classification. However, polarimetric data will not be available for ScanSAR modes, so the polarimetric modes will only be suitable for ship tracking, or perhaps for surveillance of regions with a limited spatial extent (*e.g.* in coastal passages, bays, or harbours).

Based on well-known scattering physics, new tools are being developed to analyze the polarimetric signatures from ship and ocean targets. For example, for small incidence angles, ship backscatter is dominated by a double bounce scattering mechanism.

Therefore, circular polarization (*e.g.* RR – right/right circular) is expected to be a good candidate for ship signature enhancement. For this circularly polarized antenna

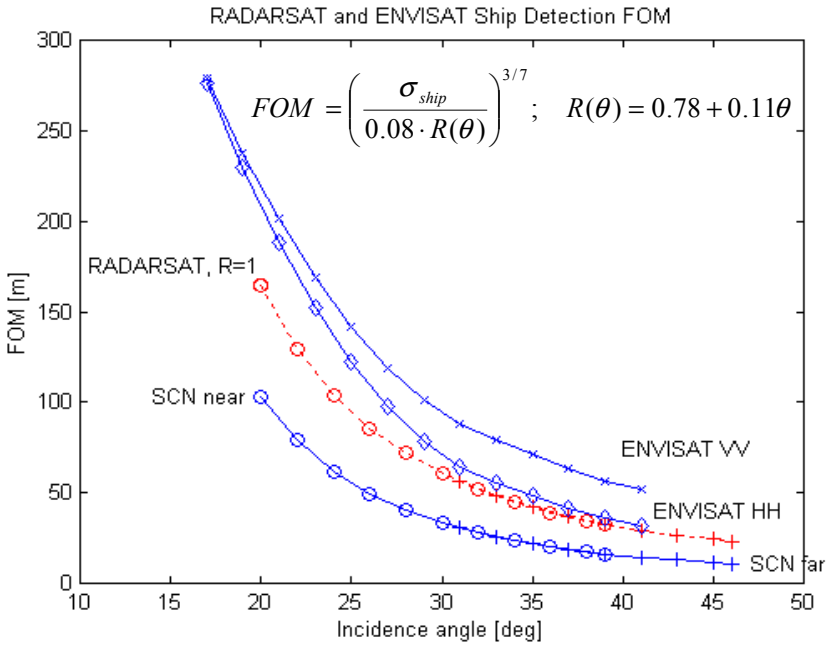


**Figure 3.7.2-4** Ship detection Figure-of-Merit (FOM) showing the minimum detectable ship size for RADARSAT-1 ScanSAR Narrow (SCN) and ENVISAT ASAR with two different polarization choices (see Olsen *et al.*, 2000). The function *R(θ)* describes the empirically-derived incidence angle dependence for the radar cross section of ships. RADARSAT results are provided with two versions of this function to illustrate the range of model predictions that are possible.

configuration, the receive antenna is matched to the transmit antenna to maximize the double bounce response, and in turn, the backscatter from ships.

A new tool referred to as the “Polarization Entropy” has also been developed for ship detection. This tool, which is an effective measure of target non-stationarity (see Touzi, 2000), has been shown to enhance the ship-sea contrast, thus providing an improved ship detection capability, especially for small incidence angles. At incidence angles of less than 60°, the Polarization Entropy can reveal ships that were only weakly visible in the HH polarization channel. Figure 3.7.2-5 shows an HH-polarization image that includes some ships along with the corresponding Polarization Entropy image. This image pair clearly illustrates enhanced ship-sea contrast and the resulting increased ship detectability by using the Polarization Entropy. This is quantified in Figure 3.7.2-6, which shows the ship-sea contrasts for all available linear polarizations, circular polarization (RR), as well as for the Polarization Entropy. For incidence angles that are relevant to RADARSAT-2, these results suggest that the polarization entropy will provide the best detectability, followed by circular polarization (RR), cross polarization (HV or VH), and HH polarization

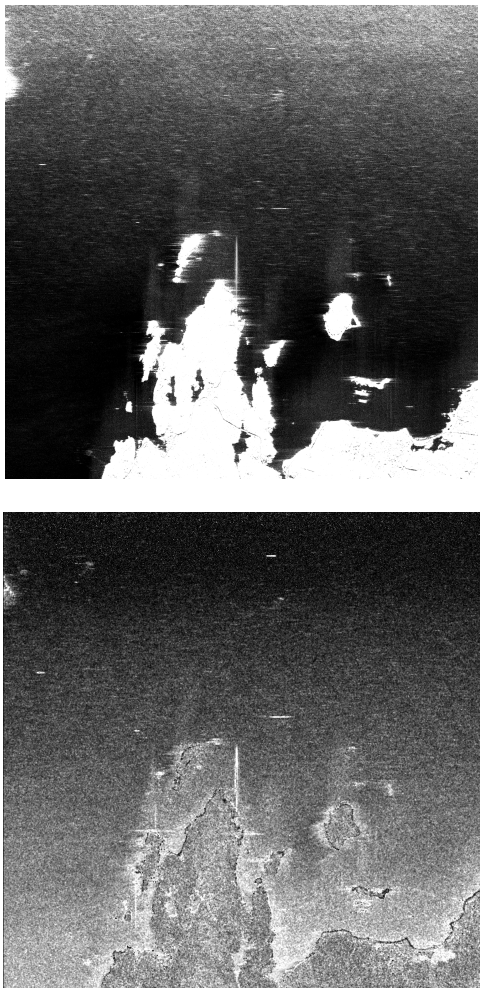

**Figure 3.7.2-5** An HH Polarization image off the coast of Nova Scotia acquired by the CV-580 SAR in Sept. 1997 covering incidence angles from 46° to 70° from top-to-bottom (top); the corresponding image of Polarization Entropy (bottom).

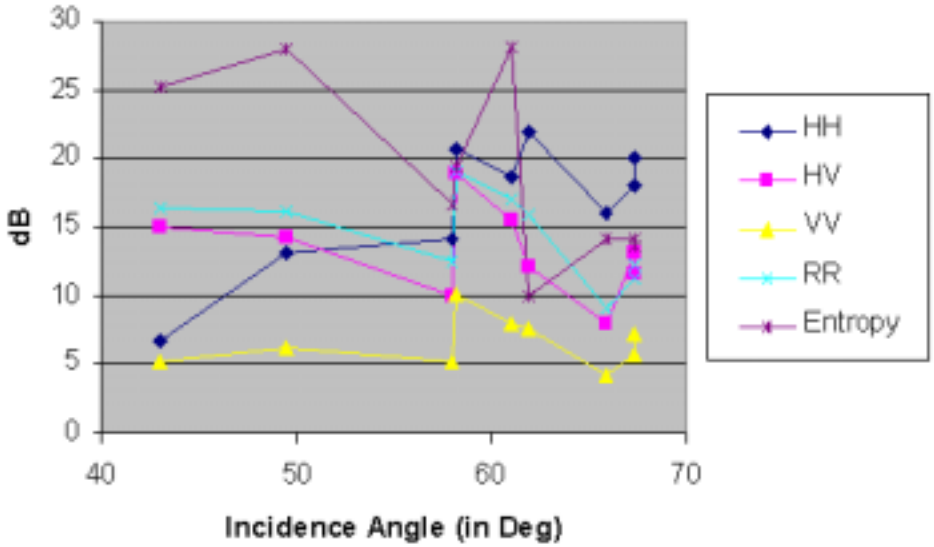


**Figure 3.7.2-6** Ship-sea contrasts as a function of the incidence angle for all choices of linear polarization, RR polarization, and the Polarization Entropy.

The advanced capabilities of RADARSAT-2 will provide improved ship-sea contrast with polarimetric data, both ship and wake detection with dual polarimetric VH and VV polarization channels, and detailed ship analysis and perhaps classification with high-resolution imagery. These advances will result in improved ship detection from SAR images by providing more complete and reliable information than is available today from RADARSAT-1 C-HH imagery.

### 3.7.3 Waves

The derivation of a closed-form expression for the "forward" transformation from an ocean wave spectrum to a synthetic aperture radar (SAR) image spectrum (Hasselmann and Hasselmann, 1991; Krogstad, 1992) has allowed the development of nonlinear "inverse" transformation schemes. These inversion schemes are based upon the minimization of a cost function and have been demonstrated for the inversion of ERS SAR image spectra to ocean wave spectra (see for example, Heimbach *et al.*, 1998) and to test assimilation schemes into operational wave models (for example, Breivik *et al.*, 1998; and Dunlap *et al.*, 1998). A weakness in all of these inversion procedures is that they require *a priori* knowledge of the ocean wave field (usually taken from ocean wave models) and of the forward mapping transfer functions. *A priori* knowledge of the wave field is required to resolve the 180º ambiguity in wave propagation direction and to provide spectral information outside of the SAR's azimuthal passband. The transfer functions are required for correct modelling of the forward transform.

The recently introduced inter-look cross-spectrum methodology (Engen *et al.*, 1995), in which the cross spectrum between individual SAR looks replaces the usual SAR image spectrum, resolves the wave propagation direction by responding to wave propagation during the short time interval between looks (see Vachon and Raney, 1991). Furthermore, it simplifies the inversion process by suppressing the speckle noise contribution to the SAR image spectrum since the speckle is not correlated between the individual looks. Dowd *et*

*al.* (2001) provide a treatment and validation of spectral inversion from inter-look cross spectra for the RADARSAT-1 SAR.

An ongoing problem in SAR ocean wave imaging and spectral inversion is the estimation of the real aperture radar (RAR) modulation transfer function (MTF). The RAR MTF describes the modulation of the radar cross section by the long waves, and depends on the long waves themselves, the wind stress, the wind and wave imaging geometry, and the radar frequency and polarization. The RAR MTF is most important for the imaging of waves travelling in the near range direction and may be estimated by direct measurement from a SAR image spectrum. However, these estimates cannot be completely explained by existing theoretical formulations.

The availability of multi-polarization SAR data presents new inversion opportunities. Individual image looks may be calculated from raw or single look complex image data. Each look represents a unique view of the wave field at an offset interval of time. Multiple channels are achieved by combining look pairs from separate polarizations. For example, the HH-HH spectrum uses look 1 from HH-polarization and look 2 from HH-polarization, while the HH-VV spectrum uses look 1 from HH-polarization and look 2 from VV-polarization. Other channel combinations can also be calculated, including the use of cross-polarization channels if the signal-to-noise ratio permits. The RAR MTF may be estimated by minimizing a cost function over the linear region of each SAR image spectrum (*i.e.* near zero azimuth wavenumber).

As part of our SAR ocean validation efforts, the Sea Truth and Remote Sensing (STARS) experiment was carried out from the Bedford Institute of Oceanography (BIO) research

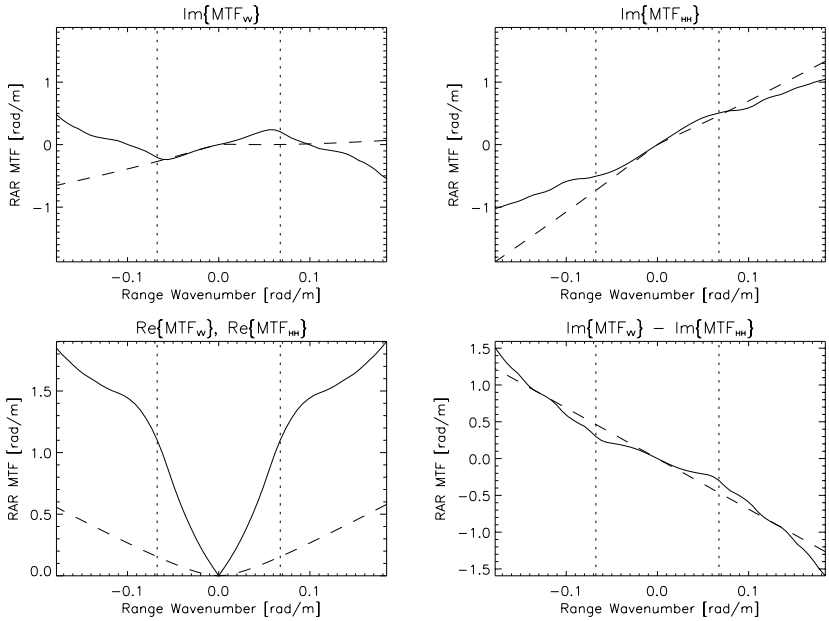


**Figure 3.7.3-1** Theoretical and estimated RAR MTFs derived from dual co-polarimetric data from the CV-580 C-band SAR, acquired on 3 Dec. 1994 over the Grand Banks of Newfoundland. Upper plots: imaginary part of the VV and HH polarization MTFs. Lower left: the real parts of the MTFs. Lower right: the difference in the imaginary parts between the VV and HH polarization MTFs (solid line - estimated; dashed line - theoretical). The vertical dotted line shows the location of the spectral maximum along the range axis.

vessel CSS *Parizeau* in December 1994. We deployed Minimet (MM) and Directional Wave Rider (DWR) buoys on the Grand Banks of Newfoundland and ran a wave model in hindcast mode. In addition to ERS-1 SAR image data, the CV-580 SAR was deployed on three separate occasions, providing us with C-band dual-polarization (HH and VV) SAR imagery (the VH and HV channels were available as well, but they suffered from a poor signal-to-noise ratio) and calibrated wind and wave data for validation purposes.

Engen *et al.* (2000) demonstrated the benefits of dual-polarization data for ocean wave measurement by using the four cross-spectra combinations available from the HH and VV co-polarization channels of the CV-580 data. The inversion to a wave spectrum was based on minimizing a cost-function and included some symmetry and functional from constraints. The inversion was further constrained by requiring that each channel or channel combination returned an identical ocean wave spectrum. Our analysis results show (Figure 3.7.3-1) that the SAR tends to measure higher RAR MTF amplitudes than are predicted by theory and that the deviation is largest for HH polarization. For the phase, the measured values in most cases are lower than theoretical predictions for both VV and HH data.

We found that the observed and best-fit average inter-look cross spectra are in good agreement, verifying that global minima have been found during the cost function minimization procedure. Since we used a coupled RAR MTF and wave spectrum estimation scheme, the final wave spectrum can reproduce all of the cross spectra within a single SAR acquisition (*i.e.* for all combinations of HH and VV polarizations). For each date, the inverted SAR spectra are in good agreement with available wave model and *in situ* observations (Figure 3.7.3-2, note the agreement of the significant wave height, in particular).

Wave spectrum estimation benefits from the available multiple channels since the underlying wave spectrum must be the same for each channel. The estimated wave spectra, when forward mapped using the estimated RAR MTF, showed good agreement with the observed cross spectra. In our work, the inversions were autonomous (*i.e.* without any externally supplied information) and were consistent with both the wave model and the DWR spectra. It is evident that dual polarization mode data from RADARSAT-2 (that is, with the HH and VV co-polarization channels extracted from polarimetric mode acquisitions) will permit more accurate and complete ocean wave spectrum retrieval than is available from the current generation of single channel spaceborne SARs.

A promising new approach to wave estimation using polarimetric data has been proposed by Kasilingam *et al.* (2000). They used fully polarimetric AIRSAR observations of ocean waves to estimate azimuth wave slopes and then to estimate fully directional wave slope spectra. Rangeward slopes were also estimated, based on the phase difference between the HH and VV channels. RADARSAT-2 will provide an opportunity to experimentally validate this approach.

Although dual-polarization will offer benefits for ocean wave observations, it must also be understood that RADARSAT-2, as with RADARSAT-1 and all polar orbiting spaceborne SARs that preceded it, will suffer from other ocean wave imaging fidelity limitations (see Vachon *et al.*, 1997a). Specifically, RADARSAT-2 will acquire data with a large platform range-to-velocity (R/V) ratio. This parameter controls the degree of non-linearity in ocean wave imaging by causing an azimuthal cut-off phenomenon, whereby shorter waves with an azimuthal wavenumber component cannot be imaged by the radar. With values of

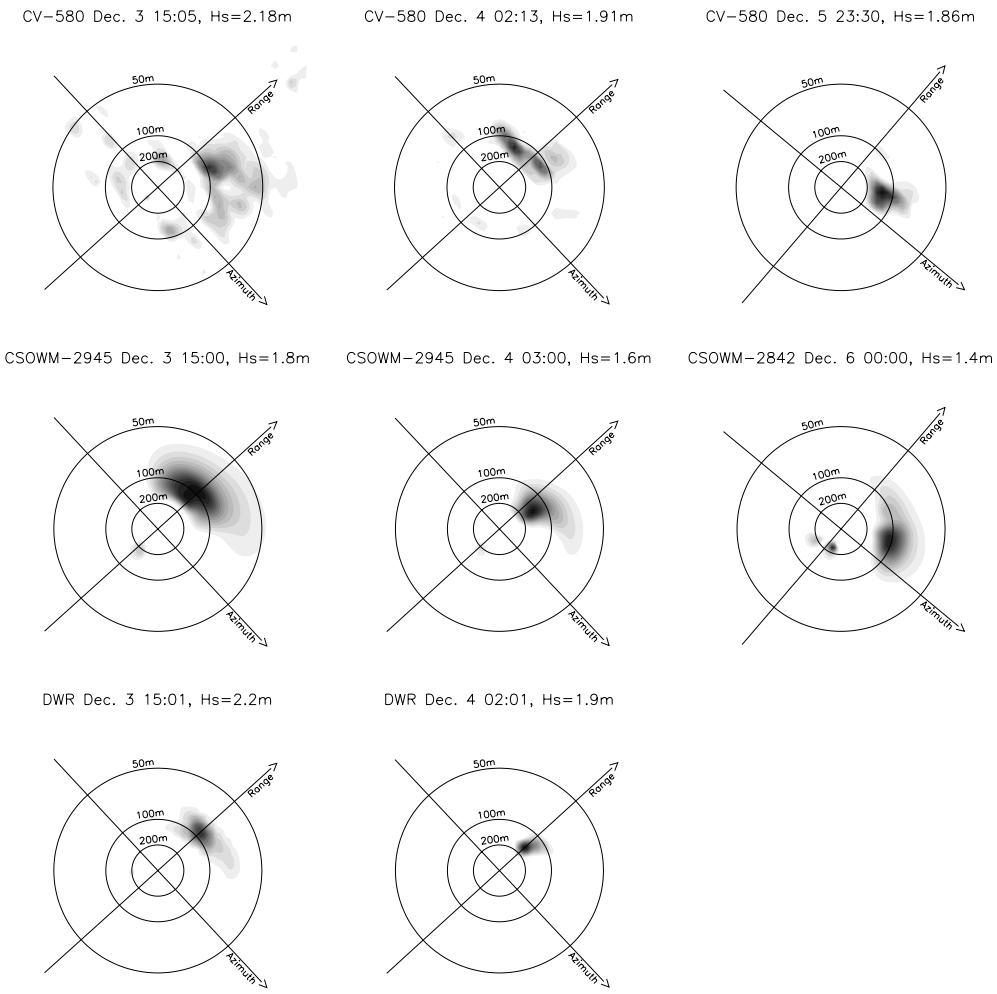


**Figure 3.7.3-2** Estimated ocean wave spectra from CV-580 C-band SAR, the Canadian Spectral Ocean Wave Model (CSOWM), and a Directional Wave Rider (DWR) buoy for December 1994 over the Grand Banks of Newfoundland. Hs refers to the significant wave height.

R/V > 115 s, RADARSAT-2's geometry, in general, is not favourable for ocean wave observation unless the waves are long or the wave heights are low.

### 3.7.4 Currents

Ocean currents may appear in SAR images through several mechanisms (see Johannessen *et al.*, 1996). Natural film often expresses spiral eddies by damping the ocean clutter by up to 10 dB. Filaments of natural film often concentrate in convergence zones that are oriented parallel to the mean flow direction. Wind speeds greater than 7 m/s, or so, will tend to disperse and mix the natural film downward, which will spoil the effectiveness of this imaging mechanism. On the other hand, meandering fronts may appear in SAR images due to short wave-current interactions that locally modify the surface roughness, resulting in both bright and dark radar cross section perturbations of several dB. Local convergence and divergence zones may accentuate these interactions. Wind speeds greater than 10 m/s, or

so, will tend to mask this short wave-current interaction imaging mechanism. This latter mechanism also applies to the imaging of underwater topography. In this case, the current (usually tidal in origin) interacts with the bottom topography, which in turn modulates the surface current and the local surface roughness.

There is rather limited observational evidence for multipolarization imaging of ocean current features. SIR-C provides the best data sets and a useful study of the Gulf Stream using data from that source was published by Ufermann and Romeiser (1999a). In their paper, they compare SIR-C observations with model predictions to address the effects of atmospheric stability (*i.e.* a temperature front), changing currents, and changing winds. All of these phenomena impact the appearance of the Gulf Stream front in their model calculations. Multifrequency response was as important to their study as multipolarization. Unfortunately, the available *in situ* observations of currents were not adequate to properly drive their imaging models.

In a companion paper, Ufermann and Romeiser (1999b) studied the signatures of atmospheric convective cells in SIR-C images. They conclude that radar signatures of oceanic phenomena are stronger for HH polarization than for VV polarization, while atmospherically induced radar signatures are stronger for VV polarization than for HH polarization. This is consistent with observations made elsewhere that ocean clutter is larger for VV polarization, and that the RAR MTF is larger for HH polarization (leading to increased modulation depth relative to VV polarization when imaging ocean waves, for example). Ufermann and Romeiser also suggest that HV or VH polarization should be beneficial for observing ocean current effects, but available observations have suffered from poor signal-to-noise ratios, so results are inconclusive.

An approach to obtaining quantitative ocean current information (radial component) is to carry out a detailed Doppler analysis and to ascribe any systematic components to ocean current effects (van der Kooij, 1999). This procedure has been demonstrated for both RADARSAT-1 and ERS SAR data. The RADARSAT-1 geometry with its larger available incidence angles is more favourable for this application since a larger radial velocity component is projected to wards the radar. On the other hand, the ERS polarization (VV) provides a better signal-to-noise ratio for ocean images. RADARSAT-2 with its VV polarization and larger incidence angles will provide a better opportunity to make this type of measurement. Improved satellite orientation information for RADARSAT-2 in comparison to RADARSAT-1 will also facilitate the use of RADARSAT-2 for this type of analysis.

Dual polarimetric and fully polarimetric RADARSAT-2 data will be beneficial to improving our understanding of the imaging of ocean currents, particularly if contemporaneous, high-resolution validation data can be obtained. Candidate validation data sources include HF radar and along-track InSAR.

### 3.7.5 Coastal zones

A disproportionate percentage of the global population lives in coastal areas. Consequently, these areas are under intense pressures resulting from urban growth, commerce, industry and tourism. A prerequisite for sustainable management of these environmentally sensitive areas is the availability of accurate and up-to-date information on their extent, state, natural dynamics and rate of change. Remote sensing satellites make potentially outstanding tools to collect information in support of coastal zone management because they are capable of

imaging any area of interest in a systematic, synoptic, and repetitive manner. Examples of coastal applications that may benefit from the use of radar data are coastline (change) mapping, mapping of tidal and near-shore terrestrial areas, and mapping of near-shore bathymetry.

The use of space-borne SAR data for application to coastline mapping and monitoring is reported in e.g. Lee and Jurkevich (1990), Mason and Davenport (1996), Schwäbisch *et al.* (1997), Corbley (2000), Romaneeßen *et al.* (2000) and Trebossen (2000). Extraction of shorelines from radar images is facilitated by a large contrast in the backscatter signals as received from the water and the land. Moderate to high wind conditions and small incidence angles are know to complicate the identification of shorelines in C-band VV images, in particular. This explains why RADARSAT-1 data have been found to be more suited for shoreline delineation than ERS data (Tittley and Werle, 1997).

The capability of RADARSAT-2 to acquire HV polarised images in the selective single polarisation mode is likely to enhance its potential for application to shoreline mapping. Regardless of the incidence angle, HV polarised images are expected to show a large water-land backscatter contrast that is less dependent on wind conditions than in HH (see also Figures 3.7.1-2 and 3.8.1-1). The modelling results presented by Ufermann and Romeiser (1999a) confirm the limited effect of wind speed variations on the HV return signal of water. Yeremy *et al.* (2000) address the potential of polarimetric radar data for coastline mapping. They successfully exploit the phase difference between the HV and VH channels to help distinguish between water (moving) and land (stable) in areas where wave action reduces the water-land backscatter contrast. Moreover, these authors illustrate the potential of polarimetric radar data for the estimation of the slopes of beaches that happen to be oriented in parallel with the radar look direction (see also section 3.2.3). The potential of a variable identified as the polarisation entropy for the extraction of cliff type shorelines has been noted by Touzi (2001) (see Figure 3.7.2-5).

Thematic maps of tidal and near-shore terrestrial areas provide a basis for coastal zone sensitivity assessments. The potential of RADARSAT-1 data for coastal zone sensitivity mapping in parts of Nova Scotia and Newfoundland is discussed in Tittley and Werle (1997) and CHART (1999), respectively. Both these studies show that there are few features in the coastal zone that are clearly separated in terms of the range of their C-band HH backscatter responses. This precludes effective and reliable application of digital image classification procedures. RADARSAT-2, thanks to its selective dual polarisation and fully polarimetric imaging modes, is likely to become a much better source of data for coastal zone mapping. The capability to image in different polarisations will make the system more sensitive to structural differences in the targets observed, e.g. to coarse versus fine substrates and vegetated versus bare areas (See Figure 3.7.5-1).

Knowledge of (changes in) the near-shore bathymetry supports the development of plans for the construction of coastal defences, the dredging of harbours and approaches, and the management of coastal resources. De Loor (1981) was among the first to report the visibility of underwater topography in radar images of coastal waters. The responsible process is the modulation of the sea surface roughness by surface currents, which in turn are modulated by sea bottom topography. The radar images the sea surface roughness variations. The process of bathmetric mapping by means of ERS SAR data is well developed and its limitations are understood (e.g. Vogelzang *et al.*, 1995; Wensink *et al.*, 1999; Hesselmans *et al.*, 2000). In contrast, little research and development seems to have been undertaken concerning the potential of RADARSAT data for this purpose. Findings reported by

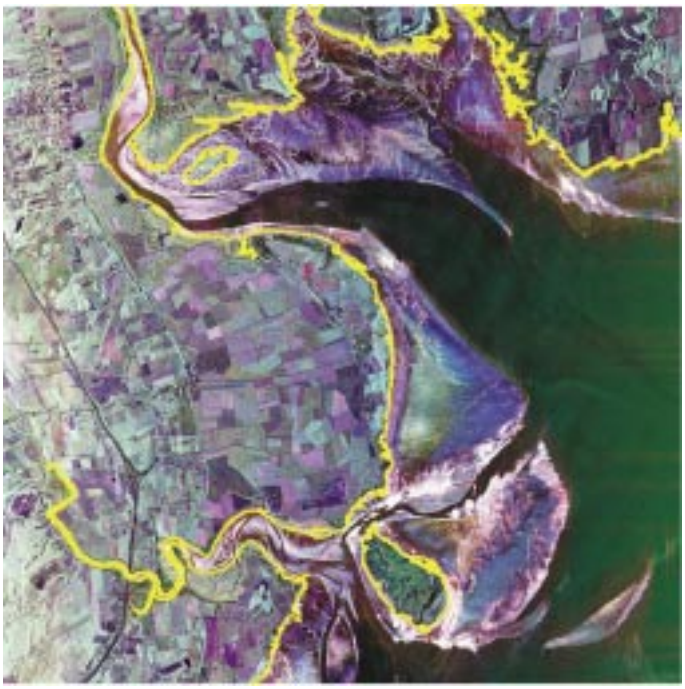

**Figure 3.7.5-1** Convair-580 SAR multi-polarization composite of the Minas Basin, N.S. during low tide conditions. The HH, HV, and VV polarized images are shown in red, green and blue, respectively. The yellow line marks the boundary between the dry land and the tidal plane. The backscatter contrasts in these two areas were enhanced independently to produce the image shown. The colourful patterns present illustrate the differences in the information content of the three images.

Ufermann and Romeiser (1999b) indicate that HH and HV polarisation are more suited to bathymetric mapping than VV polarisation. The potential of fully polarimetric data is largely unknown but could be better given the increased sensitivity of such data to the structural characteristics of the targets observed.

Undoubtedly, coastal applications will benefit from the capability of RADARSAT-2 to acquire images that show more spatial detail. According to Cracknell (1999), spatial resolution has long been the primary constraint for the application of satellite remote sensing data to coastal zone management.

As is the case for most other applications, no single sensor has the capacity to provide all of the information required for coastal zone management. Hence, there will always be a need to complement RADARSAT images with data from other remote sensing or *in situ* sources.

## 3.8 Sea and Land Ice

One of the primary drivers behind the development of the RADARSAT-1 program was the potential for spaceborne SAR to effectively monitor Canadian ice-covered waters in support of shipping operations. RADARSAT-1 has proven highly successful in addressing the information requirements for this application area and Canada is recognized as a world leader in operational use of spaceborne SAR for sea ice monitoring. With regard to land ice, RADARSAT-1 was the first satellite to accomplish complete high resolution mapping of the

Antarctic continent. The RADARSAT-1 Antarctic Mapping Mission has revealed a wealth of information about the surface conditions of the ice sheet, including the discovery of two new ice streams and has therefore become a landmark in the history of Antarctic study.

RADARSAT-2 offers a number of improvements that should provide an incremental benefit to these application areas. For operational sea ice monitoring, the beam mode of choice is ScanSAR due to its relatively high spatial resolution (as compared to other available satellite data sources) and its relatively wide swath coverage. Although other narrower beam modes (Wide, Standard) are used operationally; these are usually chosen to focus on specific target areas of interest. Based on the capabilities of RADARSAT-2 there are a number of areas where improvements are expected and these are discussed in the following sections.

### 3.8.1 Sea ice edge and ice concentration

The primary task for sea ice mapping is to be able to identify the boundary between ice and open water, or the ice edge. Generally speaking, backscatter from ice is greater than from open water. However, this depends on the ice type, ice deformation/roughness, and the ocean clutter level. Thus, it is the backscatter contrast between the ice and ocean/water that determines the capability to accurately define the ice edge. In relation to incidence angle, the ocean clutter level is highest at steeper. Increased surface roughness due to wind and waves will also increase the ocean clutter level. Thus, the most problematic situation for reduced ice-ocean backscatter contrast is when these two conditions occur together.

Presently with RADARSAT-1 its HH polarization is an improvement over the VV polarization available from the ERS satellites. However, clear definition of the ice edge can still be difficult with RADARSAT-1, particularly when the area of interest is imaged at less than around 35 degrees incidence (i.e. in the near half of the swath for ScanSAR Wide) and when wind roughening of the ocean surface occurs. It is preferable to attempt to “place” the ice margin in the far range of the swath when doing planning, but this is not always feasible. RADARSAT-2 with its cross-polarization capability is foreseen to improve the potential for clear ice edge definition, as the ocean backscatter is much reduced. The cross-polarization backscatter response from water is low and is relatively independent of wind induced surface roughness conditions. Thus, the ice-ocean contrast is greater than for either of the like-polarization channels. The SSP and SDP modes of RADARSAT-2 will allow the acquisition of cross-polarization data in all currently available RADARSAT-1 modes, including ScanSAR, which, as noted above, is the mode of choice for ice monitoring. Figure 3.8.1-1 (CCRS, 2000) illustrates the improved ice/water definition potential of cross-polarization data. Also illustrated is the result of calculating and displaying the co-polarization ratio between the HH and VV channels. This provides similar ice edge detection capabilities to the cross-polarization channel alone. However, other than for the narrow swath QP modes, the two like-polarization channels will not be acquired and thus will not be useful for the sea ice application. Accurate estimation of ice concentration is a derivative of the ability to discriminate between ice and open water. Thus, it is expected that the statements above on the utility of cross-polarization for ice/water separation will hold for improved ice concentration estimation.

In addition to the utility of the polarization capabilities, there are other proposed enhancements to the RADARSAT-2 mission that should prove beneficial not just to ice edge and concentration mapping but to the sea ice application field as a whole. A few of these benefits are discussed below.

The proposed functionality to perform slew manoeuvres to switch from left- to right-looking or vice versa in nominally 10 minutes, may provide the opportunity to increase the revisit capability of imaging activities. This capability would be of benefit to sea ice monitoring, particularly at mid-latitudes where current revisit with RADARSAT-1 is every 2-3 days. However, the operational scenarios and the availability of tasking slew manoeuvres during routine satellite operations are unknown at present.

RADARSAT-2 is expected to have improved geometric and radiometric accuracy. Although for most ice monitoring applications RADARSAT-1 is adequate, improvements in image quality, particularly for ScanSAR products, would be beneficial. Correction of some of the problems (e.g. ADC saturation, Doppler-centroid estimation, beam-seaming, etc.) which have resulted in some visual image quality artefacts with RADARSAT-1, would be beneficial as consistent visual image quality is important. Also, improved radiometric stability and accuracy of ScanSAR (and other mode) products would be most welcome, particularly as algorithms are developed for multi-polarization and/or polarimetric data analysis and information extraction.

The order handling system proposed for RADARSAT-2 promises to handle shorter lead times for satellite tasking, on the order of up to 2 days before acquisition, for routine ordering. Although improved lead-time for ordering would be of some benefit to ice

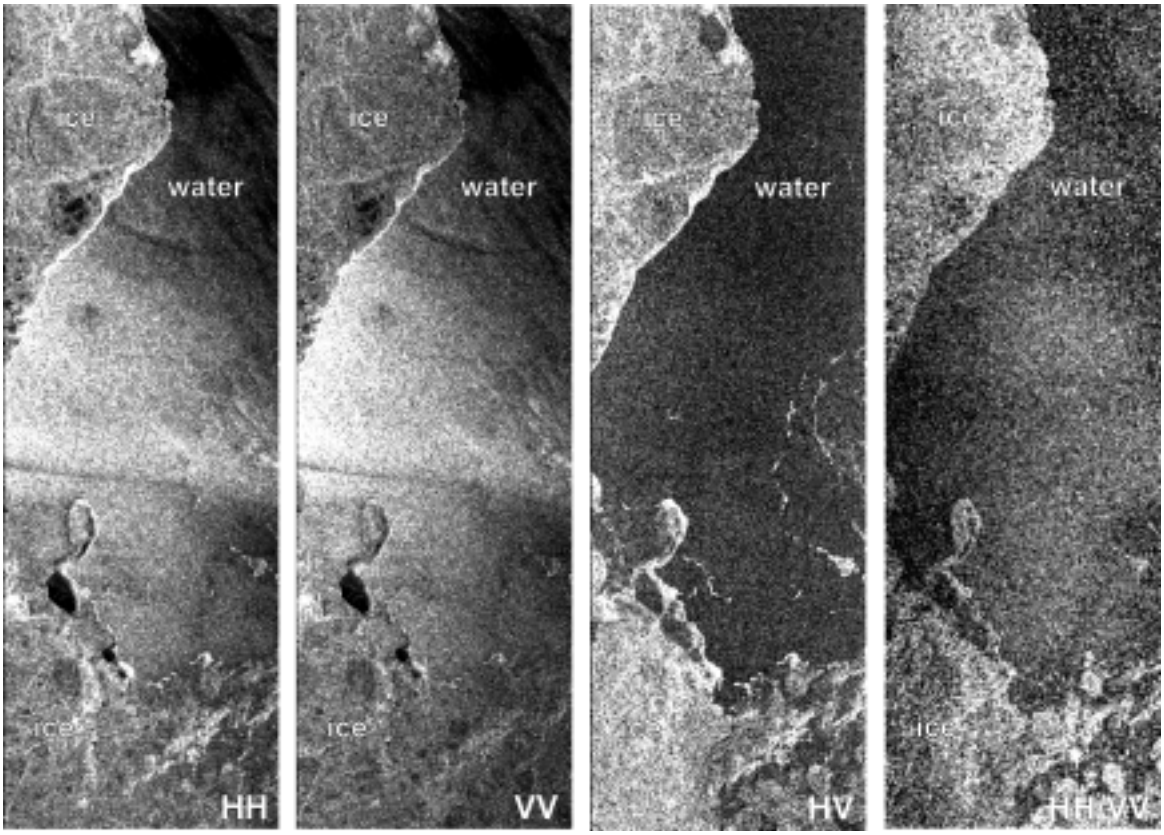


(a) (b) (c) (d)

**Figure 3.8.1-1 (a-d)** C-band radar images illustrating the effect of polarization on the ice / water contrast (**a**) HH-polarization (**b**) VV-polarization (**c**) HV-polarization (**d**) HH/VV polarization ratio. Images acquired by SIR-C on April 18, 1994 over the Labrador Sea.

operations, it is preferable to plan a minimum of 3-5 days in advance of acquisition to co-ordinate with coast guard and icebreaker planning.

Currently with RADARSAT-1, a beam mode switch requires a minimum of 13 seconds which equates roughly to an imaging gap of around 100 km. RADARSAT-2 promises a 10 microsecond beam mode switch operation which is would result in virtually no data gap when switching from one mode to another. This “instantaneous” switching capability this may be useful for operational ice mapping as it could minimize mode conflicts and also allow more efficient use of ScanSAR for wide area ice monitoring in conjunction with higher resolution acquisitions over targeted areas of interest. Figure 3.8.1-2 simulates what this functionality may be able to provide for ice monitoring in the Gulf of St. Lawrence and Northumberland Strait, a critical area for navigation.

### 3.8.2 Sea ice type

Ice type mapping is dependent on the discrimination of small-scale surface roughness characteristics, surface versus volume scattering, and large-scale ice structures and deformation. Backscatter at C-band is dominated by surface scattering (new and first-year ice) and near-surface volume scattering (multi-year ice) and offers acceptable discrimination of these ice types in cold conditions. Under wet conditions, volume and surface scattering from overlying snow becomes the dominant return, thus masking the contrasts between the

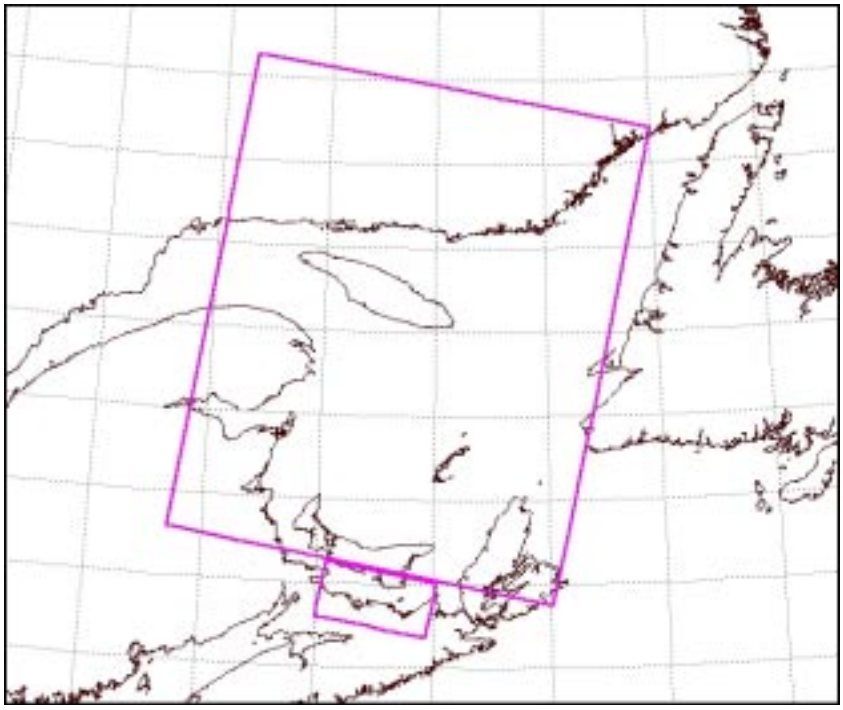

**Figure 3.8.1-2** Illustration of utility of potential “instantaneous” beam-mode switch capability of RADARSAT-2 for sea ice monitoring. The figure shows a descending pass ScanSAR Wide acquisition for Gulf of St. Lawrence to achieve moderate resolution wide spatial coverage, and a higher resolution Wide 2 acquisition of Northumberland Strait on the same pass to map greater detail. The fast beam-switching capability of RADARSAT-2 should allow these types of acquisitions to be planned with minimal gap between switching modes.

underlying ice types. HH-polarization data from RADARSAT-1 does an acceptable job at discriminating between the two major categories of multi-year and first-year ice.

Backscatter from multi-year ice is primarily a function of the air bubbles in the ice volume which depolarize the incident wave. Conversely, first-year ice backscatter is primarily a function of surface roughness, which has minimal depolarizing effect. Cross-polarization data alone has demonstrated better separation between multi-year ice and first-year ice than like-polarized returns (Flett, 1997; Onstott, 1992). Thus, cross-pol ScanSAR data would be advantageous if maximum discrimination between these two primary ice types is needed. The cross-polarization ratio may also improve potential in discriminating multi-year ice from first-year ice as the multi-year ice will have a strong depolarized response while first-year ice will not, thus maximizing the ratio difference between the two. As noted previously the capability to calculate this parameter will not be available in the modes of choice for sea ice mapping.

The separation of thin and new ice types from open water is one of the major problems with current single-channel SARs, for similar reasons as those given in the previous section. Although there appears to be some incremental benefit to be achieved with the availability of cross-polarization ScanSAR data for multi-year/first-year discrimination, use of cross-polarization for thin ice detection is not recommended as intensity differences due to surface scatter are suppressed (Onstott, 1992). Eriksson *et al.* (1998) looked at a multi-frequency SIR-C data set of the Weddell Sea and found that it was easier to find a good combination of parameters in L-Band than in C-band for thin ice discrimination. However, for C-band the best two-parameter combination was using the co-polarization ratio with one or the other of the like-polarization channels (HH or VV), although the conclusion was that they could not achieve good thin ice separation with only C-band parameters. Thomsen *et al.* (1998) looking at C-band polarimetric sea ice data in the Greenland Sea, found some improved separation beyond either like-polarization channel between two distinct thin ice types when using the co-polarized ratio. They note that no single polarimetric parameter can adequately discriminate between all ice types, but by combining various polarimetric information, better classification can be achieved. The overall conclusions of the study indicate that a) information on the co-polarization phase difference can be used for separating water from a range of thin ice types, b) detailed information of the scattering mechanism symmetries can be used to separate frazil and congelation ice in newly formed leads and open water, and c) that the co-polarization ratio is useful for separating multi-year ice from rough thin ice and open water. This is similar to the conclusions from the earlier work of Drinkwater *et al.* (1991) which concludes that additional phase information embedded in the correlations between the different polarized waves is the real power of polarimetric data for ice typing and classification. Furthermore, the use of measures that include phase differences could allow separation of all ice types from open water unambiguously and discrimination of multi-year, thin, and thick ice types. Although this is promising for sea ice information analysis, exploitation of this type of information from RADARSAT-2 would require acquisition of fully polarimetric mode data, available only in narrow swath modes.

Regardless of the work described in the preceding paragraph, it is still relatively unknown what additional ice information will be retrievable from polarimetric data that will be of utility to ice monitoring. There has been a relatively limited body of work on analysis of polarimetric sea ice data sets, particularly over a variety of surface and environmental conditions. In this respect, polarimetric data from RADARSAT-2 will be useful to more fully explore polarimetric dimensionality and potential for ice applications. Currently, the Canadian Ice Service is exploring the use of RADARSAT-1 data for assessing the state of ice decay. Part of this

relies on the ability to accurately determine when ponding begins on the ice surface and when the water begins to drain though the ice, a precursor to fracture and breakup and an indication of weakening or decay. Cross-polarization data should assist in resolving some of the ambiguity as to the presence or absence of surface water now encountered with like-polarization data, particularly under high wind conditions (De Abreu, 2001). Polarimetric data may shed more light on this and other ice applications, but at present this is unknown.

### 3.8.3 Sea ice topography and structure

Ice topography and structure and ice deformation features, such as ridging, are important parameters as these features pose a significant hazard and impediment to navigation. Cross-polarization data is known to be more sensitive to and provide enhancement of structural information and has demonstrated some utility for enhancing discrimination between smooth and deformed ice. This is a function of the combined volume scattering and multiple-reflection surface scattering in the ice ridges enhancing the cross-polarization radar returns (Livingstone, 1994). Observations of C-band scatterometer measurments of Baltic sea ice by Makynen and Hallikainen (1998) quantitatively illustrated that the backscatter contrast between level ice and ice ridges is larger at cross-polarization than co-polarization. Figure 3.8.3-1 illustrates this enhancement with C-band HH and HV data for cold winter ice

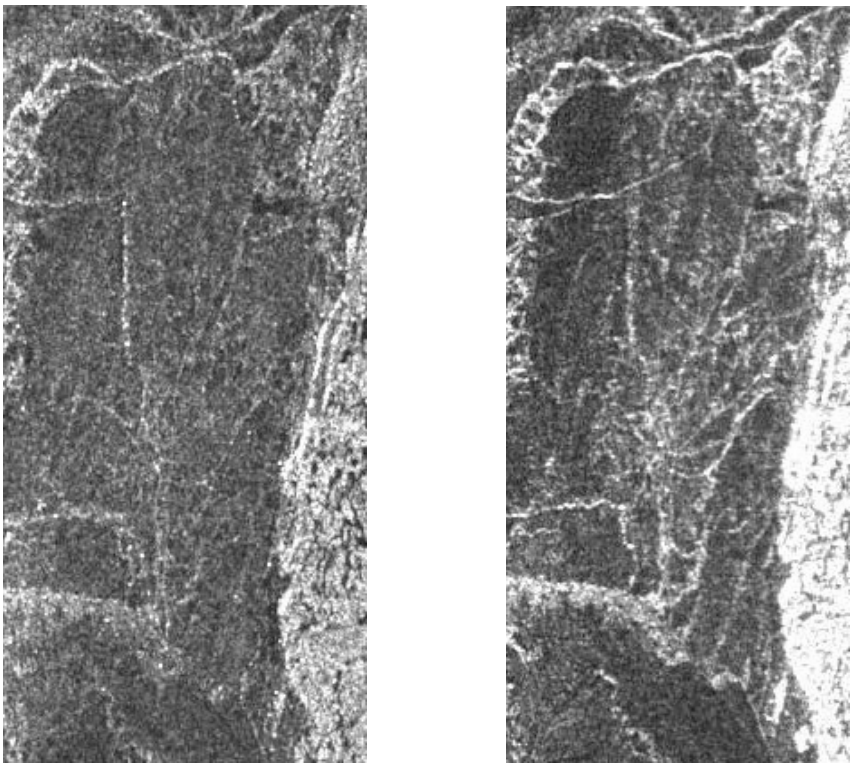

(a) (b)

**Figure 3.8.3-1 (a-b)** C-band radar images acquired by the Convair-580 over the Resolute Passage in May 1993 (**a**) HH-polarized image (**b**) HV-polarized image. The left-hand two-thirds of each image is first-year ice with ridging and deformation throughout. The brighter feature at the right-hand side of each image is a multi-year ice floe. The HV image (b) shows much greater ice surface topography and structural detail within the first-year ice than the HH image (a).

conditions (Flett, 1997). As a result, cross-polarization ScanSAR data from RADARSAT-2 should be an improvement over the current like-polarization case for better detection of ice topography and structure.

It is noted that lower-frequency systems such as L-band allow greater penetration into both first- and multi-year ice types, and are thus dominated by volume scattering behaviour. This reduces the contrast between ice types but enhances large-scale deformations, fractures and ice structures. A multi-frequency system would be expected to provide complementary information on ice type and structures, as well as provide improved penetration through snow cover under wet conditions.

### 3.8.4 Icebergs

The radar backscatter from an iceberg arises from two mechanisms, specifically surface and volume scattering (Haykin *et al.,* 1994). Volume scattering, which is most dominant, is due to the low absorption of the non-saline glacial ice allowing considerable penetration of the radar energy into the iceberg volume. The penetrated energy is then scattered by dielectric discontinuities that are due to trapped air pockets. Surface scattering is dependent on the specific surface structure of individual icebergs, including variations due to any snow or water on the surface of the iceberg, which may also reduce or alter the signal penetration. Thus, the orientation of local surface roughness, and vertical relief relative to other portions of the iceberg and/or the sea surface, are contributing factors in the total backscattered intensity. Therefore, the response for an iceberg generally contains a significant contribution from intensities above the ocean backscatter (clutter). Only in instances with high clutter and small icebergs relative to the resolution of the SAR will the response be indistinguishable from the speckle.

As a result of the scattering mechanisms described above, icebergs, like ships, manifest themselves in C-band radar images as bright point targets. Thus, similar to the ship detection case, cross-polarization data will be advantageous for detecting icebergs, particularly at steeper incidence angles below 35 degrees and in high sea states. The availability of cross-polarization from RADARSAT-2 in all currently available RADARSAT-1 beam modes is particularly useful, as various modes could be used depending on area of coverage and resolution required. Some discrimination of ships from icebergs is currently possible with single channel systems primarily using higher resolution (e.g. Fine) beam modes (C-CORE, 2000). It is expected that information contained in data acquired by fully polarimetric radar systems will further facilitate the discrimination of icebergs from ships. Additionally, those new modes, such as Ultra-Fine, will also enhance the capabilities for iceberg detection, albeit for limited swath widths.

### 3.8.5 Polar glaciology

Continuing study and monitoring of polar regions is important because of the climate related changes which appear to be taking place in some areas of both the Arctic and the Antarctic. For example, regional warming has affected ice shelves on the Antarctic Peninsula (Vaughan and Doake, 1996) and a warming trend has led to the thinning of the sea ice cover in the Arctic (Rothrock *et al.*, 1999). RADARSAT-2 will provide the capability to continue to study and monitor change for various polar sea ice and glaciological sites and conditions.

The ability of RADARSAT-2 to easily change from a right- to left-looking mode is very important to Antarctic glacial ice monitoring. It appears that during its life, RADARSAT-2 will have a unique capability to image parts of Antarctica not accessible by other high resolution remote sensing satellites. In this way, the pioneering results achieved during the 1997 Antarctic Mapping Mission (AMM) with RADARSAT-1 can be repeated, and change in ice flow patterns can be studied in a way and at a scale not possible prior to the RADARSAT program. The left-looking mode also will enable monitoring parts of the large floating ice shelves in Antarctica not visible by the Envisat ASAR, or by other high resolution satellites.

In the Arctic, the fine and standard mode acquisitions with RADARSAT-2 will help provide information on glacier equilibrium line position, and change in the outline of a glacier or ice cap. RADARSAT repeat-pass interferometry can also provide information on ice motion, at least under cold freezing conditions. Coupled with other information, this will provide information on change in mass balance. It is not clear that whether the polarimetric capability of RADARSAT-2 will add significantly to the capability for glacial ice monitoring; more research is required. However, in the Arctic, RADARSAT-2 data will provide continuity of the temporal record of SAR coverage, which will become more and more important as we try to better understand the impacts of climate change in the north.

Research is still required to study the changes associated with melting of permafrost and ground ice. The implications of thaw subsidence ('thermokarst') on roads, pipelines, northern industry, communities, tourism, etc. is significant, and under some conditions the areal extent of thermokarst may be amenable to mapping with satellite radar interferometry. Work is underway now to evaluate the contribution of RADARSAT-1 data for mapping changes in ground ice conditions; particularly changes in permafrost, ground ice and coastal erosion. If successful, this is a potentially a very important application for RADARSAT-2. The improved orbit maintenance and knowledge of satellite position will improve the interferometric capabilities of RADARSAT-2 in relation to RADARSAT-1.

## 3.9 Applications Summary

Table 3.9-1 summarises our assessment of the effect of the most important technical enhancements of RADARSAT-2 on the information content and hence the application potential of it's data. Our expectations regarding the combined effect of these technical enhancements on the overall application potential of RADARSAT-2 are rated in Table 3.9-2. This table also lists our ratings for RADARSAT-1 and hence illustrates to what degree the progress in space-borne SAR technology as embodied by RADARSAT-2 is expected to improve the application potential of it's data products. Evidently, the applicability of the RADARSAT-2 data will govern the satellite's economic viability and as such it's contribution to the operationalisation of space-borne radar remote sensing.

In the Selective Single Polarization (SSP) mode of operation RADARSAT-2 will image in the HH, HV, VV or VH polarization. Table 3.9-1 shows that this capability will moderately advance the potential of RADARSAT-2 for applications the information needs of which can generally be met by single channel C-band data but for which the HH-polarization as offered by RADARSAT-1 is not the most favourable. As a rule, the information needs associated with hurricanes, oil spills and winds are better met through application of VV-polarized images. Similarly, the requirements pertaining to clearcuts, fire-scars, ships, and selected

**Table 3.9-1** Anticipated effect of new RADARSAT-2 features on applications potential in terms of data information content. Key: '-' minor, '-/+' moderate, '+' major.

| Application | RADARSAT-2 Feature | | | | | |
|---|---|---|---|---|---|---|
| | Selective Single Polarization | Selective Dual Polarization | Quad Polarization | Ultra-Fine Spatial Resolution | Selective Look Direction | Improved Orbit Control |
| Agriculture | | | | | | |
| Crop type | - | -/+ | + | - | - | - |
| Crop condition | - | -/+ | + | -/+ | -/+ | - |
| Crop yield | - | - | -/+ | -/+ | - | - |
| Cartography | | | | | | |
| DEM interferometry | - | - | - | + | - | + |
| DEM stereoscopy | - | - | - | + | - | -/+ |
| DEM polarimetry | N.A. | N.A. | + | N.A. | - | -/+ |
| Cartographic feature extraction | - | - | -/+ | + | - | -/+ |
| Disaster Management | | | | | | |
| Floods | - | - | - | - | + | - |
| Geological hazards | - | -/+ | -/+ | -/+ | + | - (+) [1] |
| Hurricanes | -/+ | - | -/+ | - | + | - |
| Oil spills | -/+ | - | - | -/+ | + | - |
| Search and rescue | - | - | + | -/+ | + | -/+ (+) [1] |
| Forestry | | | | | | |
| Forest type | - | - | -/+ | -/+ | - | - |
| Clearcuts | -/+ | - | - | -/+ | - | - |
| Fire-scars | -/+ | - | - | -/+ | - | - |
| Biomass | - | - | - | - | - | - |
| Geology | | | | | | |
| Terrain mapping | - | -/+ | -/+ | -/+ | - | - (+) [1] |
| Structure | - | -/+ | -/+ | -/+ | - | - |
| Lithology | - | - | - | - | - | - |
| Hydrology | | | | | | |
| Soil moisture | - | - | -/+ | - | -/+ | - |
| Snow | - | - | -/+ | - | -/+ | - |
| Wetlands | - | -/+ | -/+ | -/+ | - | - |
| Oceans | | | | | | |
| Winds | -/+ | - | - | - | - | - |
| Ships | -/+ | - | -/+ | + | -/+ | -/+ |
| Waves | - | - | -/+ | - | - | - |
| Currents | - | - | - | - | - | - |
| Coastal zones | - | -/+ | -/+ | -/+ | - | - |
| Sea and Land Ice | | | | | | |
| Sea ice edge and ice concentration | -/+ | - | -/+ | - | -/+ | - |
| Sea ice type | - | - | -/+ | - | - | - |
| Sea ice topography and structure | -/+ | -/+ | -/+ | - | - | - |
| Icebergs | -/+ | - | -/+ | + | -/+ | -/+ |
| Polar glaciology | -/+ | -/+ | -/+ | - | + | - (+) [1] |

1) Using InSAR techniques.

sea and land ice applications are more easily satisfied when HV or VH images can be applied.

When operating in the Selective Dual Polarization (SDP) mode of operation RADARSAT-2 will acquire two coincident images either in the HH and HV or the VV and VH polarization. This capability is projected to moderately improve the capability of RADARSAT-2 to provide information in support of applications dealing with targets that include transparent vegetation / ice volumes with varying structural properties or land / ice surfaces with varying degrees of roughness. Applications that are expected to gain little information from having access to two image channels instead of one image channel (in SSP mode) have been given the 'minor' rating. Unfortunately, the SDP mode will not allow for simultaneous acquisition of HH- and VV-polarized data. Application fields that would benefit from this capability are those focusing on soil moisture, waves and sea ice edge / concentration. RADARSAT-2 will be capable of acquiring coincident HH- and VV-polarized images in the Quad Polarization mode. However, the swath width of these images will be substantially smaller than the swath width of the images acquired in the SDP mode.

In the Quad Polarization (QP) or fully polarimetric mode the SAR onboard of RADARSAT-2 will measure the amplitude and phase of the backscattered wave for the four available transmit and receive linear antenna polarization combinations (HH, HV, VV, VH). These measurements will enable the computation of a wide variety of variables that relate to the strengths, polarizations or phases of the radar return signals as received from the observed objects. Table 3.9-1 shows that the introduction of the QP imaging mode is expected to moderately advance the potential of RADARSAT-2 for most applications. Applications for which the QP data are anticipated to be particularly valuable or essential ('major' rating) are concerned with crop type, crop condition, DEM polarimetry, and search & rescue. Once again, 'minor' ratings have been given whenever the increase in terms of radar data is not expected to result in a significant increase in applicable information. Due to technical limitations the swath width of the images acquired in the QP mode is restricted to 25 km. This narrow swath width poses a definite problem for the operational use of QP data in applications that require information on extended geographical areas, e.g. forestry, oceans and sea ice applications.

RADARSAT-2's capacity to acquire images with Ultra-Fine spatial resolutions (nominally 3 m by 3 m and single look) is restricted to the SSP imaging mode of operation. As indicated in Table 3.9-1 it is our expectation that this capability will enhance the potential of RADARSAT-2 for cartographic applications and applications concerned with point targets, that is, ships and icebergs, in particular. In addition there is a considerable number of applications that are foreseen to moderately benefit from the upcoming availability of these very high resolution space-borne SAR data. Like the QP data products, the Ultra-Fine data products have a limited swath width (20 km). Again, this will obstruct the operational use of this data type in certain applications, e.g. the mapping of clearcuts and fire-scars and ship and iceberg surveillance. Yet, the narrow swath width is not so much an obstacle for the tracking of ships and icebergs.

The selective look direction feature of RADARSAT-2 is expected to have a 'major' effect on its potential for applications in the fields of disaster management and polar glaciology. Applications in the context of disaster management will benefit form the reduced average response time and the generally increased revisit frequency. On the other hand, the polar glaciology application will gain from the fact that the left-looking configuration will enable

**Table 3.9-2** Application potential of RADARSAT-1 and RADARSAT-2 [1]. Key: '-' minimal, '-/+' limited, '+' moderate, '++' strong.

| Application | Satellite | |
|---|---|---|
| | **RADARSAT-1** | **RADARSAT-2** |
| Agriculture | | |
| Crop type | -/+ | ++ |
| Crop condition | -/+ | ++ |
| Crop yield | - | -/+ |
| Cartography | | |
| DEM interferometry | + | + |
| DEM stereoscopy | ++ | ++ |
| DEM polarimetry | N.A. | -/+ |
| Cartographic feature extraction | + | ++ |
| Disaster Management | | |
| Floods | ++ | ++ |
| Geological hazards | -/+ | + |
| Hurricanes | + | + |
| Oil spills | + | + |
| Search and rescue | -/+ | + |
| Forestry | | |
| Forest type | -/+ | -/+ |
| Clearcuts | -/+ | + |
| Fire-scars | -/+ | + |
| Biomass | - | - |
| Geology | | |
| Terrain mapping | -/+ | + |
| Structure | + | ++ |
| Lithology | -/+ | -/+ |
| Hydrology | | |
| Soil moisture | -/+ | + |
| Snow | -/+ | + |
| Wetlands | -/+ | + |
| Oceans | | |
| Winds | + | ++ |
| Ships | + | ++ |
| Waves | -/+ | -/+ |
| Currents | -/+ | + |
| Coastal zones | -/+ | + |
| Sea and Land Ice | | |
| Sea ice edge and ice concentration | + | ++ |
| Sea ice type | + | + |
| Sea ice topography and structure | -/+ | ++ |
| Icebergs | -/+ | + |
| Polar glaciology | + | + |

1) Use of single date images assumed.

RADARSAT-2 to routinely image the most southerly regions on earth including Antarctica. Applications expected to benefit from the increase in the number of imaging opportunities but dealing with circumstances that are not usually life-threatening have been given the 'moderate' rating. For example, the crop condition application would gain from having an image available immediately after the onset of an infestation has been reported.

The improved knowledge about and control over the RADARSAT-2 orbit will enhance the potential of the image data products for applications that make use of interferometric processing techniques in particular. Table 3.9-1 therefore shows the 'major' rating in connection with the following applications: DEM interferometry, geological hazards, search and rescue, terrain mapping and polar glaciology. The cartographic mapping applications and other applications will benefit considerably from the improved accuracy with which scenes will be georeferenced have been given the 'moderate' rating. For the remaining applications the enhancements in terms of orbit knowledge and control are projected to be useful but not essential ('minor' rating).

Table 3.9-2 shows our assessments of the overall application potential of RADARSAT-1 and the anticipated overall application potential of RADARSAT-2. The difference in the ratings for the two satellites illustrates the degree to which we expect the technical innovations contained in RADARSAT-2 to enhance the information content of the data products and hence to expand the applications potential of these products. With regard to Table 3.9-2 it is important to note that we assume application of single date images. The use of images acquired on different dates would enhance the application potential in fields dealing with vegetation in particular. For example, the rating associated with RADARSAT-1 and crop type mapping would have been 'moderate' rather than 'limited' if the application of multi-temporal data had been considered.

Comparison of the ratings for RADARSAT-1 and –2 shows that the biggest improvement in application potential is projected to be associated with the crop type, crop condition and sea ice topography / structure fields (change in ratings from 'limited' to 'strong'). This is primarily the result of the enhancement of RADARSAT-2 in terms of polarization. Of the 29 remaining applications fields, the DEM polarimetry field is one that cannot currently be attended to with data from RADARSAT-1. The potential of RADARSAT-2 for this particular application is rated as 'limited' because of the minimal flexibility in terms of viewing geometry and the fact that the elevation information is limited to the azimuth direction. For 18 out of the 32 fields considered we predict that the introduction of RADARSAT-2 will result in a modest increase in application potential. Going from RADARSAT-1 to RADARSAT-2 the potentials associated with these applications are ranked one category higher. The RADARSAT-2 features that instigate these changes in application potential may differ from one application to another. For 10 fields we foresee no increase in application potential. Among these are the applications concerned with DEM stereoscopy and floods, that is, applications for which the potential of RADARSAT-1 data products is already ranked as 'strong'. For the DEM interferometry and hurricanes fields the application potential stalls at the 'moderate' rating because of restraints imposed by atmospheric conditions and swath width, respectively. The orbital characteristics of RADARSAT-1 and RADARSAT-2 make that the application potential for the waves field halts at the 'limited' rating. Generally speaking, the information requirements of the five remaining applications can only be better satisfied by low- or multi-frequency SAR systems (e.g. forest type, forest biomass, sea ice type) or by optical remote sensing systems (e.g. oil spills, lithology).

# 4 Recommendations for Research and Development

Consistent with the objectives, the following recommendations for applications research and development (R&D) will focus on the new RADARSAT-2 data products. Outstanding R&D issues that relate to the application of the current SAR satellite data can be expected to carry forward into the RADARSAT-2 era. These may concern the development of new application fields, the transfer of applications from one environment to another, the fine-tuning of known applications or the development of complete solutions. The new RADASAT-2 data products may prove to help resolve these issues in some ways and complicate them in other ways. For example, the Selective Dual Polarization images may both ease and burden application development because they contain more information and constitute a larger data volume, respectively.

We have demonstrated in Chapter 3 that, for most applications, the information content of RADARSAT-2 images is likely to exceed that of ERS-1/2 and RADARSAT-1 images. This is largely thanks to the enhancement of the RADARSAT-2 SAR in terms of spatial resolution and polarization. In general, the change in the image information content as a function of spatial resolution can easily be reckoned with. Hence, we expect that the successful application of the new high-resolution RADARSAT-2 image products does not require major research efforts at this time. Existing techniques for information extraction can probably be applied to these data without further ado. Efforts to develop operational applications for the Ultra-Fine mode data will have to confront the high data volume per unit ground area and the limited swath width. These problems are best addressed following the launch of the satellite. By that time they may well have lost weight thanks to the ongoing development of compression techniques for data from other (remote sensing) sources.

Although recognized in most application fields, the effect of the polarization on the image information content is not well understood in many of those fields. R&D in the context of RADARSAT-2 should focus on alleviating the lack of understanding concerning polarization and image information content because it will hinder the application of certain RADARSAT-2 image products. Primarily thanks to the availability of data from ERS-1/2 and RADARSAT-1, the current knowledge about the information in and hence the application potential of C-band VV and C-band HH image products is considerable. The understanding with respect to application potential of C-band HV (VH) is less developed mainly because it rests on a limited number of data sets that have been acquired by space-borne, airborne or ground based radar systems during short-lived operations. This implies that there is an explicit requirement for R&D relating to the Selective Single Polarization (SSP) HV (VH) polarized data products and the Selective Dual Polarization (SDP) data products.

However, the primary R&D challenge lies in the extraction and application of the information as contained in the data acquired in the Quad Polarization (QP) image mode. Even though fully polarimetric C-band SAR data have been acquired in an experimental fashion for more than 10 years their potential for many application fields is poorly understood. This is evident from the literature and is partly due to the fact that most of the data were acquired by multi-frequency systems, i.e. the NASA JPL AIRSAR and the SIR-C SAR. Researchers that have worked with these data tend to focus on the multi-frequency rather than the polarimetric aspect of these data. To a large degree this is explained from the fact that the information content of images acquired in different wavelengths often exceeds that of images acquired in different polarizations. By and large, good results are therefore achieved more easily

through the extraction and application of information resulting from diversity in frequency rather than from diversity in polarization. This contributes to the noted lack of knowledge concerning C-band polarimetric data but also gives good reason for a cautionary message in reference to RADARSAT-2. The preference of the research community for multi-frequency data shows that the market for RADARSAT-2 products could diminish considerably when the existing plans for multi-frequency SAR satellites (e.g. TerraSAR) become reality (Infoterra, 2001).

R&D concerning the extraction and exploitation of information from C-band SAR images with polarizations other than HH and VV can be based on either archived or newly acquired data sets. The value of data sets available from archives often proves to be limited because the corresponding ground reference data are missing or incomplete. Available archived data sets include those as acquired by the Convair-580 SAR, NASA JPL AIRSAR and SIR-C SAR.

For the acquisition of new data in Canada, the airborne Convair-580 SAR is most readily available and hence the sensor of choice. The capabilities of this system are described in Appendix I of this report. The truck-mounted scatterometer system from CCRS could be deployed to accurately measure the C-band HH, HV, VH and VV backscatter responses of targets in a small-scale but regulable or at least definable setting. Technical enhancements would be required to enable the system to operate in a fully polarimetric mode. Experiments with this scatterometer would facilitate detailled studies into the relationships between the radar return signal and the dielectric and structural characteristics of the targets observed. Knowledge of these relationships supports the development of applications for similar data from imaging radar systems greatly. Applications concerned with crop type, crop condition, crop yield, soil moisture and snow are most suited to ground-based scatterometer experiments.

New data for areas of interest located beyond Canada's borders can possibly be obtained through participation in forthcoming missions from the AIRSAR system. The Advanced Synthetic Aperture Radar (ASAR), which is mounted on the Envisat-1 satellite, represents an important future source of multi-polarized (not fully polarimetric) C-band data. Scheduled for launch in October of 2001, the ASAR will be capable of imaging in the following polarization modes: HH, VV, HH+VV, HH+HV or VV+VH (ESA, 2001). In terms of incidence angle, viewing geometry, spatial coverage and repeat cycle the ASAR data will resemble the RADARSAT-2 data more closely than the data from airborne systems. Hence, the Envisat-1 ASAR data will make a valuable basis for applications R&D in preparation for RADARSAT-2. A prerequisite for all data to be investigated in the context of RADARSAT-2 is that they are well calibrated.

In Table 3.9-1 of Section 3.9 we have summarised our expectations concerning the degree to which the applications considered will benefit from, among others, RADARSAT-2's capabilities to image in new and multiple polarizations. R&D to prepare for the exploitation of the extended polarization capabilities should focus on application fields that hold the most promise for operational use of the related RADARSAT-2 products. Application fields that are anticipated to benefit moderately from the HV (VH) polarized SSP products have to do with the mapping and monitoring of clearcuts, fire-scars, ships and selected sea and land ice properties. The SDP data products are expected to have a moderately increased potential for application to the mapping and monitoring of crop type, crop condition, geological hazards, geological terrain features, geological structures, wetlands, coastal zones, sea ice topography, and polar glaciology. RADARSAT-2's QP data products are expected to

become a major source of information for operational application to the crop type, crop condition and search and rescue field. Operational use of these in the generation of DEMs is unlikely since the elevation information is restricted to the azimuth direction. As noted in Section 3.9, the potential of the QP data for operational application is generally compromised by the narrow swath width.

The present text conveys an initial assessment of the applications potential of the future RADARSAT-2 satellite. This preview is based on our current understanding about the state-of–the-art with respect to the extraction and application of information from RADARSAT-2 type data. Progress in R&D is likely to advance our knowledge on this topic and may therefore call for the adjustment of the presented preliminary assessment. In subsequent assessments the application potential of products in which RADARSAT-2 data are fused with other data sources, both in-situ and remote, should also be considered.

BLANK PAGE

# References


Ahern, F.J., and J.A. Drieman. (1988). “Assessment of Clearcut Mapping Accuracy With C-Band SAR”, In: Proceedings of IGARSS'88, Vol. 3, pp. 1335-1338.

Ahern, F.J., J.S. Paterson, R. Landry, D. Boucher and I. McKirdy. (1995). “Forest Landcover Information Content of Multi-frequency Multi-polarized SAR Data of a Boreal Forest”, In: *Proceedings of the 17th Canadian Symposium on Remote Sensing*, Vol. 2, pp. 537-549.

Ahern, F.J., R. Landry, I. McKirdy, V. Janusauskas, A. Banner, J. Russell, and T. Balce. (1997). "Factors affecting clearcut mapping accuracy from single-date RADARSAT images", In: *Proceedings of GER'97, Geomatics in the Era of RADARSAT*, Ottawa, 25-30 May 1997, Vol. I, CD-ROM.

Altese, E., O. Bolognani, M. Mancini, and P.A. Troch. (1996). “Retrieving soil moisture over bare soil from ERS-1 synthetic aperture radar data: Sensitivity analysis based on a theoretical surface scattering model and field data”, *Water Resources Research*, Vol. 32, No. 3, pp.653-661.

Amelung, F., D.L. Galloway, J.W. Bell, H.A. Zebker, and R.J. Laczniak. (1999). “Sensing the ups and downs of Las Vegas: InSAR reveals structural control of land subsidence and aquifer-system deformation”, *Geology*, Vol. 27, No. 6, pp. 483-486.

Amelung, F., S. Jónsson, H. Zebker, and P. Segall. (2000). “Widespread uplift and 'trapdoor' faulting on Galápagos volcanoes observed with radar interferometry”, *Nature*, Vol. 407, pp. 993-996.

Armenakis, C., A. Dow, L. Gray, K. Mattar, and M. Van Der Kooij. (2000). ”Evaluation of spaceborne InSAR generated DEM”, In: *Proceedings of the American Society of Photgrammetry and Remote Sensing*, Washington D.C., May 2000.

Armour, B., A. Tanaka, H. Ohkura, and G. Saito. (1998). “Radar Interferometry for Environmental Change Detection”, In *Remote Sensing Change Detection* (Ross S. Lunetta and Christopher D. Elvidge, Eds.), Ann Arbor Press, Ann Arbor, MI, pp. 245-279.

Barber, D.G., K. P. Hochheim, R. Dixon, and M.J. McMullan. (1996). “The role of earth observation technologies in flood mapping: a Manitoba case study”, *Canadian Journal of Remote Sensing*, Vol. 22, No. 1, pp.137-143.

Baronti, S., F. Del Frate, P. Ferrazzoli, S. Paloscia, P. Pampaloni and G. Schiavon. (1995). “SAR polarimetric features of agricultural areas”, *International Journal of Remote Sensing*, Vol. 14, pp. 2639-2656.

Beaudoin, A., T. Le Toan, S. Goze, E. Nezry, A. Lopes, E. Mougin, C.C. Hsu, H.C. Han, J.A. Kong, and R.T. Shin. (1994). “Retrieval of Forest Biomass From SAR Data”, *International Journal of Remote Sensing*, Vol. 15, No. 14, pp. 2777-2796.

Bernier, M. (1994). “The potential and limitations of ERS-1 SAR data to estimate the now water equivalent”. In: *Proceedings of the NHRI Symposium on Applications of Remote Sensing in Hydrology*, No. 14, pp.113-125.

Bernier, M. and J-P. Fortin. (1998). “The Potential of Time Series of C-Band SAR Data to Monitor Dry and Shallow Snow Cover”. *IEEE Transactions on Geoscience and Remote Sensing*, Vol.36, No. 1, pp. 226-243.

Blom, R.G., L.R. Schenck, and R.E. Alley. (1987). “What are the Best Radar Wavelengths, Incidence Angles and Polarizations for Discrimination Among Lava Flows and Sedimentary Rocks? A Statistical Approach”, *IEEE Transactions on Geosciences and Remote Sensing*, Vol. 25, No. 2, pp. 208-213.

Blumberg, D.G. (1998). “Remote Sensing of Desert Dune Forms by Polarimetric Synthetic Aperture Radar (SAR)”, *Remote Sensing of Environment*, Vol. 65, pp. 204-216.

Brakenridge, G.R., J.C. Know, E.D. Paylor, and F.J. Magilligan. (1994). “Radar remote sensing aids study of the great flood of 1993”. EOS transaction, *American Geophysical Union*, Vol. 75, No. 45, pp.526-527.

Braun, N., M. Gade, and G. Schymura. (2000). “Multi-frequency/multi-polarization measurements of radar backscatter under different rain and wind conditions”, In: *Proceedings of the IEEE 2000 International Geoscience and Remote Sensing Symposium (IGARSS 2000)*, 24 to 28 July 2000, Honolulu, Hawaii, USA, pp. 123-125.

Breivik, L.-A., M. Reistad, H. Schyberg, J. Sunde, H.E. Krogstad, and H. Johnsen. (1998). “Assimilation of ERS SAR wave spectra in an operational wave model”, *Journal of Geophysical Research*, Vol. 103, No. C4, pp. 7887-7900.

Brisco B. and T.J. Pultz. (1998). “Wetland Mapping and Monitoring with RADARSAT”. In: *Proceedings of the 20th Canadian Symposium on Remote Sensing*, Calgary, May 11-14 1998, 3 p.

Brown, C.E. and M.F. Fingas. (1998). "Oil spill remote sensors", In: R.A.Meyers (Ed.), Encyclopedia of environmental analysis and remediation*,* New York etc*.,* John Wiley & Sons, Inc., pp. 3200-3207.

Brown, C.E., M.F. Fingas, and W.C. Bayer. (1999). "The Future of the Convair-580 SAR Facility", In: *Proceedings of the 21st Canadian Symposium on Remote Sensing*, Ottawa, Ontario, June 21-24, pp. I-463 - I-467.

Brown, N. (2000). “Practical commercial remote sensing applications in the Ontario precision farming marketplace”, In: *Proceedings of the Second International Conference on Geospatial Information in Agriculture and Forestry,* Lake Buena Vista*,* Florida, 10-12 January 2000, Vol. I, pp. 6-13.

Brown, R.J., B. Brisco, R. Leconte, D.J. Major, J.A. Fischer, G. Riechert, K.D. Dorporal, P.R. Bullock, H. Pokrant, and J. Culley. (1993). “Potental Applications of RADARSAT data to Agriculture and Hydrololgy”, *Canadian Journal of Remote Sensing*, Vol. 19, No. 4, pp. 317-329.

Canadian Space Agency. (1998). “Bringing Radar Applications Down to Earth”, In: *Proceedings of the RADARSAT ADRO Symposium,* Montreal, Canada, 13-15 October 1998, CD-ROM.

C-CORE. (2000). *Validation Of Iceberg Detection Capabilities Of Radarsat Synthetic Aperture Radar - Final Report*. St. John’s, Newfoundland, C-CORE Contract Report 00-C5 for Canadian Ice Service, February.

CCRS, Canada Centre for Remote Sensing. (2001). *RADARSAT-2 Demonstration Website*, http://www.ccrs.nrcan.gc.ca/ccrs/tekrd/radarsat/r2demo/r2demoe.html.

CEOS. (2000a). Earthquake Hazards CEOS Disaster Management Support Project. NOAA, pp. 16-30.

CEOS. (2000b). Volcanic Hazards CEOS Disaster Management Support Project. NOAA, pp. 103-129.

CHART. (1999). *Calibration of RADARSAT data for use in a multilayered coastal habitat identification model.* St. John's, NF, Coastal Habitat Assessment Research and Technology, Inc., RSDDP Contract 23413-8-D479, 55 p.

Chunchuzov, I., P.W. Vachon, and B. Ramsay. (2000). “Detection and Characterization of Polar Mesoscale Cyclones in RADARSAT Synthetic Aperture Radar Images of the Labrador Sea”, *Canadian Journal of Remote Sensing*, Vol. 26, No. 3, pp. 213-230.

Cimino, J.B., A. Brandani, D.J. Casey, J. Rabassa, and S.D. Wall. (1986). "Multiple incidence angle SIR-B experiment over Argentina: mapping of forest units", *IEEE Transactions on Geoscience and Remote Sensing*, Vol. GE-24, No. 4, pp. 498-509.

Corbley, K.P. (2000). "Canadian firm provides turnkey solution for Indonesian coastline mapping project", *Earth Observation Magazine*, No. February 2000, pp. 25-27.

Cracknell, A.P. (1999). "Remote sensing techniques in estuaries and coastal zones - an update", *International Journal of Remote Sensing*, Vol. 19, No. 3, pp. 485-496.

Creber, K.A.M., A.R. Green, E.A. Ough, and V. Singh. (1997). "A Comparison Study of Data from RADARSAT, Landsat, A Multispectral Camera, A Field Portable Spectrometer and A High Resolution UV-Vis-NIR Spectrometer", In: *Proceedings of the International Symposium on Geomatics in the Era of RADARSAT*, May, 5 p.

Crevier, Y., and T. J. Pultz. (1996). "Analysis of C-Band SIR-C radar backscatter over a flooded environment, Red River, Manitoba", In: *Proceedings of the Third International Workshop on the Applications of Remote Sensing in Hydrology*, pp. 47-60.

CSA, Canadian Space Agency. (2001). *RADARSAT-2 website,* http://space.gc.ca/csa_sectors/earth_environment/radarsat2/rad_inf/default.asp.

Cunnningham, C.J., W. Millett, and P.W. Somers. (1994). "Multispectral Satellite Imagery for Search and Rescue", In: *Proceedings of the 8th CASI Conference on Astronautics*, Nov. 8-10, pp. 97-99 .

D'Iorio, M.A., B. Rivard, and P. Budkewitsch. (1996). "Use of Sar Wavelength and Polarization Information for Geological Interpretation of a Semi-Arid Terrain", *Canadian Journal of Remote Sensing*, Vol. 22, No. 3, pp. 305-316.

Daily, M., C. Elachi, T. Farr, and G, Schaber. (1978). "Discrimination of Geologic Units in Death Valley Using Dual Frequency and Polarization Imaging Radar Data", *Geophysical Research Letters*, Vol. 5, pp. 889-892.

Dams, R.V., D. Flett, M.D. Thompson, and M. Lieberman. (1987). "SAR (STAR-1) image analysis for Costa Rican tropical forestry applications", In: *Proceedings II Simposyum Latinoamericano de Sensores Remotos,* Bogota*,* 16-20 November 1987, Vol. pp. 23-32.

De Abreu, R.A. (2001). *Personal communication*.

de Loor, G.P. (1981). "The observation of tidal patterns, currents and bathymetry with SLAR imagery of the sea", *IEEE Journal of Oceanic Engineering*, Vol. 6, pp. 124-129.

de Matthaeis, P., P. Ferrazzoli, G. Schiavon and D. Solimini. (1992). "Agriscatt and MAESTRO: Multifrequency radar experiments for vegetation remote sensing", In: *Proceedings of MAESTRO-1/AGRISCATT: Radar Techniques for Forestry and Agricultural Applications, Final Workshop*, The Netherlands, 6-7 March, 1992, pp. 231-248.

Dellwig, L.F. and R.K. Moore. (1966). "The Geological Value of Simultaneously Produced Like- and Cross-Polarized Radar Imagery", *Journal of Geophysical Research*, Vol. 71, No. 14, pp. 3597-3601.

Dobson, M.C., F.T. Ulaby, T. Le Toan, A. Beaudoin, E.S. Kasischke and N. Christensen. (1992). "Dependence of Radar Backscatter on Coniferous Forest Biomass", *IEEE Transaction on Geoscience and Remote Sensing*, Vol. 30, No. 2, pp. 412-415.

Dowd, M., P.W. Vachon, F.W. Dobson, and R.B. Olsen. (2001). "Ocean wave extraction from RADARSAT synthetic aperture radar inter-look image spectra", *IEEE Transactions on Geoscience and Remote Sensing*, Vol. 39, No. 1, pp. 21-37.

Dowman, I.J., Z.-G. Twu, and P.H. Chen, (1997). "DEM generation from stereoscopic SAR data". In: *Proceedings of the ISPRS Joint Workshop on Sensors and Mapping from Space*, Hannover, Germany, 29 September-2 October 1997, pp. 113-122.

Dreibelbis, R., D.W. Affens, H. Rais, and A.W. Mansfield. (1999). "The Montana Project", In: *Proceedings of SPIE Conference on Automatic Target Recognition IX*, F.A. Sadjadi (Ed.), SPIE Vol. 3718, 7-9 April, Orlando, Florida, pp. 221-229.

Drieman, J.A. (1987). "Evaluation of SIR-B imagery for monitoring forest depletion and regeneration in western Alberta", *Canadian Journal of Remote Sensing*, Vol. 13, No. 1, pp. 19-25.

Drinkwater, M.R., R. Kwok, D.P. Winebrenner, and E. Rignot. (1991). "Multifrequency polarimetric synthetic aperture radar observations of sea ice", *Journal of Geophysical Research,* Vol. 96(C11), pp. 20,679-20,698.

Duncan, R., T.J. Pultz, J.B. Boisvert, and R.J. Brown. (1994). “Estimation of soil moisture using Polarimetric Radar Data”, In: *Proceedings of the Second International Workshop on the Applications of Remote Sensing in Hydrology*, NHRI Symposium, No. 14, pp.43-51.

Dunlap, E.M., R.B. Olsen, L.J. Wilson, S. De Margerie, and R. Lalbeharry. (1998). “The effect of assimilating ERS-1 fast delivery wave data into the North Atlantic WAM model”, *Journal of Geophysical Research*, Vol. 103, No. C4, pp. 7901-7915.

Durden, S.L., J.J. van Zyl, and H.A. Zebker, (1989). “Modeling and observation of radar polarization signature of forested areas*”, IEEE Transactions on Geoscience and Remote Sensing*, Vol. 27, No. 3, pp. 290-301.

Edwards, G., R. Landry, and K.P.B. Thompson. (1988). "Texture analysis of forest regeneration sites in high resolution SAR imagery", In: *Proceedings of the IGARSS 1988 Symposium; Remote Sensing: Moving Towards the 21st Century,* Edinburgh*,* 12-16 September 1988, pp. 1355-1360.

Engen, G., and H. Johnsen. (1995). “SAR-ocean wave inversion using image cross-spectra”, *IEEE Transactions on Geoscience and Remote Sensing*, Vol. 33, No. 4, pp. 1047-1056.

Engen, G., P.W. Vachon, H. Johnsen, and F.W. Dobson. (2000). “Retrieval of Ocean Wave Spectra and RAR MTFs from Dual-Polarization SAR Data”, *IEEE Transactions on Geoscience and Remote Sensing*, Vol. 38, No. 1, pp. 391-403.

Engman, E.T. and N. Chauhan. (1995). “Status of microwave soil moisture measurements with remote sensing”, *Remote Sensing of Environment*, Vol. 51, pp.189-198.

Eriksson, L., M. Drinkwater, B. Holt, E. Valjavek, and O. Nortier. (1998). “SIR-C Polarimetric Radar Results from the Weddell Sea, Antarctica”, In: *Proceedings IGARSS’98*, Seattle, Washington, July 6-10.

ESA, European Space Agency. (2001). *Envisat-1 website*, http://envisat.esa.int/.

Evans, D.L. and J.J. van Zyl. (1990). “Polarimetric Imaging Radar: Analysis Tools and Applications”, Polarimetric Remote Sensing (J.A. Kong, Ed.), Elsevier, New York, NY, pp. 371-389.

Evans, D.L. and M.O. Smith. (1991). “Separation of vegetation and rock signatures in Thematic Mapper and polarimetric SAR images”, *Remote Sensing of the Environment*, Vol. 34, pp. 63-75.

Evans, D.L., T.G. Farr, J.J. van Zyl and H.A. Zebker. (1988). “Radar polarimetry: analysis tools and applications”, *IEEE Transactions on Geoscience and Remote Sensing*, Vol. 26, pp. 774-789.

Evans, D.L., T.G. Farr, J.P. Ford, T.W. Thompson, and C.L. Werner. (1986). “Multipolarization radar images for geological mapping and vegetation discrimination”, *IEEE Transactions on Geoscience and Remote Sensing*, Vol. 24, No. 2, pp. 246-257.

Ferretti, A., C. Prati, and F. Rocca. (1999a). “Multibaseline InSAR DEM reconstruction: the wavelet approach”, *IEEE Transactions on Geoscience and Remote Sensing*, Vol. 37, No. 2, pp. 705-715.

Ferretti, A., C. Prati, and F. Rocca. (1999b). “Permanent scatteres in SAR interferometry”, In: *Proceedings of the IGARSS’99 Symposium; Remote Sensing of the System Earth – A challenge for the 21st Century*, Hamburg, 28 June – 2 July 1999, CD-ROM.

Fielding, E. J., R.G. Blom, and R.M Goldstein. (1998). “Rapid subsidence over oil fields measured by SAR interferometry”, *Geophysical Research Letters*, Vol. 25, pp. 3215.

Flett, D.G. (1997). “C-Band Polarimetric Synthetic Aperture Radar Signatures of Winter Sea Ice Conditions” *Masters Thesis*, University of Waterloo, Waterloo, Ontario, 129 pp.

Francis, P.W., G. Wadge, and P.J. Mouginis-Mark. (1996). “Satellite Monitoring of Volcanoes”, In: R. Scara and R.I. Tilling, (Eds.), Monitoring and Mitigating of Volcano Hazard: Springer- Verlag, New York, pp. 257-298.

French, N.H.F., L.L. Bourgeau-Chavez, Y. Wang, E.S. Kasischke. (1998). “Initial Observations of RADARSAT Imagery at Fire-Disturbed Sites in Interior Alaska”, *Remote Sensing of the Environment*, April.

Fruneau, B., C. Delacourt, and J. Achache. (1996). “Observation and Modelling of the Saint-Etienne-de-Tin´ ee Landslide Using SAR In-terferometry”, In: *Proceedings of the FRINGE’96*, Zurich, Switzerland. http://esrin.esa.it/fringe99

Gabriel, A.K. and R.M. Goldstein. (1988). “Crossed Orbit Interferometry: Theory and experimental results from SIR-B”, *International Journal of Remote Sensing*, Vol. 9, No. 5, pp. 857-873.

Gaddis, L. (1992). “Lava-flow characterization at Pisgah volcanic field, California, with multiparameter imaging radar”, *Bulletin of the Geological Society of America*, Vol. 104, pp. 695-703.

Gade, M., J. Scholz, and C. von Viebahn. (2000). "On the detectability of marine oil pollution in European marginal waters by means of ERS SAR imagery", In: *Proceedings of the IGARSS 2000 Symposium; Taking the Pulse of the Planet: The Role of Remote Sensing in Managing the Environment,* Honolulu*,* 24-28 July 2000, Vol. 5, pp. 2510-2512.

Gade, M., W. Alpers, H. Hühnerfuss, H. Masuko, and T. Kobayashi. (1998a). "Imaging of biogenic and anthropogenic ocean surface films by the multifrequency / multipolarization SIR-C / X-SAR", *Journal of Geophysical Research*, Vol. 103, No. C9, pp. 18,851-18,866.

Gade, M., W. Alpers, H. Hühnerfuss, V.R. Wismann, and P.A. Lange. (1998b). "On the reduction of the radar backscatter by oceanic surface films: scatterometer measurements and their theoretical interpretation", *Remote Sensing of Environment*, Vol. 66, No. 1, pp. 52-70.

Galarneau, M., R. Leconte, F. Brissette, and T.J. Pultz. (1998). “The determination of soil moisture at the field scale using RADARSAT data”, In: *Proceedings of the Fourth International Workshop on Applications of Remote Sensing in Hydrology*, November, Santa Fe, New Mexico, USA, pp.77-85.

Geng, H., Q.H. Gwyn, B. Brisco, J. Boisvert, and R.J. Brown. (1996). “Mapping of Soil moisture from C-Band radar images”, *Canadian Journal of Remote Sensing*, Vol. 22, No. 1, pp. 117-126.

Gilliam, B., S.W. McCandless Jr., L. Reeves, and B.D. Huxtable. (1999). "RADARSAT-2 for Search and Rescue", In: *Proceedings of the SPIE Conference on Automatic Target Recognition IX*, F.A. Sadjadi (Ed.), SPIE Vol. 3718, Orlando, Florida, April 7-9, pp. 189-194.

Goldstein, R. (1995). “Atmospheric limitations to repeat-pass interferometry”. *Geophysical Research Letters*, Vol. 22, No. 18, pp. 2517-2520.

Goodison, B.E, A. Banga, and R.A. Halliday. (1984). “Canada-United States Prairie Snow Cover Runoff Study”. *Canadian Water Resources Journal*, Vol. 9, No. 1, pp. 99-107.

Gray A.,L., Mattar K.M. and G. Sofko. (2000). “Influence of ionospheric electron density fluctuations on satellite interferometry”. *Geophysical Research Letters*, Vol. 27, No. 10, pp. 1451-1454.

Groot, J.S., A.C. van den Broek and A. Freeman. (1992). “An investigation of the potential of polarimetric SAR data for discrimination between agricultural crops”, In: *Proceedings of MAESTRO-1/AGRISCATT: Radar Techniques for Forestry and Agricultural Applications, Final Workshop*, The Netherlands, 6-7 March, 1992, pp.67-82.

Guinard, N.W. and C.G. Purves. (1970). *The remote sensing of oil slicks by radar.* Washington DC, Naval Research Laboratory, US Coast Guard, Project 71404-A004, 19 p.

Haefner, J., and J. Piesbergen. (1998). “Multiscale SAR snow cover monitoring in the Swiss Alps”. In: *Proceedings of the 4th International Workshop on Applications of Remote Sensing in Hydrology*, 4-6 November 1998, Santa Fe New Mexico, U.S.A.

Hasselmann, K. and S. Hasselmann. (1991). “On the nonlinear mapping of an ocean wave spectrum into a synthetic aperture radar image spectrum and its inversion”, *Journal of Geophysical Research*, Vol. 90, No. C6, pp.10713-10729.

Hawkins, R.K., R. Touzi, and C.E. Livingstone. (1999). "Calibration and Use of CV-580 Polarimetric SAR Data", In: *Proceedings of the 21st Canadian Symposium on Remote Sensing*, Ottawa, Ontario, June 21-24, pp.II-32 - II-40.

Haykin S., E.O. Lewis, R.K. Raney, and J.R. Rossiter. (1994). *Remote Sensing of Sea Ice*. John Wiley & Sons, Inc., 689 pp.

Heimbach, P., S. Hasselmann, and K. Hasselmann. (1998). “Statistical analysis and intercomparison to WAM model data with global ERS-1 SAR wave mode spectral retrievals over 3 years”, *Journal of Geophysical Research*, Vol. 103, No. C4, pp.7931-7977.

Hess, L.L., J.M. Melack, and D.S. Simonett. (1990). “Radar detection of flooding beneathe the forest canopy: A review”, *International Journal of Remote Sensing*, Vol. 11, No. 7, pp. 1313-1325.

Hesselmans, G.H.F.M., G.S. Prasetya, F.M. Seifert, K. Trismadi , G.J. Wensink, and R.J.A. Grim. (2000). *SIMBA: Sistem Informasi untak Manajemen "Bathymetry"; A bathymetry assessment system for Indonesia.* Delft, Netherlands Remote Sensing Board, BCRS report no.99-35, 33 p.

Hinds, M.R. (1989). “Ku band polarization characteristics of crops”. Master of Science thesis, University of Saskatchewan, Saskatoon, Canada, 225 pp.

Hoekman, D.H. (1985). "Textural analysis of SLAR images as an aid in automized classification of forest areas", In: *Proceedings EARSeL workshop: Microwave remote sensing applied to vegetation,* Amsterdam*,* 10-12 December 1984, Vol. ESA SP-227, pp. 99-109.

Hoekman, D.H., J.J. van der Sanden and M.A.M. Vissers. (1992). "MAESTRO-1 Flevoland/Speulderbos; Analysis Results of Multiband Polarimetric SAR Data of Forests and Agricultural Crops". In: *Proceedings of MAESTRO-1/AGRISCATT: Radar Techniques for Forestry and Agricultural Applications, Final Workshop*, The Netherlands, 6-7 March, 1992, pp. 53-58.

Huadong, G., L. Jingjuan, W. Changlin, W. Chao, T.G. Farr, and D.L. Evans. (1997). “Use of Multifrequency, Multipolarization Shuttle Imaging Radar for Volcano Mapping in the Kunlun Mountains of Western China”, *Remote Sensing of Environment*, Vol. 59, pp. 364-374.

Hühnerfuss, H., W. Alpers, H. Dannhauer, M. Gade, P.A. Lange, V. Neumann, and V. Wismann. (1996). "Natural and man-made sea slicks in the North Sea investigated by a helicopter-borne 5-frequency radar scatterometer", *International Journal of Remote Sensing*, Vol. 17, No. 8, pp. 1567-1582.

Imhoff, M.L, M. H. Story, C. Vermillion, F. Khan, and F. Polcyn. (1986). “Forest Canopy Characterization and vegetation penetration assessment with space-borne radar”, *IEEE Transactions on Geoscience and Remote Sensing*, Vol. 24, No. 4, pp. 535-542.

Infoterra. (2001). *TerraSar website*, http://infoterra-global.com/terrasar.html.

J.F. Sabourin and Associates Inc. (1998). “Water Management Plan for the Mississippi River Watershed: Phase 1: Hydrologic Data Optimization using RADARSAT”, *Radar Data Development Program Project Report prepared for the Canada Centre for Remote Sensing*, June 3.

Jackson, C.R., H. Rais, and A.W. Mansfield. (1998). "Polarimetric target detection techniques and results from the Goddard Space Flight Center Search and Rescue Synthetic Aperture Radar (SAR2) program", In: *Proceedings of Automatic Target Recognition VIII*, F.A. Sadjadi (Ed.), SPIE Vol. 3371, Orlando, Florida, April 13-17, pp. 185-193.

Johannessen, J.A., R.A. Shuchman, D.R. Lyzenga, C. Wackerman, O.M. Johannessen, and P.W. Vachon. (1996). “Coastal ocean fronts and eddies imaged with ERS-1 synthetic aperture radar”, *Journal of Geophysical Research*, Vol. 101, No. C3, pp. 6651-6667.

Kasilingam, D., H. Chen, D. Schuler, and J.-S. Lee. (2000). “Ocean wave slope spectra from polarimetric images of the ocean surface”, In: *Proceedings IEEE 2000 International Geoscience and Remote Sensing Symposium (IGARSS 2000)*, Honolulu, Hawaii, USA, 24-28 July 2000, pp. 1110-1112.

Kasischke, E.S. and L.L. Bourgeau-Chavez. (1997). “Monitoring South Florida Wetlands Using ERS-1 SAR Imagery”, *Photogrammetric Engineering & Remote Sensing*, Vol. 63, No. 3, pp. 281-291.

Kasischke, E.S., Melack, J.M., and M.C. Dobson. (1997). “The Use of Imaging Radars for Ecological Applications – A Review”. *Remote Sensing of Environment*, Vol. 59, pp.141-156.

Katsaros, K., P. Vachon, P. Black, P. Dodge, and E. Uhlhorn. (1999). “Wind fields from SAR: Could they improve our understanding of storm dynamics?”, In: *The Symposium Record of Emerging Coastal and Marine Applications of Wide Swath SAR*, 23-25 March 1999, Laurel, MD, USA, In: *A dedicated issue of Johns Hopkins APL Technical Digest*, January-March 2000, Vol. 21, No. 1, pp.86-93.

Keefer, D. (1984). “Landslides caused by earthquakes”, *Geological Society of America Bulletin*, Vol 95, pp. 406-421.

Keefer, D. (1994). “The importance of earthquake- induced landslides to long-term slope erosion and slope failure hazards in seismically active regions”, *Geomorphology*, Vol. 10, pp. 265- 284.

Kendra, J.R., K Sarabandi, and F.T. Ulaby. (1998). “Radar measurements of snow: Experiment and Analysis. *IEEE Transactions on Geoscience and Remote Sensing*, Vol. 36, No. 3, pp. 864-879.

Kerbaol, V., B. Chapron, and P.W. Vachon. (1998). “Analysis of ERS-1/2 SAR wave mode imagettes”, *Journal of Geophysical Research*, Vol. 103, No. C4, pp. 7833-7846.

Kharuk, V.I. and V.V. Yegorov. (1990). “Polarimetric indication of plant stress*”, Remote Sensing of the Environment*, Vol. 33, pp. 35-40.

Kimura, H., and Y Yamaguchi. (2000). “Detection of Landslide areas Using Radar Interferometry”, *Photogrammetric Engineering and Remote Sensing*, Vol. 66, No.3, pp. 337-344.

Kneppeck, LD., and F.J. Ahern. (1989). “Stratification of a Regenerating Burned Forest in Alberta Using Thematic Mapper and C-SAR Images”, In: *Proceedings of the IGARSS '89*, Vol. 3, pp.1391-1396.

Krishen, K. (1973). "Detection of oil spills using a 13.3-Ghz radar scatterometer", *Journal of Geophysical Research*, Vol. 78, pp.1952-1963.

Krogstad, H.E. (1992). “A simple derivation of Hasselmann’s nonlinear ocean-synthetic aperture radar transform”, *Journal of Geophysical Research*, Vol. 97, No. C2, pp.2421-2425.

Landry R, F.J. Ahern, and R. O’Neil. (1995), “Forest Burn Visibility on C-HH Radar Images”, *Canadian Journal of Remote Sensing*, Vol. 21, No. 2, pp. 204-206.

Lankester, T. (1998). "OilWatch: development of an international oil slick detection system using spaceborne SAR", *EEZ Technology*, Vol. 2, pp. 227-232.

Le Toan, T., A. Beaudoin and D. Guyon. (1992). “Relating Forest Biomass to SAR Data”, *IEEE Transaction on Geoscience and Remote Sensing*, Vol. 30, No. 2, pp. 403-411.

Leberl, F.W. (1990). *Radargrammetric image processing.* Norwood, Artech House Inc., 595 p.

Leckie, D.G. (1984). “Preliminary Results of an Examination of C-Band Synthetic Aperture Radar for Forestry Applications”, In: *Proceedings of the 8th Canadian Symposium on Remote Sensing*, pp. 151-164.

Leconte, R. (1996). “Exploring the behaviour of microwaves in a snowpack using modelling techniques”. *Canadian Journal of Remote Sensing*, Vol. 22, No. 1, pp.23-35.

Leconte, R. and T.J. Pultz. (1990).”Utilization of SAR Data in the Monitoring of Snowpack, Wetlands and River Ice Conditions”. In: *Proceedings of the Workshop on Applications of Remote Sensing in Hydrology*, Saskatoon, Saskatchewan, 13-14 February 1990 , pp. 233-247.

Lee, J.S. and I. Jurkevich. (1990). "Coastline detection and tracing in SAR images", *IEEE Transactions on Geoscience and Remote Sensing*, Vol. 28, No. 4, pp. 662-668.

Lee, Y.J. (1981). “Synthetic Aperture Radar for Identification and Monitoring Forest Conditions in British Columbia”, In: *Proceedings of the XVII IUFR0 World Congress*, pp. 428-441.

Lemoine, G.G., D.H. Hoekman and H.J.C. van Leeuwen. (1991). “Separability of agricultural fields and forest stands using multi-frequency polarimetric SAR data of the Flevoland site”, In: *Proceedings of the International Geoscience and Remote Sensing Symposium (IGARSS ’91)*, Espoo, Finland, pp. 681-684.

Li. F.K. and R.M. Goldstein. (1990). “Studies of multi-baseline spaceborne interferometric synthetic aperture radars”, *IEEE Transactions on Geoscience and Remote Sensing*, Vol. 28, No. 1, pp. 88-97.

Livingstone, C.E. (1994). “Synthetic Aperture Radar Images of Sea Ice”, In: Haykin et al. (Eds.), Remote Sensing of Sea Ice and Icebergs, John Wiley and Sons, Inc., pp.540-569.

Livingstone, C.E., A.L. Gray, R.K. Hawkins, P.W. Vachon, T.I. Lukowski, and M. Lalonde. (1995). "The CCRS Airborne SAR Systems: Radar for Remote Sensing Research", *Canadian Journal of Remote Sensing*, Vol. 21, No. 4, December, pp. 468-490.

Luckman, A.J., J.R. Baker, T.M. Kuplich, C.C.F. Yanasse, and A.C. Frery. (1997a). "A study of the relationship between radar backscatter and regenerating tropical forest biomass for spaceborne SAR instruments", *Remote Sensing of Environment*, Vol. 60, No. 1, pp. 1-13.

Luckman, A.J., A.C. Frery, C.C.F. Yanasse, and G.B. Groom. (1997b). "Texture in airborne SAR imagery of tropical forest and its relationship to forest regeneration stage", *International Journal of Remote Sensing*, Vol. 18, No. 6, pp. 1333-1349.

Lukowski T.I., P. Budkewitsch, F. Charbonneau, and J. Stix. (2000). “RADARSAT-1 Interferometric Potential for Monitoring Volcanic Activity: The Guagua Pichincha Volcano, Ecuador”, In *Proceedings of the International Geoscience and Remote Sensing Symposium*, Honolulu, Hawaii.

Lukowski, T.I. and F.J. Charbonneau. (2001). "Synthetic Aperture Radar and Search and Rescue", (Tentative title.) In Preparation.

MacKay, M.E. and P.J. Mouginis-Mark. (1997). “The Effect of Varying Acquisition Parameters on the Interpretation of SIR-C Radar Data: The Virunga Volcanic Chain”, *Remote Sensing of Environment*, Vol. 59, pp. 321-336.

Madsen, S.N. (1987). "Mapping oil at sea with an X-band dual polarized SLAR system", In: *The Archimedes 2 Experiment,* Luxembourg*,* 1987, Vol. I, pp. 71-79.

Makynen, M, and M. Hallikainen. (1998). “C-Band Backscattering Signatures of Baltic Sea Ice”, In: *Proceedings IGARSS’98: Sensing and Managing the Environment*, Seattle, Washington, July 6-10 1998.

Mason, D.C. and I.J. Davenport. (1996). "Accurate and efficient determination of the shoreline in ERS-1 images", *IEEE Transactions on Geoscience and Remote Sensing*, Vol. 34, No. 5, pp. 1243-1253.

Massonet D. and T. Raboute. (1993). “Radar interferometry: Limits and and Potential”, *IEEE Transactions on Geoscience and Remote Sensing*, Vol. 31, No. 2, pp. 455-464.

Massonet, D. and K.L. Feigl. (1995). “Discriminition of Geophysical Phenomena in Satellite Interferograms”, *Geophysical Research Letters*, Vol. 22, No. 12, pp. 1537-1540.

Massonnet, D., M. Rossi, C. Carmona, F. Adragna, G. Peltzer, K. Feigl, and T. Rabaute. (1993). “The displacement field of the Landers earthquake mapped by radar interferometry”, *Nature*, Vol. 364, pp. 138-142.

Mattar, K.E., A.L. Gray, D. Geudtner, and P.W. Vachon. (1999). “Interferometry for DEM and Terrain Displacement: Effects of Inhomogeneous Propagation”, *Canadian Journal of Remote Sensing*, Vol. 25, No. 1, pp. 60-69.

Maxfield, A.W., P. Marsh, J.W. Pomeroy, and W.L. Quinton. (1996). “Arctic Snow and soil observations by radar satellite”, *In: Proceedings of the Third International Workshop, NHRI Symposium No. 17*, Goddard Space Flight Center, Greenbelt, Maryland, USA, pp. 199-210.

McNairn, H. (1999). Radar response to crop residue cover and tillage application on post-harvest agricultural surfaces. Doctoral thesis, Laval University, Québec City, Canada, 410 p.

McNairn, H., J.J. van der Sanden, R.J. Brown, and J. Ellis. (2000a). "The potential of RADARSAT-2 for crop mapping and assessing crop condition", In: *Proceedings of the Second International Conference on Geospatial Information in Agriculture and Forestry,* Lake Buena Vista, Florida, 10-12 January 2000, Vol. II, pp. 81-88.

McNairn, H., Brown, R.J., M. McGovern, T. Huffman and J. Ellis (2000b). "Integration of multi-polarized SAR data and high resolution optical imagery for precision farming", In: *Proceedings of the 22nd Canadian Remote Sensing Symposium*, Victoria, British Columbia, 21-25 August 2000, CD-ROM.

McNairn, H., C. Duguay, B. Brisco, R.J. Brown and T.J. Pultz. (1998). "Exploring the Information Content of Polarimetric SAR Data for Tillage and Residue Mapping", In: *Proceedings of the 21st Canadian Remote Sensing Symposium,* Calgary, Alberta, 10-13 May 1998, pp. 37-40.

McNairn, H., J. Ellis, J.J. van der Sanden, T. Hirose and R.J. Brown. (2001a). "Providing crop information using RADARSAT-1 and satellite optical imagery", *International Journal of Remote Sensing* (in press).

McNairn, H., C. Duguay, J. Boisvert, E. Huffman and B. Brisco. (2001b). "Defining the sensitivity of multi-frequency and multi-polarized radar backscatter to post-harvest crop residue", *Canadian Journal of Remote Sensing* (in press).

MDA, MacDonald, Dettwiler, and Associates. (2001). *RADARSAT-2 mission requirements specification*, CDRL SE-01, February 1, 2001, 65 p.

Moeremans, B., and S. Dautrebande. (2000). "Soil moisture evaluation by means of multi-temporal ERS SAR PRI images and interferometric coherence", *Journal of Hydrology*, pp. 234:162-169.

Morain, S.A. and D.S. Simonett. (1966). *Vegetation Analysis With Radar Imagery*, University of Kansas, Lawrence, Kansas, CRES Report No. 61-9, pp. 605-622.

NASA. (2001). Search and Rescue Mission Office, SAR$^2$: http://poes2.gsfc.nasa.gov/sar/becnless.htm.

National Search and Rescue Manual (B-GA-209-001/FP-001, DFO 5449) Issued on Authority of the Chief of the Defence Staff and the Minister of Fisheries and Oceans, May, 1998.

Neville, R.A., V. Thomson, A.L. Gray, and R.K. Hawkins. (1984). "Observation of two test oil spills with a microwave scatterometer and a synthetic aperture radar", In: *NATO Challenges of Modern Society, 6: Remote Sensing for the Control of Marine Pollution,* New York, pp. 257-266.

Oh, Y., K. Sarabandi and F.T. Ulaby. (1992). "An Empirical Model and an Inversion Technique for Radar Scattering from Bare Soil Surfaces", *IEEE Transactions on Geoscience and Remote Sensing*, Vol. 30, No. 2, pp. 370-382.

Olsen, R.B., P.W. Vachon, and T. Wahl. (2000). "Vessel detection using SAR imagery: Current status and some views for the future", In: *AMRS Ship Detection in Coastal Waters Workshop*, Digby, Nova Scotia, 31 May to 2 June 2000.

Onstott, R.G., (1992). "SAR and Scatterometer Signatures of Sea Ice", In: F.D. Carsey (Ed.), Microwave Remote Sensing of Sea Ice, Geophysical Monograph 68, American Geophysical Union, pp. 73-104.

Ormsby, J. P., J. P. Blanchard, and A.J. Blanchard. (1985). "Detection of lowland flooding using active microwave systems", *Photogrammetric Engineering and Remote Sensing*, Vol. 5, No. 3, pp. 317-328.

Parashar, S., E. Langham, J. McNally, and S. Ahmed. (1993). "RADARSAT mission requirements and concept', *Canadian Journal of Remote Sensing*, Vol. 19, No. 4, pp. 280-288.

Pedersen, J.P., L.G. Seljelv, G.D. Strom, O.A. Follum, J.H. Andersen, T. Wahl, and A. Skoelv. (1995). "Oil spill detection by use of ERS SAR data", In: *Proceedings of the Second ERS Applications Workshop,* London, 6-8 December 1995, Vol. pp. 1-7.

Pellemans, A.H.J.M., W.G. Bos, and H. Konings. (1995). *Oil spill detection on the North Sea using ERS-1 SAR data.* Delft, BCRS - Netherlands Remote Sensing Board, 94-30, 53 p.

Pohl, C., Y. Wang, and B.N. Koopmans. (1995). “The 1995 flood in the Netherlands from space”, *ITC Journal*, pp. 414-415.

Polidori, L. (1997). *Cartographie radar*. Amsterdam, The Netherlands, Gordon and Breach Science Publishers, 287 p.

Pope, K.O., J.M. Rey-Benayas, and J.F. Paris. (1994). “Radar remote sensing of forest and wetland ecosystems in the Central American tropics”, *Remote Sensing of Environment*, Vol. 48, No. 2, pp. 205-219.

Pope, K.O., Rejmankova, E., Paris, J.F., and R. Woodruff. (1997). “Detecting Seasonal Flooding Cycles in Marches of the Yucatan Peninsula with SIR-C Polarimetric Radar Imagery”, *Remote Sensing of Environment*, Vol. 59, pp. 157-166.

Prati, C. and F. Rocca. (1990). “Limits to the resolution of elevation maps from stereo SAR images”, *International Journal of Remote Sensing*, Vol. 11, No. 12, pp. 2215-2235.

Prevot, L., I. Champion and G. Guyot. (1993). “Estimating Surface Soil Moisture and Leaf Area Index of a Wheat Canopy using a Dual Frequency (C- and X-Bands) Scatterometer”, *Remote Sensing of Environment*, Vol. 46, No. 3, pp. 331-339.

Proisy C., E. Mougin, E. Dufrene, and V. Le Dantec. (2000). "Monitoring seasonal changes of a mixed temperature forest using ERS SAR observation", *IEEE Transactions on Geoscience and Remote Sensing*, Vol. 38, No. 1, pp. 540-552.

Pultz T.J., Y. Crevier, and J. Boisvert. (1997). “Monitoring local environmental conditions with SIR-C/X-SAR”. *Remote Sensing of Environment*; Vol.59, No.2, pp. 248-255

Pultz, T.J. and Y. Crevier. (1996). “Early Demonstrations of RADARSAT for Applications in Hydrology”. *Remote Sensing*, Vol. 20, No. 15, pp. 3125-3129.

Pultz, T.J., R. Leconte, L. St.Laurent, and L. Peters. (1991). “Flood mapping with airborne SAR imagery”, *Canadian Water Resource Journal*, Vol. 16, No. 2, pp.173-189.

Quesney, A., S. Le Hegarat-Mascle, O. Taconet, D. Vidal-Madjar, J.P. Wigneron, C. Loumagne, and M. Normand. (2000). “Esitmation of Watershed Soil Moisture Index from ERS/SAR Data”, *Remote Sensing of Environment*, Vol. 72, pp. 290-303.

Radarsat International and Spot Image. (1995). *RADARSAT 3 - commercial and economic forecast.* Vancouver, 52 p.

Raggam, J., A. Almer, W. Hummelbrunner, and D. Strobl, (1993). “Investigation of the stereoscopic potential of ERS-1 SAR data”, In: *Proceedings of the Fourth International Workshop on Image Rectification of Spaceborne Synthetic Aperture Radar*, Loipesdorf, Austria, 26-28 May 1993, pp. 81-87.

Raney, R.K. (1998). “Radar fundamentals: technical perspective”, In: *R.A. Ryerson (Editor-in Chief), The Manual of Remote Sensing, 3rd Edition: Principles and Applications of Imaging Radar*, Volume 2, American Society of Photogrammetry and Remote Sensing, pp. 9-130.

Raney, R.K., A.P. Luscombe, E.J. Langham, and S. Ahmed. (1991), “RADARSAT”, *Proceedings of the IEEE*, Vol. 79, No. 6, pp. 839-849.

Rauste, Y., T. Hame, J. Pulliainen K. Heiska and M. Hallikainen. (1994). “Radar-Based Forest Biomass Estimation”, *International Journal of Remote Sensing*, Vol. 15, No. 14, pp. 2797-2808.

Reeves, L.A. (2000). "The RADARSAT-2/3 Topographic Mapping Mission", In: *Proceedings of the 11th Conference on Astronautics; Opportunities and Challenges for Space Applications Technology,* Ottawa*,* 7-9 November 2000, Vol. 1, pp. 375-378.

Refice, A., F. Bovenga, J. Wasowski, and L. Guerriero. (2000). “Use of InSAR Data for Landslide Monitoring: A Case Study from Southern Italy”, In: *Proceedings of the IGARSS 2000*, Hawaii, U.S.A., 3 p.

Richards, J. A., P. W. Woodgate, and A. K. Skidmore. (1987). “An explanation of enhanced radar backscattering from flooded forests”, *International Journal of Remote Sensing*, Vol. 8, No. 7, pp. 1093-1100.

Romaneeßen, E., S. Lehner, A. Niedermeier, and J. Horstmann. (2000). "Morphodynamic in the Elbe estuary as seen by ERS synthetic aperture radar", In: *Proceedings of the Sixth International Conference on Remote Sensing for Marine and Coastal Environment,* Charleston*,* 1-3 May 2000, Vol. I, pp. I-296-I-302.

Rothrock, D., Y. Yu and G. Maykut. (1999). “Thinning of the Arctic Ice Cover”, *Geophysical Research Letters*, Vol. 26, pp. 3469-3472.

Rott, H. and A. Siegel. (1999). “Analysis of mass movements in Alpine terrain by means of SAR interferometry”, In: *Proceedings of the IGARSS’99 Conference*, Hamburg.

Rott, H., R.E. Davis, and J. Dozier. (1992). “Polarimetric and multifrequency SAR signatures of wet snow”. *IEEE Transactions on Geoscience and Remote Sensing*, Vol. 30, pp. 1645-1660.

Sader, S.A. (1987). “Forest Biomass, Canopy, Structure, and Species Composition Relationships With Multipolarization L-band Synthetic Aperture Radar Data”, *Photogrammetric Engineering and Remote Sensing*, Vol. 53, No. 2, pp. 193-202.

Saint-Jean, R., V. Singhroy, and M. Rheault. (1999). “Multi-polarized Airborne C-SAR images for Geological Mapping at Lac Volant, Quebec”, In: *Proceedings of Applied Geologic Remote Sensing*, Vancouver, pp. 411-418.

Saint-Jean, R., V. Singhroy, and R. Hawkins. (2000). “Geological Mapping in the Canadian Shield: Implications for RADARSAT-2”, Presented at the *22nd Canadian Remote Sensing Symposium*, August 21-25, 2000. Victoria, pp. 299-306.

Saint-Jean, R., V. Singhroy, and S. M Khalifa. (1996). “Geological interpretation of the integrated SAR images in the Azraq area of Jordan”, Canadian Journal of Remote Sensing Vol. 21, No. 4, pp. 511-517.

SARSAT (2001): http://www.dnd.ca/menu/SAR/eng/sar/gicossar.htm.

Schaber, G.G., J.F. McCauley, and C.S. Breed. (1997). “The Use of Multifrequency and Polarimetric SIR-C/X-SAR Data in Geologic Studies of Bir Safsaf, Egypt”, *Remote Sensing of Environment*, Vol. 59, pp. 337-363.

Schmullius, C.C. and D. L. Evans. (1997). “Synthetic aperture radar (SAR) frequency and polarization requirements for applications in ecology, geology, hydrology, and oceanography: a tabular status quo after SIR-C/X-SAR”, *International Journal of Remote Sensing*, Vol. 18, No. 13, pp. 2713-2722.

Schuler, D.L., J.S. Lee, and G. De Grandi. (1996). “Measurement of topography using polarimetric SAR images*”*, *IEEE Transactions on Geoscience and Remote Sensing*, Vol. 34, No. 5, pp. 1266-1277.

Schuler, D.L., J.S. Lee, and K.W. Hoppel. (1993). “Polarimetric SAR image signatures of the ocean and Gulf Stream features*”*, *IEEE Transactions on Geoscience and Remote Sensing*, Vol. 31, No. 5, pp. 1210-1221.

Schuler, D.L., T.L. Ainsworth, J.S. Lee, and G.F. De Grandi. (1998). “Topography mapping using polarimetric SAR data*”*, *International Journal of Remote Sensing*, Vol. 19, No. 1, pp. 141-160.

Schwäbisch, M., S. Lehner, and N. Winkel. (1997). "Coastline extraction using ERS SAR interferometry", In: *Proceedings of the Third ERS Symposium,* Florence*,* 17-20 March 1997, Vol. I, pp. 1-12.

Search and Rescue in Canada (2001): http://www.dnd.ca/menu/SAR/eng/sar/index.htm.

Seglenieks, F., E.D. Soulis, and N.Kouwen. (1998). “Establishment of a relationship between Radarsat backscatter and soil moisture at hydrological modelling scales”, In: *Proceedings of the Fourth International Workshop on Applications of Remote Sensing in Hydrology*, November, Santa Fe, New Mexico, USA, pp.375-386.

Sempere, J.-P. (1998). “Quantitative evaluation of the planimetric potential of RADARSAT images”, In: *Proceedings of the ADRO Symposium “Bringing radar applications down to Earth”*, Montreal, Canada, 13-15 October 1998, CD-ROM.

Shi, J. and J. Dozier. (1997). “Mapping Seasonal Snow with SIR-C/X-SAR in Mountainous Areas”. *Remote Sensing of Environment*, Vol. 59, pp. 294-307.

Shi, J., H. Rott, and J. Dozier. (1993). “Deriving snow liquid water content using C-band polarimetric SAR”. In: *Proceedings of IGARSS’93*, August 18-21, Tokyo, Japan, pp. 1038-1041.

Shi, J., J. Wang, A. Hsu, P. O’Neill, and E.T. Engman. (1996). “Estimation of bare surface soil moisture and surface roughness parameters using L-Band SAR image data”. In: *Proceedings of the Third International Workshop,* NHRI Symposium No. 17, Goddard Space Flight Center, Greenbelt, Maryland, USA, pp. 323-335.

Shi, J. (1994). “Active Microwave Remote Sensing of Snow Cover”. In: *Proceedings of the Second International Workshop,* NHRI Symposium No. 14*, October, Saskatoon, Saskatchewan.*

Singhroy V., K. Mattar and L. Gray. (1998). “Landslide characterization in Canada using interferometric SAR and combined SAR and TM images”, *Advances in Space Research*, Vol. 2, No. 3, pp. 465-476.

Singhroy, V. (1996). “Environmental and Geological site characterization in vegetated areas: Image enhancement guidelines”. In: *Remote Sensing and GIS: Applications and Standards*. ASTM Special Technical Publication #1279. V. Singhroy, D. Nebert. and A. Johnson (Eds.), American Society for Testing and Materials. pp.5-17.

Singhroy, V., J.E. Loehr, and A.C. Correa. (2000a). “Landslide Risk Assessment with High Spatial Resolution Remote Sensing Satellite Data”, In: *Proceedings of the IGARSS 2000*, Hawaii, pp. 2501-03.

Singhroy, V. and K. Mattar. (2000b). “SAR Image Techniques for Mapping Areas of Landslides”, In: *Proceedings of the ISPRS Congress*, Amsterdam, pp. 1395- 1402.

Singhroy, V. (2000c). “Landslide Hazard Assessment from Earth Observation”, *CEOS Disaster Management Support Project*, NOAA, pp. 82-89.

Singhroy, V., R. Saint-Jean, and M. R Momani. (1996). “Mapping Surface Characteristics of Aquifers in Jordan from Integrated SAR Images”, In: *Proceedings of ERIM Exploration Geology,* Las Vegas, Nevada, pp 691-697.

Sivertson, W.E., Jr. (1976). A Global Search and Rescue Concept Using Synthetic Aperture Radar and Passive User Targets NASA Technical Report NASA -TN- D-8172, *NASA Langley Research Center*, Hampton, Va., U.S.A., April, 1976, 29 p.

Skriver, H., H.B. Mortensen and P. Gudmandsen. (1994). “Calibration and Modelling of MAESTRO-1 Polarimetric SAR Data of Forest Areas at Les Landes, France”, *International Journal of Remote Sensing*, Vol. 15, No. 14, pp. 2737-2754.

Soeters, R. and C.J. van Westen. (1996). “Slope instability recognition, analysis, and zonation”, In: A. K. Turner and R. L. Schuster (Eds), Landslides. Investigation and mitigation, Transportation Research Board Spec. Rep. 247. Nat. Academy Press, 673 p.

Sokol J., T.J. Pultz T. J., and A.E. Walker. (1998). “Investigating snow pack parameters using passive and active microwave remote sensing”. In: *Proceedings of the Fourth International Workshop on Applications of Remote Sensing in Hydrology*, 4-6 November 1998, Santa Fe, New Mexico, pp.

Sokol J., T.J. Pultz, and V. Bulzgis. (2000). “Investigating Labrador fens and bogs using multi-temporal ERS-2 and RADARSAT Data”. In: *Proceedings of the 22nd Canadian Symposium on Remote Sensing*, Victoria, B.C., 21-25 August 2000, pp. 357-364

Sokol, J., T.J. Pultz, and A.E. Walker. (1999). “Passive and Active Airborne Microwave Remote Sensing of Snow Cover”. In: *Proceedings of the 4th International Airborne Remote Sensing Conference/21st Canadian Symposium on Remote Sensing*, Ottawa, June 21-24 1999, Volume I, pp.146-153.

Sun G., and K.J. Ranson. (1993). *Polarimetric Radar Data Decomposition and Interpretation*, Summaries of the Fourth Annual JPL Airborne Geoscience Workshop, Vol. 3, pp. 65-68.

Taconet, O., D. Vidal-Madjar, Ch. Emblanch, and M. Normand. (1996). “Taking into account vegetation effects to estimate soil moisture from C-band radar measurements”, *Remote Sensing of Environment*, Vol. 56, pp. 52-56.

Tarayre, H., and D. Massonet. (1996). “Atmospheric propagation heterogeneities revealed by ERS-1 interferometry”, *Geophysical Research Letters*, Vol. 23, No. 9, pp. 989-992.

Thompson, A.A. and C.E. Livingstone. (2000). "Moving target performance for RADARSAT-2 ", In: Proceedings of the IGARSS 2000 Symposium: Taking the Pulse of the Planet: The Role of Remote Sensing in Managing the Environment, Honolulu, 24-28 July 2000, Vol. 5, pp. 2599-2601.

Thomsen, B.B., S.V. Nghiem, and R. Kwok. (1998). “Polarimetric C-band SAR Observations of Sea Ice in the Greenland Sea”, In: *Proceedings IGARSS’98: Sensing and Managing the Environment*, Seattle, Washington, July 6-10 1998.

Tittley, B. and D. Werle. (1997). *Using RADARSAT-1 SAR imagery for coastal zone sensitivity mapping in Nova Scotia.* Halifax, NS, AERDE Environmental Research, EOP3 Contract 23413-5-D550, 72 p.

Toutin, Th. (1996). “Opposite-side ERS-1 SAR stereo mapping over rolling topography”*, IEEE Transactions on Geoscience and Remote Sensing*, Vol. 34, No. 2, pp. 543-549.

Toutin, Th. (1999). “Error tracking of radargrammetric DEM from RADARSAT images”, *IEEE Transactions on Geoscience and Remote Sensing*, Vol. 37, No. 5, pp. 2227-2238.

Toutin, Th. (2000). “Evaluation of radargrammetric DEM from RADARSAT images in high relief areas”, *IEEE Transactions on Geoscience and Remote Sensing*, Vol. 38, No. 2, pp. 782-789.

Toutin, Th. (2001). “Potential of Road Stereo Mapping with RADARSAT Images”, To be published in *Photogrammetry Engineering & Remote Sensing*, Vol. 67.

Toutin, Th. and A.L. Gray. (2000). “Elevation Modeling from SAR Satellite Data: A Review”, *ISPRS Journal of Photogrammetry and Remote Sensing*, Vol. 55, No. 1, pp. 13-33.

Toutin, Th. and B. Rivard, (1997). *“Value-added RADARSAT Products for Geoscientific Applications*”, Canadian Journal of Remote Sensing, Vol. 23, No. 1, pp. 63-70.

Toutin, Th., and S. Amaral, (2000). “Stereo RADARSAT data for canopy height in Brazilian forest”, *Canadian Journal for Remote Sensing*, Vol. 26, No. 3, pp. 189-199.

Touzi R. and Sasitiwarih A. (1998). “Radarsat Potential for Trail and Road Detection in Indonesian Forests”, In: *Proceedings of the EUSAR’98 Conference*, Friedrichshafen, Germany, 25-27 May 1998, pp. 543-546.

Touzi R., S. Goze, T. Le Toan , A. Lopes, and E. Mougin. (1992). “Polarimetric discriminators for SAR images”, *IEEE Transactions on Geoscience and Remote Sensing*, Vol.30, No. 5, pp. 973-980.

Touzi, R. (2000). “Calibrated polarimetric SAR data for ship detection”, In: *Proceedings of the 22nd Canadian Symposium on Remote Sensing*, Victoria, British Columbia, 21 to 25 August 2000, pp. 93-96.

Touzi, R., R. Landry, and F. Charbonneau. (2001). “Forest target discrimination using SAR polarization information”, To be published, In: *Proceedings of the Canadian Symposium on Remote Sensing*, Quebec, August.

Trebossen, H., J.P. Rudant, B. Fruneau, and N. Classeau. (2000). "Contribution of RADAR SAR imagery for mapping coastal's areas: examples of sedimentationnal and erosionnal zones in French Guiana and Mauritania", In: *Proceedings of the Sixth International Conference on Remote Sensing for Marine and Coastal Environments,* Charleston, South Carolina*,* 1-3 May 2000, Vol. II, pp. II-398-II-405.

Ufermann, S. and R. Romeiser. (1999a). "A new interpretation of multifrequency / multipolarization radar signatures of the Gulf Stream front", *Journal of Geophysical Research*, Vol. 104, No. C11, pp. 25,697-25,705.

Ufermann, S. and R. Romeiser. (1999b). "Numerical study on signatures of atmospheric convective cells in radar images of the ocean", *Journal of Geophysical Research*, Vol. 104, No. C11, pp. 25,707-25,719.

Ulaby, F.T. and W.H. Stiles. (1981). "Microwave Response of Snow". *Advance Space Research*, Vol. 1, pp. 131-149.

Ulaby, F.T., D. Held, M.C. Dobson, K.C. McDonald and T.B.A. Senior. (1987). "Relating polarization phase difference of SAR signals to scene properties", *IEEE Transactions on Geoscience and Remote Sensing*, Vol. 25, pp. 83-92.

Ulaby, F.T., F. Kouyate, B. Brisco, and T.H. Lee. (1986). "Textural information in SAR images", *IEEE Transactions on Geoscience and Remote Sensing*, Vol. GE-24, No. 2, pp. 235-245.

Vachon, P.W., and F.W. Dobson. (1996). "Validation of wind vector retrieval from ERS-1 SAR images over the ocean", *The Global Atmosphere and Ocean System*, Vol. 5, pp. 177-187.

Vachon, P.W., and F.W. Dobson. (2000). "Wind retrieval from RADARSAT SAR images: Selection of a suitable C-band HH polarization wind retrieval model", Canada Journal of Remote Sensing, Vol. 26, No. 4, pp. 306-313, 2000.

Vachon, P.W., and R.K. Raney. (1991). "Resolution of the ocean wave propagation direction in SAR imagery", *IEEE Transactions on Geoscience and Remote Sensing,* Vol. 29, No. 1, pp. 105-112.

Vachon, P.W., D. Geudtner, A.L. Gray and R. Touzi. (1995). "ERS-1 Synthetic Aperture Radar Repeat-Pass Interferometry Studies: Implications for RADARSAT", *Canadian Journal of Remote Sensing*, Vol. 21, No. 4, pp. 441-454.

Vachon, P.W., J.W.M. Campbell, and F.W. Dobson. (1997a). "Comparison of ERS and RADARSAT SARs for wind and wave measurement", In: *Proceedings of the 3rd ERS Symposium on Space at the Service of our Environment*, Florence, Italy, 17-21 March 1997, ESA SP-414, Vol. 3, pp. 1367-1372.

Vachon, P.W., J.W.M. Campbell, C. Bjerkelund, F. W. Dobson, and M.T. Rey. (1997b). "Ship detection by the RADARSAT SAR: Validation of detection model predictions", *Canadian Journal of Remote Sensing*, Vol. 23, No. 1, pp. 48-59.

Vachon, P.W., S.J. Thomas, C.J. Cranton, H.R. Edel, and M.D. Henschel. (2000). "Validation of ship detection by the RADARSAT Synthetic Aperture Radar and the Ocean Monitoring Workstation", *Canadian Journal of Remote Sensing*, Vol. 26, No. 3, pp. 200-212.

Valenzuela, G.R. (1968). "Scattering of electromagnetic waves from a tilted slightly-rough surface*"*, *Radio Science,* Vol. 11, No. 3, pp. 1057-1066.

van der Kooij , M., W. Hughes, and S. Sato. (1999). "Doppler current velocity measurements: A new dimension to spaceborne SAR data", In: *Proceedings of the 2nd International Symposium on Operationalization of Remote Sensing*, Enschede, 16-20 August 1999; Available from: http://www.itc.nl/ags/research/ors99/ors99.htm.

van der Sanden, J.J. (1997). *Radar remote sensing to support tropical forest management*. Wageningen (Wageningen Agricultural University), Tropenbos-Guyana Series 5, Ph.D. thesis, 330 p.

van der Sanden, J.J. and D.H. Hoekman. (1999). "Potential of airborne radar to support the assessment of land cover in a tropical rain forest environment", *Remote Sensing of Environment*, Vol. 68, No. 1, pp. 26-40.

van Kuilenburg, J. (1975). "Radar observations of controlled oil spills", In: *Proceedings of the Tenth Symposium on Remote Sensing of Environment,* Ann Arbor*,* pp. 243-250.

Van Zyl, J.J. (1989). “Unsupervised classification of scattering behaviour using radar polarimetry data”, *IEEE Transactions on Geoscience and Remote Sensing*, Vol. 27, pp. 36-45.

Vaughan, D.G. and C.S.M. Doake. (1996). “Recent atmospheric warming and retreat of ice shelves on the Antarctic Peninsula”, *Nature*, Vol. 379 (6563), pp. 328-331.

Vogelzang, J., H.S.F. Greidanus, G.J. Wensink, and R. van Swol. (1995). *Mapping of sea bottom topography with ERS-1 C-band SAR.* Delft, Netherlands Remote Sensing Board, BCRS report no.94-27, 108 p.

Wagner, W., J. Noll, M. Borgeaud, and H. Rott. (1999). “Monitoring soil moisture over the Canadian Prairies with the ERS Scatterometer”, *IEEE Transactions on Geoscience and Remote Sensing*, Vol. 37, No. 1, pp. 206-216.

Wallace, R.G., D.W. Affens, and H. Rais. (1997). "Beaconless Search and Rescue Overview - History, Development, and Achievements", In: *Proceedings of Automatic Target Recognition VII*, F.A. Sadjadi (Ed.), SPIE Vol. 3069, pp.162-166.

Wang, J.R. and T. Mo. (1990). “The polarization phase difference of orchard trees”, *International Journal of Remote Sensing*, Vol. 11, pp. 1255-1265.

Wensink, G.J., C.J. Calkoen, G.H.F.M. Hesselmans, J. Vogelzang, J.M.M. Kokke, H.S.F. Greidanus, J.A. Roelvink, V. Rocher de Grimal, and H. Gerritsen. (1999). *Coastal sediment transport assessment using SAR imagery (C-Star).* Delft, Netherlands Remote Sensing Board , BCRS report no.99-18, 30 p.

Werle, D., J. Drieman, F.J. Ahern, and R. O' Neil. (1991). “Synthetic Aperture Radar (SAR) - A Promising Tool for Assessing Recently Burned Forest in Canada?”. In: *Proceedings of the 14th Canadian Symposium on Remote Sensing*, pp. 470-474.

Wismann, V., M. Gade, and W. Alpers. (1998). "Radar signatures of marine mineral oil spills measured by an airborne multi-frequency radar", *International Journal of Remote Sensing*, Vol. 19, No. 18, pp. 3607-3623.

Witte, F. (1985). "Detecting oil at sea by means of a VV polarized side looking airborne radar", In: *The Archimedes 1 Experiment,* Luxembourg*,* 1985, Vol. I, pp. 65-80.

Wu, S.-T. and S.A. Sader. (1987). "Multipolarization SAR data for surface feature delineation and forest vegetation characterization", *IEEE Transactions on Geoscience and Remote Sensing*, Vol. GE-25, No. 1, pp. 67-76.

Yamagata, Y. and Y. Yasuoka. (1993). “Classification of wetland vegetation by texture analysis methods using ERS-1 and JERS-1 Images”. In: *Proceedings of IGARSS’93*, Vol 4, pp. 1614-1616.

Yelizavetin, I.V. (1993). “Digital terrain modeling from radar image stereopairs*”, Mapping Sciences and Remote Sensing*, Vol. 30, No. 2, pp. 151-160.

Yeremy, M., J.D. Beaudoin, G.M. Walter, and A. Beaudoin. (2000). "Shoreline mapping from SAR imagery: a polarimetric approach", In: *Proceedings of the 22nd Canadian Remote Sensing Symposium,* Victoria, B.C.*,* 21-25 August 2000, Vol. I, pp. 365-374.

Zebker H.A., C.L. Werner, P.A. Rosen, and S. Hensley. (1994). “Accuracy of topographic maps derived from ERS-1 interferometric radar”, *IEEE Transactions on Geoscience and Remote Sensing*, Vol. 32, No. 4, pp. 823-836.

BLANK PAGE

# Appendix I - Convair-580 SAR System

RADARSAT-2 will entertain a wide variety of modes, imaging geometries, and resolutions. Among these are a first in spaceborne SAR: full polarimetric capability. This same capability has been available to the remote sensing research community on a number of airborne platforms including the system developed by CCRS. Environment Canada now operates the system. Many of the demonstration products for RADARSAT-2 are based on products from this system. Table 1 lists selected technical specifications of the Convair-580 SAR and RADARSAT-2.

Note in every case, except swath, the aircraft system has superior or equivalent performance to RADARSAT-2 and as such provides a reasonable tool for evaluating the potential of RADARSAT-2. It is important to note, however, that the range of incidence angle covered in an airborne image is very much larger than a spaceborne SAR. For this reason, any comparison of simulated data from airborne platforms will carry with it a rider concerning this property.

**Table 1** Selected specifications of the Convair-580 SAR and RADARSAT-2.

| Characteristic | Convair-580 SAR | RADARSAT-2 | Units |
|---|---|---|---|
| Resolution (1 x 1 Look) (Gr Rg x Az) | 1 x 6 | 3 x 3 | m |
| Polarization | Polarimetric | Polarimetric | |
| Power | 16 | ~4 | kW |
| Swath | 20-60 | 20-500 | km |
| Frequency | 5.3 | 5.43 | GHz |
| Incidence angle | 0-86 | 10-60 | deg |
| Look direction | Left or Right | Left or Right | |
| Revisit | < 1 | 24 | days |
| Aspect angles | Any | 4 | |
| Noise-equivalent $\sigma^{\circ}$ | < -40 | < -24 | dB |
| Cross polarization isolation | < -35 | < - 20 | dB |
| Availability | “Any time” | Dec 2003 (TBC) | |

# Standard Convair-580 SAR Geometry for Land and Ice Applications

## RK Hawkins[2]

## CCRS-TN-2001-003

### Canada Centre for Remote Sensing

### *Abstract*

This document very briefly describes a *preferred geometric* configuration for polarimetric imaging of Land and Sea Ice with the Environment Canada Convair-580 SAR system. This configuration reduces the calibration error bars and increases the stability and consistency of the data.

### Table of Contents



[2] Bob Hawkins can be reached at (613) 995-1067 or email: Robert. Hawkins@CCRS.NRCan.gc.ca for further discussion.

# 1 Introduction

The Convair-580 SAR system was developed as an experimental SAR with a very large number of degrees of freedom. The general modes were described in a number of CCRS brochures[3], the latest of which was issued in 1994. They included the following general modes assuming a flying height of approximately 21000 ft.

**Table 1. Nominal Geometric Operating Modes of the Convair-580 SAR System.**

| | *Nominal Geometric Mode* | *Slant Range Sampling (m)* | *Swath (km)* | *Incidence Angles (°)* |
|---|---|---|---|---|
| 1 | Nadir | 4 | 22 | 0-74 |
| 2 | Narrow | 4 | 18 | 45-76 |
| 3 | Wide | 16 | 63 | 45-85 |

These nominal geometric modes could be used for data collection in a number of SAR configurations including: X/C mode in selected polarizations, C-band polarimetry, C-band along-track interferometry, and C-band cross-track interferometry. This note only concerns itself with data collection in the C-band Polarimetry configuration.

# 2 Preferred Geometry for Polarimetry

The radar however offers a continuous range of geometries that the operators can access by appropriate offsets. The one shown in Figure 1 has been shown to provide excellent imagery

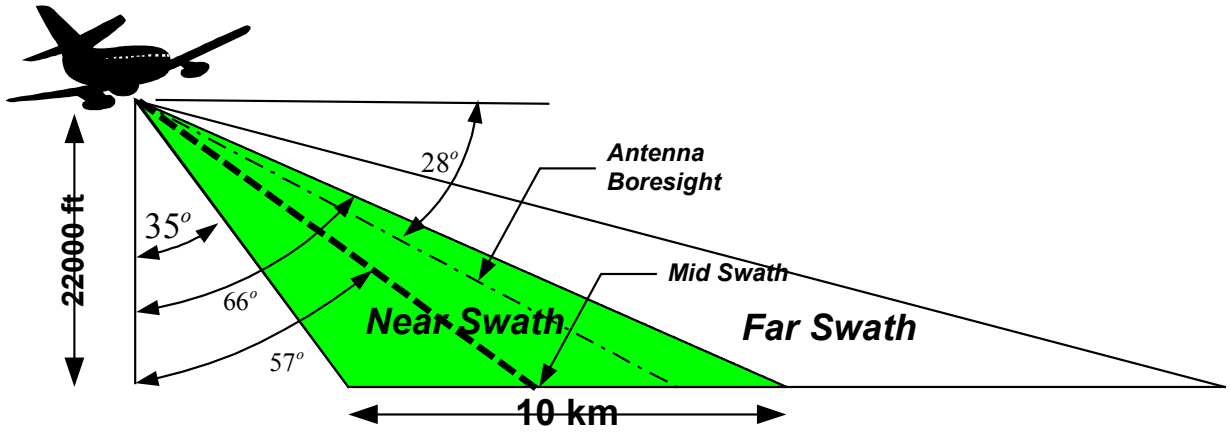


**Figure 1. Preferred Acquisition Geometry for Polarimetric Applications over Land.** The green area is the near half swath which has been optimized for incidence angle of interest and fidelity of polarimetric calibration. The centre of the near swath is about 57°.

[3] "Airborne C/X-SAR", Ministry of Supply and Services, Canada, 1994. Cat. No. M77-42/19994E.

over the near swath for land applications under the restrictions normally imposed on the operation of the SAR in the C-band polarimetric configuration. This preferred is further characterised by the geometry parameters shown in Figure 2. The units are in nautical miles (1 nm = 1.852 km) because that is normally how aircraft navigation is specified.

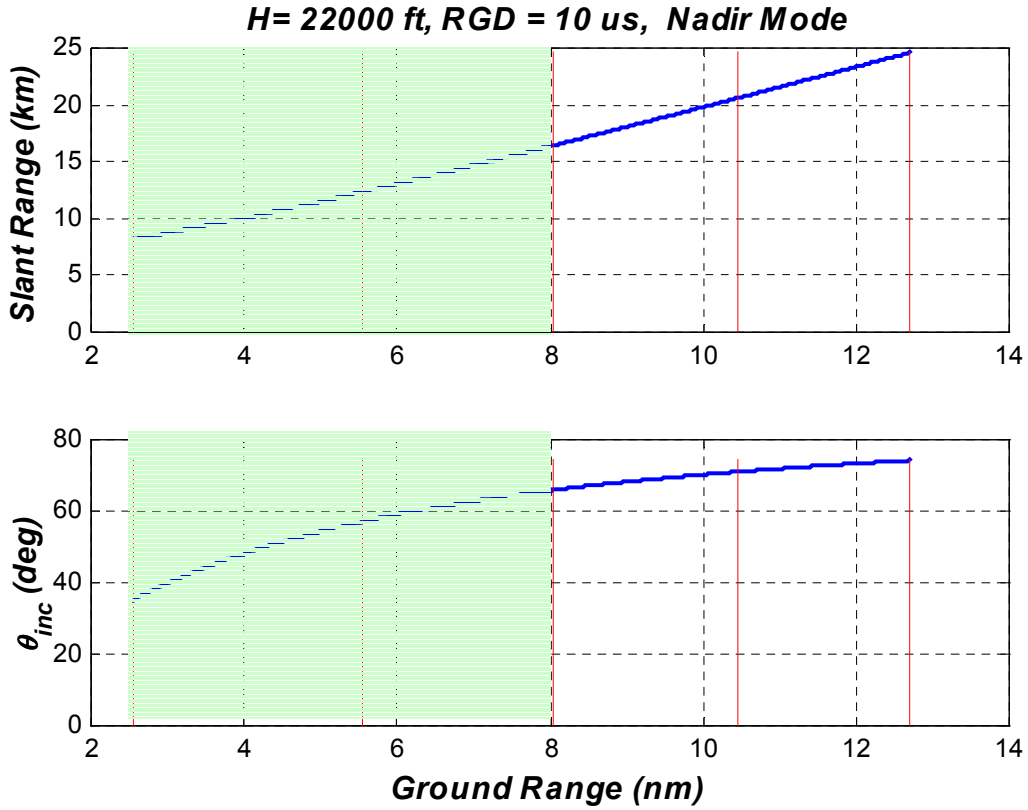


**Figure 2. Slant Range and Incidence Angle Available in Preferred Acquisition Geometry.** At the top is the slant range sample range accessed in the geometry as a function of ground range in nautical miles from the nadir position. The vertical red lines represent the ¼ swath boundaries of the data. At the bottom is the associated incidence angle that is accessed in the data. In the first ½ swath, the incidence angle range is from about 35˚ to 66˚. The green shaded area represents the near swath and corresponds to green area in Figure 1. A ground swath of approximately 10 km = (8 nm – 2.6 nm)x 1.852 km/nm is indicated. .

In this geometry, the very steep angles are not imaged because they are normally poorly calibrated, both in terms of phase and radiometry, and suffer from banding due to poorly defined antenna pattern. The range from 35 to 66˚ is however well characterized[4]. The full swath of data is recorded in signal form during an acquisition for all four polarimetric channels; however, because of the image quality restrictions and to reduce the data volume, only the near half swath is normally processed.

[4] See for instance: Hawkins, RK, R Touzi, CE Livingstone, ``Calibration and use of CV-580 airborne polarimetric SAR data", in *Proc. Fourth International Airborne Remote Sensing Conference and* Exhibition/ 21st Canadian Symposium on Remote Sensing, Ottawa, Ontario, 21-24 June 1999., 10p.

# 3 Flight Planning

For flight planning, the mid swath is at and incidence angle of about 57˚ with an aircraft offset of about 5.5 nm. Consideration needs to be given to azimuth direction and length of swath.

# 4 Recommendations

CCRS has the most experience with processing and calibration of Convair-580 SAR acquisition of any organization. Although the system can sustain data acquisition in many other configurations, these can only be used at the risk of complicating the calibration and processing and even jeopardizing the quality of the data. For land and sea-ice applications, the geometry shown in this note is recommended.

Because processing is a very arduous and time consuming, well thought out experiments which minimize the data acquisition and processing is highly recommended.